



2014.
GODINA
LVII

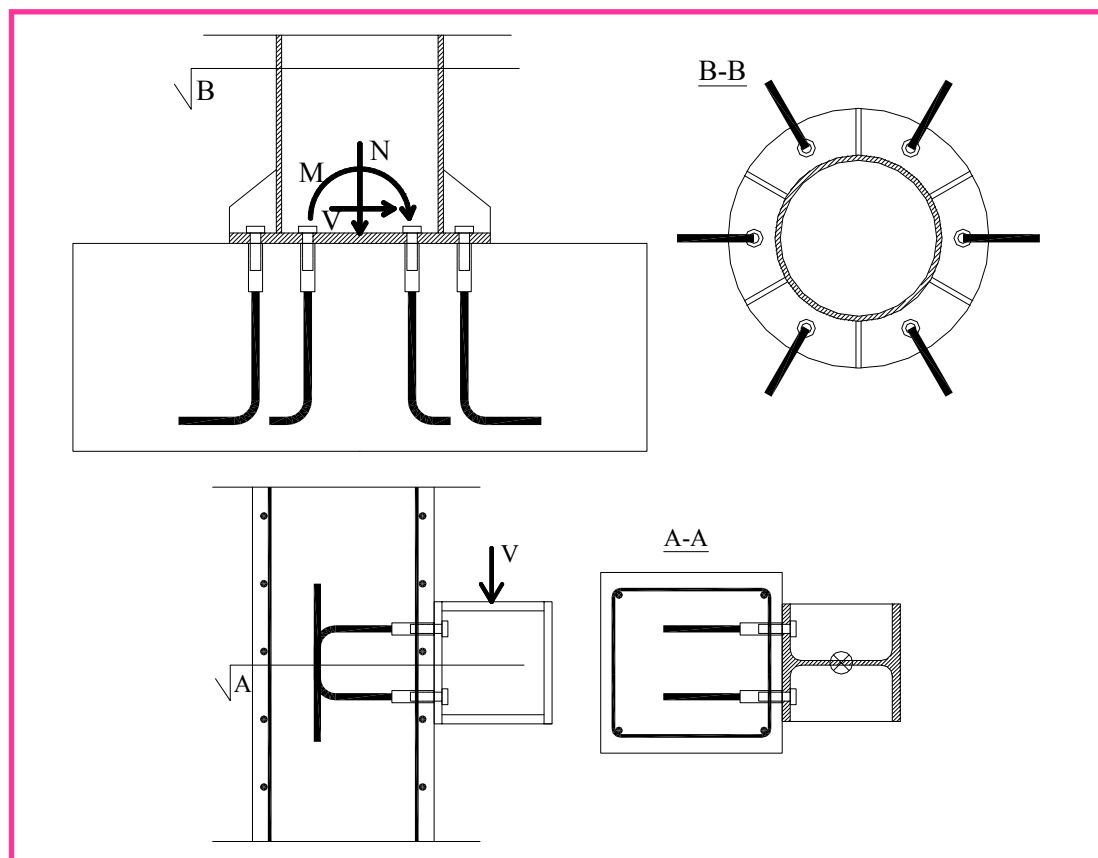


GRAĐEVINSKI MATERIJALI I KONSTRUKCIJE

2

BUILDING MATERIALS AND STRUCTURES

ČASOPIS ZA ISTRAŽIVANJA U OBLASTI MATERIJALA I KONSTRUKCIJA
JOURNAL FOR RESEARCH OF MATERIALS AND STRUCTURES



Odlukom Skupštine ***Društva za ispitivanje materijala i konstrukcija***, održane 19. aprila 2011. godine u Beogradu, promenjeno je ime časopisa **Materijali i konstrukcije** i od sada će se časopis publikovati pod imenom **Gradevinski materijali i konstrukcije**.

According to the decision of the Assembly of the **Society for Testing Materials and Structures**, at the meeting held on 19 April 2011 in Belgrade the name of the Journal Materijali i konstrukcije (Materials and Structures) is changed into **Building Materials and Structures**.

Professor Radomir Folic
Editor-in-Chief

GRAĐEVINSKI MATERIJALI I KONSTRUKCIJE

BUILDING MATERIALS AND STRUCTURES

ČASOPIS ZA ISTRAŽIVANJA U OBLASTI MATERIJALA I KONSTRUKCIJA
JOURNAL FOR RESEARCH IN THE FIELD OF MATERIALS AND STRUCTURES

INTERNATIONAL EDITORIAL BOARD

Professor **Radomir Folić**, Editor in-Chief
Faculty of Technical Sciences, University of Novi Sad, Serbia
Fakultet tehničkih nauka, Univerzitet u Novom Sadu, Srbija
e-mail:folic@uns.ac.rs

Professor **Mirjana Malešev**, Deputy editor
Faculty of Technical Sciences, University of Novi Sad,
Serbia
Fakultet tehničkih nauka, Univerzitet u Novom Sadu, Srbija
e-mail: miram@uns.ac.rs

Dr **Ksenija Janković**
Institute for Testing Materials, Belgrade, Serbia
Institut za ispitivanje materijala, Beograd, Srbija

Dr **Jose Adam, ICITECH**
Department of Construction Engineering, Valencia,
Spain.

Professor **Radu Banchila**
Dep. of Civil Eng. „Politehnica“ University of
Temisoara, Romania

Professor **Dubravka Bjegović**
Civil Engineering Institute of Croatia, Zagreb, Croatia

Assoc. professor **Meri Cvetkovska**
Faculty of Civil Eng. University "St Kiril and Metodij",
Skopje, Macedonia

Professor **Michael Forde**
University of Edinburgh, Dep. of Environmental Eng.
UK

Dr **Vladimir Gocevski**
Hydro-Quebec, Motreal, Canada

Dr. Habil. **Miklos M. Ivanyi**
UVATERV, Budapest, Hungary

Professor **Asterios Liolios**
Democritus University of Thrace, Faculty of Civil
Eng., Greece

Predrag Popović
Wiss, Janney, Elstner Associates, Northbrook,
Illinois, USA.

Professor **Tom Schanz**
Ruhr University of Bochum, Germany

Professor **Valeriu Stoin**
Dep. of Civil Eng. „Poloitehnica“ University of
Temisoara, Romania

Acad. Professor **Miha Tomažević**, SNB and CEI,
Slovenian Academy of Sciences and Arts,

Professor **Mihailo Trifunac**, Civil Eng.
Department University of Southern California, Los
Angeles, USA

Lektori za srpski jezik: Dr **Miloš Zubac**, profesor
Aleksandra Borojević, profesor
Proofreader: Prof. **Jelisaveta Šafranj**, Ph D
Technical editor: Stojan Todorović, e-mail: saska@imk.grf.bg.ac.rs

PUBLISHER

Society for Materials and Structures Testing of Serbia, 11000 Belgrade, Kneza Milosa 9
Telephone: 381 11/3242-589; e-mail: dimk@ptt.rs, veb sajt: www.dimk.rs

REVIEWERS: All papers were reviewed
COVER: Veza preko zavrtanja i mehaničke spojnica
Bolt-Rebar Coupler Connection

Financial supports: Ministry of Scientific and Technological Development of the Republic of Serbia

GRAĐEVINSKI MATERIJALI I KONSTRUKCIJE

BUILDING MATERIALS AND STRUCTURES

ČASOPIS ZA ISTRAŽIVANJA U OBLASTI MATERIJALA I KONSTRUKCIJA
JOURNAL FOR RESEARCH IN THE FIELD OF MATERIALS AND STRUCTURES

SADRŽAJ

Jan RAVINGER STABILNOST I VIBRACIJE U GRAĐEVINARSTVU Originalni naučni rad	3
Branko MILOSAVLJEVIĆ MEHANIČKO NASTAVLJANJE ARMATURE Stručni rad	19
Ksenija JANKOVIĆ Dragan BOJOVIĆ Marko STOJANOVIĆ Ljiljana LONČAR OTPORNOST MATERIJALA NA BAZI METALURŠKOG CEMENTA NA DEJSTVO KISELINA Originalni naučni rad	29
Anina SARKIC Milos JOČKOVIC Stanko BRCIC METODE ANALIZE FLATERA U FREKVENTNOM I VREMENSKOM DOMENU Originalni naučni rad	39
Uputstvo autorima	57

CONTENTS

Jan RAVINGER STABILITY AND VIBRATION IN CIVIL ENGINEERING Original scientific paper	3
Branko MILOSAVLJEVIĆ MECHANICAL REBAR SPLICING Professional paper.....	19
Ksenija JANKOVIĆ Dragan BOJOVIĆ Marko STOJANOVIĆ Ljiljana LONČAR RESISTANCE OF CEM III/B BASED MATERIALS TO ACID ATTACK Original scientific paper	29
Anina SARKIC Milos JOČKOVIC Stanko BRCIC FREQUENCY- AND TIME-DOMAIN METHODS RELATED TO FLUTTER INSTABILITY PROBLEM Original scientific paper	39
Preview report	57

CIP - Каталогизација у публикацији
Народна библиотека Србије, Београд

620.1

GRAĐEVINSKI materijali i konstrukcije :
časopis za istraživanja u oblasti materijala
i konstrukcija = Building Materials and
Structures : journal for research of
materials and structures / editor-in-chief
Radomir Folić. - God. 54, br. 1 (2011)-
- Beograd (Kneza Miloša 9) : Društvo za
ispitivanje i istraživanje materijala i
konstrukcija Srbije, 2011- (Novi Beograd :
Hektor print). - 30 cm

Tromesečno. - Je nastavak: Materijali i
konstrukcije = ISSN 0543-0798
ISSN 2217-8139 = Građevinski materijali i
konstrukcije
COBISS.SR-ID 188695820



STABILITY AND VIBRATION IN CIVIL ENGINEERING

STABILNOST I VIBRACIJE U GRAĐEVINARSTVU

Ján RAVINGER

ORIGINALNI NAUČNI RAD
ORIGINAL SCIENTIFIC PAPER
UDK: 624.072.2.046

1 INTRODUCTION

Taking into account the stiffness and inertia forces, dynamic behaviour of structures can be investigated. Dynamic investigation usually starts with an example of free vibration. It means to evaluate the natural frequency. The simplest stability problem of structures is buckling of a column. This problem can be arranged preparing the equilibrium conditions on a deformed structure. In general, however, for the evaluation of the stability problems strains should be evaluated for a deformed differential element what means to apply geometric non-linear theory.

Combination of dynamics and stability yields in a lot of problems: dynamic buckling, dynamic post buckling behaviour, parametric resonance, etc. Introduction example – vibration of a column loaded in compression is simple but its investigation still represents a lot of problems.

The natural frequency can be measured by using rather simple equipment. The comparison of frequencies measured experimentally and evaluated numerically is the basis of non-destructive methods for investigation of structure properties. Generally, it can be said that in structural design stability effects have to be taken into consideration. These two ideas are the reason for our investigation of the combination of vibration and stability.

Leonard Euler was probably the first scientist who had analyzed stability problems. The former solutions are supposed to be the linear stability. It means that we suppose an ideal structure. The differences between theory and reality inspired researchers to search for more accurate models. Especially the slender web as the main part of thin-walled structure has significant post-buckling reserves and it is necessary to accept a geometric non-linear theory for their description. The problem of the vibration of the non-linear system was

formulated by Bolotin². Burgreen³ analysed the problem of the vibration of an imperfect column in early 50's. Some valuable results have been achieved by Volmir⁷. Combination of dynamics and stability is still a subject of research all over the world.

2 DYNAMIC POST-BUCKLING BEHAVIOUR OF SLENDER WEB

2.1 Post-buckling behaviour of slender web – displacement model

As it was already mentioned, slender web is the main constructional element of thin-walled structure. If we assume an "ideal" slender web and a distribution of the in-plane stresses are not the function of the out-of plane (the plate) displacements, the problem leads to eigenvalues and eigenvectors. From the obtained eigenvalues elastic critical load can be evaluated and eigenvector characterizes the mode of buckling.

Post-buckling behaviour can be assumed as follows (Fig.1)

Displacements of the point of the middle surface are

$$\mathbf{q} = [u, v, w]^T \quad (1)$$

In the post-buckling behaviour of the slender web the plate displacements are much larger than in-plane (web) displacements ($w \gg u, v$) and so the strains are

$$\boldsymbol{\varepsilon} = \begin{Bmatrix} u_{,x} \\ v_{,y} \\ u_{,y} + v_{,x} \end{Bmatrix} + \frac{I}{2} \begin{Bmatrix} w_{,x}^2 \\ w_{,y}^2 \\ 2w_{,x}w_{,y} \end{Bmatrix} - z \begin{Bmatrix} w_{,xx} \\ w_{,yy} \\ w_{,xy} \end{Bmatrix} \quad (2)$$

where "z" is the coordinate of the thickness. The indexes "x, y" denote partial derivations.

Dr.h.c. prof. Ing. Ján Ravinger, DrSc. Slovak University of Technology, Faculty of Civil Engineering
Radlinského 11, 813 68 Bratislava, Slovakia. E-mail
jan.ravinger@stuba.sk

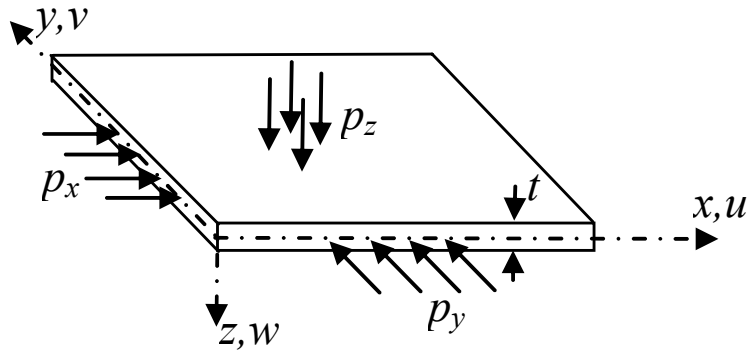


Figure 1. Notation of the quantities of slender web

For the next investigation, slender web with initial deformations is assumed. Initial deformations are the plate types only.

$$\mathbf{q}_\theta = [0, 0, w_0]^T \quad (3)$$

Due to that the initial strains are

$$\boldsymbol{\varepsilon}_0 = \frac{1}{2} \begin{Bmatrix} w_{0,x}^2 \\ w_{0,y}^2 \\ 2w_{0,x}w_{0,y} \end{Bmatrix} - z \begin{Bmatrix} w_{0,xx} \\ w_{0,yy} \\ 2w_{0,xy} \end{Bmatrix} \quad (4)$$

The "w" represents the global displacements and "w₀" is part related to the initial displacement.

The linear elastic material has been assumed

$$\boldsymbol{\sigma} = \begin{Bmatrix} \sigma_x \\ \sigma_y \\ \tau \end{Bmatrix} = \mathbf{D}(\boldsymbol{\varepsilon} - \boldsymbol{\varepsilon}_0) + \boldsymbol{\sigma}_w,$$

where $\mathbf{D} = \frac{E}{1-\nu^2} \begin{bmatrix} 1 & \nu & 0 \\ \nu & 1 & 0 \\ 0 & 0 & \frac{1-\nu}{2} \end{bmatrix}$ (5)

E, ν are the Young's modulus and Poisson's ratio, $\boldsymbol{\sigma}_w = [\sigma_{xw}, \sigma_{yw}, \tau_w]^T$ are the residual stresses.

The global potential energy of the slender web is

$$U = U_i + U_e \quad (6)$$

where

$U_i = \frac{1}{2} \int_V (\boldsymbol{\varepsilon} - \boldsymbol{\varepsilon}_0)^T \boldsymbol{\sigma} dV$ - is the potential energy of the internal forces,

$U_e = - \int_{\Gamma} (\mathbf{q} - \mathbf{q}_\theta)^T \mathbf{p} d\Gamma$ - the potential energy of the external forces,

where V is the volume of the slender web, Γ is the in-plane surface.

The displacements are assumed as the product of the variational functions and the displacements parameters

$$\mathbf{q} = \mathbf{B}\boldsymbol{\alpha} \quad (7)$$

The minimum of the global potential energy gives the system of conditional equation

$$\mathbf{K}_G(\boldsymbol{\alpha})\boldsymbol{\alpha} = \mathbf{f} \quad (8)$$

where \mathbf{K}_G is the stiffness matrix as the function of the displacement parameters – non-linear stiffness matrix, \mathbf{f} is the vector of the external load.

2.2 Post-buckling behaviour of slender web loaded in compression – illustrative example

For the simplification we suppose the square rectangular slender web loaded in compression simply supported all around.

We do not need to suppose the external load as the constant along the edge. But the external force must be

defined as $F = \int_0^b t \sigma dy$. Consequently, the average

stress can be defined as $\sigma = \frac{F}{b \cdot t}$. For the approximate solution, we take displacement functions as

$$w = \alpha S_{x1} S_{y1},$$

$$w_0 = \alpha_0 S_{x1} S_{y1},$$

$$u = \beta_1 \left(1 - \frac{2x}{b} \right) + \beta_2 S_{x2} C_{y2} + \beta_3 S_{x2},$$

$$v = \gamma_1 \left(1 - \frac{2y}{b} \right) + \gamma_2 C_{x2} S_{y2} + \gamma_3 S_{y2},$$

$$\text{where } S_{xi} = \sin \frac{i\pi x}{b}, \dots, C_{yi} = \cos \frac{i\pi y}{b}.$$

We have divided the variational parameters into:

- plate $\boldsymbol{\alpha}_D = \boldsymbol{\alpha}$,

- in-plane $\boldsymbol{\alpha}_S = [\beta_1, \beta_2, \beta_3, \gamma_1, \gamma_2, \gamma_3]^T$.

The in-plane displacements parameters are

$$\alpha_s = \frac{\pi}{16b} (\alpha^2 - \alpha_0^2) [\pi, I, -I + v, \pi, I, -I + v]^T$$

Introducing $\sigma_E = \frac{\pi^2 Et^2}{12(1-v^2)b^2}$ (Euler's elastic critical stress), the dimensionless load as $\bar{\sigma} = \frac{\sigma'}{4\sigma_E} = \frac{\sigma'}{\sigma_{cr}}$, ($\sigma_{cr} = 4\sigma_E$) and the dimensionless parameters of the displacements function $\bar{\alpha} = \frac{\alpha}{t}$, $\bar{\alpha}_0 = \frac{\alpha_0}{t}$, the result can be arranged into the final equation

$$0.34125(\bar{\alpha}^2 - \bar{\alpha}_0^2) + 1 - \frac{\bar{\alpha}_0}{\bar{\alpha}} = \bar{\sigma} \quad (9)$$

The parameters α and α_0 represent the amplitudes of the out of plate displacements of the slender web. Eq. (9) is arranged in Fig. 2.

It is evident that slender web could be loaded above the level of the elastic critical load. Due to that "the post-buckling behaviour" can be introduced.

It has to be noted that the presented example represents an approximate solution.

2.3 System of non-linear algebraic equations

First, we present a note related to the solution of geometric non-linear problems.

We use (for example) the Ritz variational method. The functions of the displacements are sums of the products of the basic functions and the variational coefficients.

$$q = B \cdot \alpha \quad (10)$$

These equations could be written in the mode

$$u, w \Rightarrow \alpha \uparrow 1 \quad (11)$$

The sign „ \uparrow “ is used as the exponent.

The elongations taking into account non-linear parts have the variational coefficients in quadrates and can be recorded as

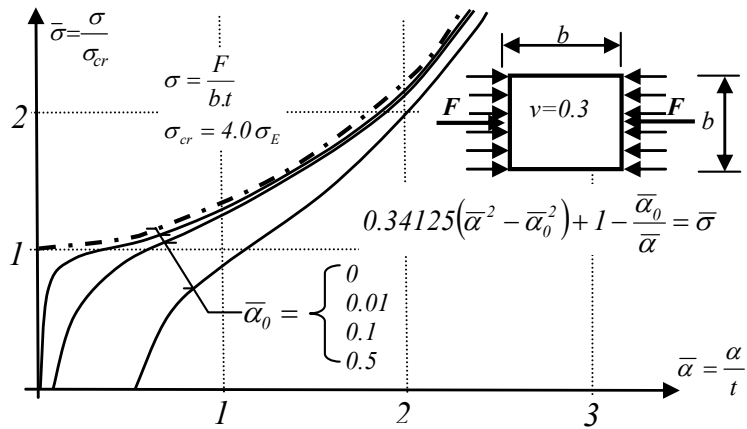


Figure 2. Post-buckling behaviour of slender web loaded in compression

$$\varepsilon = u_{,x} + \frac{1}{2} w_{,x}^2 - z \cdot w_{xx} \Rightarrow \alpha \uparrow 2 \quad (12)$$

Assuming the linear elastic material, the stresses are in quadrates as well.

$$\sigma = E(\varepsilon - \varepsilon_0) \Rightarrow \alpha \uparrow 2 \quad (13)$$

The potential energy of the internal forces is a product of the elongations and the stresses, then, finally, the variational coefficients are of the fourth power

$$U_i = \frac{1}{2} \boldsymbol{\varepsilon}^T \cdot \boldsymbol{\sigma} = (\alpha \uparrow 2) \cdot (\alpha \uparrow 2) = \alpha \uparrow 4 \quad (14)$$

The system of conditional equations may be arranged as a partial derivation according to the variational coefficients

$$\frac{\partial U}{\partial \alpha_i} = \dots = \alpha \uparrow 3 \quad (15)$$

Finally, we obtain the **system of cubic algebraic equations**.

A partial approval of our explanation can be seen in the example of the post buckling behaviour of the slender web (Part 2.2, Eq.(9) where we have got the cubic algebraic equation).

Note. In the example of the buckling of the column, the cubic terms have been eliminated. This "special case" is the consequence of the constant normal force along the column.

Let us continue with our former considerations.

The system of linear algebraic equations can be arranged as a matrix (two dimensional area). The system of quadratic algebraic equations could be arranged as a three dimensional matrix. The cubic algebraic equations are a four dimensional matrix. We are not able to imagine the four dimensional matrix, but modern computers are able to compile it.

One typical property of the finite element method is a large number of parameters (many thousands). To arrange 1000 cubic algebraic equations represents in computer memory $1000^4 = 1 \cdot 10^{12}$ real numbers and this is beyond possibilities.

The way how to solve these non-linear systems has been found. The idea is to use the Newton-Raphson iteration without compilation of the system of non-linear (cubic) algebraic equations. It will be explained in the following parts.

2.4 Incremental formulation

As it has been already explained in the previous part, we are forced to arrange the iterative method. It can be prepared from the incremental formulation, and so we must prepare all the regulars in increments.

Note. All the rules for one dimensional problem (beams, columns) are prepared. For the solution of the two dimensional problems (webs, plates) all the steps are similar.

As the first step, the increments and variations for the elongations must be prepared.
If we have the linear function as

$$f\left(\frac{du}{dx}\right) = \frac{du}{dx} = u_{,x} \quad (16)$$

For the increments $u + \Delta u$, we get the increments of the function

$$\begin{aligned} \Delta f &= f\left(\frac{d(u + \Delta u)}{dx}\right) - f\left(\frac{du}{dx}\right) = \frac{du}{dx} + \frac{d\Delta u}{dx} - \frac{du}{dx} = \\ &= \frac{d\Delta u}{dx} = \Delta u_{,x} \end{aligned} \quad (17)$$

We do the same steps for the non-linear function

$$f\left(\frac{dw}{dx}\right) = \frac{1}{2}\left(\frac{dw}{dx}\right)^2 = \frac{1}{2}w_{,x}^2 \quad (18)$$

We have for the increment of this function

$$\begin{aligned} \Delta f &= f\left(\frac{d(w + \Delta w)}{dx}\right) - f\left(\frac{dw}{dx}\right) = \frac{1}{2}\left(\frac{d(w + \Delta w)}{dx}\right)^2 - \\ &- \frac{1}{2}\left(\frac{dw}{dx}\right)^2 = \frac{1}{2}\left(\left(\frac{dw}{dx}\right)^2 + 2\frac{dw}{dx} \cdot \frac{d\Delta w}{dx} + \left(\frac{d\Delta w}{dx}\right)^2\right) - \\ &- \frac{1}{2}\left(\frac{dw}{dx}\right)^2 = \frac{dw}{dx} \cdot \frac{d\Delta w}{dx} + \frac{1}{2}\left(\frac{d\Delta w}{dx}\right)^2 = \\ &= w_{,x} \cdot \Delta w_{,x} + \frac{1}{2} \Delta w_{,x}^2 \end{aligned} \quad (19)$$

According to these rules the increment of the strain can be arranged as follows

$$\Delta \varepsilon_{,x} = \Delta u_{,x} + w_{,x} \cdot \Delta w_{,x} + \frac{1}{2} \Delta w_{,x}^2 - z \cdot \Delta w_{xx} \quad (20)$$

Then the variation of the increment of the elongation is prepared

$$\delta \Delta \varepsilon_{,x} = \delta \Delta u_{,x} + w_{,x} \cdot \delta \Delta w_{,x} + \delta \Delta w_{,x} \cdot \Delta w_{,x} - z \cdot \delta \Delta w_{xx} \quad (21)$$

2.5 The Hamilton's principle

In this step, we prepare the rules for the dynamic process. In order to neglect the inertial forces, we get the static problems.

The Hamilton's principle means: in each time interval, the variation of the kinetic and potential energy and the variation of the work of the external forces is equal zero. This rule is valid for the increments as well:

$$\int_{t_0}^{t_1} \delta(\Delta T - \Delta U) dt + \int_{t_0}^{t_1} \delta \Delta W dt = 0 \quad (22)$$

where $\Delta T = \int_V \frac{1}{2} \rho \Delta q^T \Delta q dV$ is the increment of the

kinetic energy, $\Delta U = \int_V \left(\frac{1}{2} \Delta \varepsilon \cdot \Delta \sigma + \Delta \varepsilon \cdot \sigma \right) dV$ – the

increment of the potential energy of the internal forces,

$\Delta W = \int_V \Delta q^T \cdot (\mathbf{p} + \Delta \mathbf{p}) dV$ – the increment of the work of

the external forces, t_0, t_1 – the time intervals, ρ – the mass density, V – the volume (in our case it is the volume of the beam – column), $\mathbf{p}, \Delta \mathbf{p}$ – the external load, the increment of the external load.

The dots mean the time derivation.

We assume the linear elastic material (Eq. (5)). For the increments, we have

$$\Delta \sigma = D \Delta \varepsilon$$

In the case of the beam type of structures, the volume integration can be changed into the integration over the cross section and the integration over the length:

A, I – the cross section area, the moment of inertia.

The longitudinal axis is situated into centre of the gravity of the cross section.

We use the Ritz variational method

$$u = \mathbf{B}_S \cdot \boldsymbol{\alpha}_S, \quad w = \mathbf{B}_D \cdot \boldsymbol{\alpha}_D, \quad (23)$$

We have the incremental model and the variational coefficients $\boldsymbol{\alpha}_S$ a $\boldsymbol{\alpha}_D$ are timeless functions.

For the increments of the displacements functions, the independent basic variational functions can be used. The increments of the variational coefficients are the function of the time

$$\Delta u = \mathbf{B}_{S1} \cdot \Delta \boldsymbol{\alpha}_S(t), \quad \Delta w = \mathbf{B}_{D1} \cdot \Delta \boldsymbol{\alpha}_D(t) \quad (24)$$

Note. In some dynamic processes where there can be different boundary condition for the static behaviour and for the vibration, it is useful to have different basic variational functions for the displacements and for the increment of the displacements.

Finally, Eq. (22) leads to the system of conditional equation. This system could be arranged into the mode

$$\begin{aligned} \mathbf{K}_{M-D} \Delta \ddot{\alpha}_D + \mathbf{K}_{INC-D} \Delta \alpha_D + \mathbf{K}_{INC-DS} \Delta \alpha_S + \mathbf{f}_{INT-D} - \mathbf{f}_{EXT-D} - \Delta \mathbf{f}_{EXT-D} &= \mathbf{0} \\ \mathbf{K}_{M-S} \Delta \ddot{\alpha}_S + \mathbf{K}_{INC-S} \Delta \alpha_S + \mathbf{K}_{INC-SD} \Delta \alpha_D + \mathbf{f}_{INT-S} - \mathbf{f}_{EXT-S} - \Delta \mathbf{f}_{EXT-S} &= \mathbf{0} \end{aligned} \quad (25)$$

where $\mathbf{K}_{M-D} = \int_0^a \mathbf{B}_{DI}^T \rho A \mathbf{B}_{DI} dx$ is the mass matrix of

the "bending" displacements,

$\mathbf{K}_{INC-D} = \mathbf{K}_{INC-DL} + \mathbf{K}_{INC-DG}$ □ the incremental stiffness matrix of the bending,

$\mathbf{K}_{INC-DL} = \int_0^a \mathbf{B}_{DI}^T EI \mathbf{B}_{DI} dx$ □ the linear part,

$\mathbf{K}_{INC-DG} = \int_0^a \mathbf{B}_{DI}^T EA \left(\frac{3}{2} w_{,x}^2 - \frac{1}{2} w_{\theta,x}^2 \right) \mathbf{B}_{DI} dx$ □ the non-linear part of the incremental stiffness matrix of the bending stiffness,

$\mathbf{K}_{INC-DS} = \int_0^a \mathbf{B}_{DI}^T EA (w_{,xx} + u_{,x} w_{,x}) \mathbf{B}_{SI} dx$ □ the incremental "bending – axial" stiffness matrix,

$\mathbf{f}_{INT-D} = \int_0^a \mathbf{B}_{DI}^T EI (w_{,xx} - w_{0,xx}) dx + \int_0^a \mathbf{B}_{DI}^T EA (u_{,x} + \frac{1}{2} w_{,x}^2 u_{,x} - \frac{1}{2} w_{\theta,x}^2 u_{,x}) dx$ □ the vector of the bending internal forces,

$\Delta \mathbf{f}_{EXT-D} = \int_0^a \mathbf{B}_{DI}^T \Delta p_D dx$ □ the increment of the vector of the bending external forces,

$\mathbf{K}_{M-S} = \int_0^a \mathbf{B}_{SI}^T \rho A \mathbf{B}_{SI} dx$ □ the mass matrix of the "axial" displacements,

$\mathbf{K}_{INC-S} = \int_0^a \mathbf{B}_{SI}^T EA \mathbf{B}_{SI} dx$ □ the incremental stiffness matrix of the axial stiffness.

It can be proved that $\mathbf{K}_{INC-SD} = \mathbf{K}_{INC-DS}^T$ – the incremental "axial – bending" stiffness matrix,

$\mathbf{f}_{INT-S} = \int_0^a \mathbf{B}_{SI}^T EA \left(u_{,x} + \frac{1}{2} w_{,x}^2 - \frac{1}{2} w_{\theta,x}^2 \right) dx$ □ the vector of the axial internal forces,

$\mathbf{f}_{EXT-S} = \int_0^a \mathbf{B}_{SI}^T p_S dx$ – the vector of the axial external forces,

$\Delta \mathbf{f}_{EXT-S} = \int_0^a \mathbf{B}_{SI}^T \Delta p_S dx$ – the increment of the vector of the axial external forces.

It is evident that Eq.(25) represents the system of the differential equations of the second degree.

The axial and the bending displacement can be joined as

$$\Delta \boldsymbol{\alpha} = \begin{cases} \Delta \alpha_D \\ \Delta \alpha_S \end{cases}, \quad \boldsymbol{\alpha} = \begin{cases} \alpha_D \\ \alpha_S \end{cases}$$

The system of conditional equations (Eq. (25)) could be written as

$$\mathbf{K}_M \Delta \ddot{\boldsymbol{\alpha}} + \mathbf{K}_{INC} \Delta \boldsymbol{\alpha} + \mathbf{f}_{INT} - \mathbf{f}_{EXT} - \Delta \mathbf{f}_{EXT} = \mathbf{0} \quad (26)$$

where

$$\mathbf{K}_M = \left[\begin{array}{c|c} \mathbf{K}_{M-D} & \\ \hline & \mathbf{K}_{M-S} \end{array} \right],$$

$$\mathbf{K}_{INC} = \left[\begin{array}{c|c} \mathbf{K}_{INC-D} & \mathbf{K}_{INC-DS} \\ \hline \mathbf{K}_{INC-SD} & \mathbf{K}_{INC-S} \end{array} \right]$$

$$\Delta \mathbf{f}_{EXT} = \begin{cases} \Delta \mathbf{f}_{EXT-D} \\ \Delta \mathbf{f}_{EXT-S} \end{cases}, \quad \mathbf{f}_{EXT} = \begin{cases} \mathbf{f}_{EXT-D} \\ \mathbf{f}_{EXT-S} \end{cases}, \quad \mathbf{f}_{INT} = \begin{cases} \mathbf{f}_{INT-D} \\ \Delta \mathbf{f}_{INT-S} \end{cases}$$

Static behaviour

The inertial forces can be neglected for the solution of the static behaviour of the structure

$$\mathbf{K}_M \cdot \Delta \ddot{\boldsymbol{\alpha}} \approx \mathbf{0} \quad (27)$$

Note. In the case of the static behaviour, except the Hamilton's principle, (Eq.(28)) the principle of the minimum of the increment of the global potential energy can be applied.

The system of the differential equations (Eq. (25)) will be changed into the system of the linear algebraic equation related to the increments of the displacements

$$\mathbf{K}_{INC} \Delta \boldsymbol{\alpha} + \mathbf{f}_{INT} - \mathbf{f}_{EXT} - \Delta \mathbf{f}_{EXT} = \mathbf{0} \quad (28)$$

If the problem is not established in the increments, but in the displacement parameters, we get the system of the cubic algebraic equations in the mode

$$\mathbf{f}_{INT} - \mathbf{f}_{EXT} = \mathbf{0} \quad (29)$$

As previously explained in the introduction Part 2.3, this system of cubic algebraic equations cannot be compiled. (Note. This system can be arranged in some simple examples only.)

Eq. (28) is the basis for the incremental solution and for the Newton-Raphson iteration as well.

2.6 Incremental solution

We assume the system in equilibrium represented by the parameters of the displacements " $\boldsymbol{\alpha}$ ". Then it is valid that

$$\mathbf{f}_{INT} - \mathbf{f}_{EXT} = \mathbf{0} \quad (30)$$

The increment of the external load is obtained. The increments of the parameters of the displacements can be obtained from Eq. (28)

$$\Delta\alpha = \mathbf{K}_{INC}^{-1} \Delta f_{EXT} \quad (31)$$

The displacement parameters of the new level are

$$\alpha_D^i = \alpha_D + \Delta\alpha_D \quad (32)$$

2.7 Newton-Raphson iteration

We do not assume any system in equilibrium represented by the parameters of the displacements " α^i ". Then we have the vector of residuum

$$r^i = f_{INT} - f_{EXT} \quad (33)$$

For the correction of the roots (displacement parameters), we assume the constant level of the external load ($\Delta f_{EXT} = 0$). Then it can be evaluated from Eq. (28)

$$\Delta\alpha^i = -\mathbf{K}_{INC}^{-1} \cdot r^i \quad (34)$$

The new approximation of the displacement parameters is

$$\alpha^{i+1} = \alpha^i + \Delta\alpha^i \quad (35)$$

Eqs. (33 – 35) represent the Newton-Raphson iteration.

We have a large amount of parameters. For the completing the iterative process, it is necessary to use suitable norms. One of them could be

$$\|n\| = \frac{(\alpha^{i+1})^T \cdot \alpha^{i+1} - (\alpha^i)^T \cdot \alpha^i}{(\alpha^{i+1})^T \cdot \alpha^i} \leq 0.001, (0.0001) \quad (36)$$

Using the terminology of the Newton-Raphson iteration, we have

$$\mathbf{K}_{INC} = \mathbf{J} \quad (37)$$

The incremental stiffness matrix is the same as the Jacoby matrix of the Newton-Raphson iteration. The Jacoby matrix characterizes the tangent plane to the non-linear surface and is defined as

$$\mathbf{J}_{ij} \equiv \frac{\partial}{\partial \alpha_i} \mathbf{K}_{Gnel-ij}^* \quad (38)$$

where \mathbf{K}_{Gnel}^* is the system of non-linear (in our case cubic) algebraic equations.

2.8 Bifurcation point

In the case of the non-linear problems, many results can be obtained represented by many paths (curves) illustrating relation of load versus the displacement parameters. Especially in the case of the stability problems, stable and unstable paths should be distinguished.

The global potential energy represents the surface. The local minimum of this surface is the point of stable path of the non-linear solution. From the theory of the quadratic surfaces for the local minimum, the Jacoby matrix (in our case, the incremental stiffness matrix) must be positively defined and all the principle minors must be positive as well

$$D = \left| \mathbf{K}_{INC} \right|_{det} > 0, D_k > 0. \quad (39)$$

If any condition of Eq. (39) is not satisfied, the path is unstable. The point between the stable and unstable paths is called **the bifurcation point**. In the bifurcation point, we have

$$D = \left| \mathbf{K}_{INC} \right|_{det} = 0 \quad (40)$$

2.9 Vibration of the structure

The conditional equations have been arranged as a dynamic process. The static behaviour is taken as a partial problem. From the viewpoint of the dynamic, we consider only the problem of the vibration. We are able to evaluate the vibration of the structure in different load levels including the effects of initial imperfections. We assume the structure in equilibrium and zero increment of the load

$$\Delta f_{EXT} = 0 \quad (41)$$

The system of conditional equations (Eq.(25) will be reduced

$$\mathbf{K}_M \Delta \ddot{\alpha} + \mathbf{K}_{INC} \Delta \alpha = 0 \quad (42)$$

Related to the increments of the displacements parameters, this system represents a homogeneous differential equation with constant coefficient. The solution has the mode

$$\Delta \alpha = \Delta \bar{\alpha} \sin(\omega t) \quad (43)$$

where ω is the circular frequency.

Putting this into Eq. (42), we get

$$-\omega^2 \mathbf{K}_M \Delta \bar{\alpha} \sin(\omega t) + \mathbf{K}_{INC} \Delta \bar{\alpha} \sin(\omega t) = 0 \quad (44)$$

The non-trivial solution leads to the problem of eigenvalues and eigenvectors

$$\left| \mathbf{K}_{INC} - \omega^2 \mathbf{K}_M \right|_{det} = 0. \quad (45)$$

The eigenvalues represent the squares of circular frequencies, and eigenvectors are the parameters of the modes of the vibration.

Note. Incremental stiffness matrix includes level of the load, deformation of structure and initial imperfections as well.

3 STABILITY AND VIBRATION

3.1 Vibration of simply supported column loaded in compression

In Part 2.5, the derivation has been started by using the Hamilton's principle and generally prepared the conditional equation for the dynamic process. In Part 2.10., we have arranged the equations for the evaluation of the vibration.

Another simple and interesting example is the vibration of the imperfect column. For the application of the action of the force, we must suppose one support as the hinge and the other support as the roller (the sliding support (Fig 3.)). (Note: The column is displayed in horizontal position.)

The axial inertial forces are neglected and the displacement functions are

$$w = \alpha_1 \sin \frac{\pi x}{l}, \quad w_0 = \alpha_0 \sin \frac{\pi x}{l}, \quad u = \begin{bmatrix} x, \sin \frac{2\pi x}{l} \end{bmatrix}^T \begin{bmatrix} \alpha_2 \\ \alpha_3 \end{bmatrix}$$

The parameters of axial displacements are

$$\alpha_2 = -\frac{F}{EA} - \frac{\pi^2}{l^2} (\alpha_1^2 - \alpha_0^2), \quad \alpha_3 = -\frac{\pi}{8l} (\alpha_1^2 - \alpha_0^2)$$

The equation of the static behaviour can be arranged in the form

$$\bar{F} = \left(1 - \frac{\alpha_0}{\alpha_1} \right), \text{ where } \bar{F} = \frac{F}{F_{EU}}, \quad F_{EU} = \frac{\pi^2 EI}{l^2} \text{ is}$$

Euler's elastic critical force.

The incremental stiffness matrix is

$$\mathbf{K}_{INC} = \frac{\pi^4 EI}{l^4} \frac{l}{2} - \frac{\pi^2}{l^2} \frac{l}{2} F$$

Putting this into Eq.(9.59), obtained result is
 $\omega^2 = \omega_0^2 (1 - \bar{F})$

where $\omega_0^2 = \frac{\pi^4 EI}{\rho A l^4}$ is the square of the circular frequency of the simply supported column

(46)

We have obtained a trivial result of the linear relation of the square of the circular frequency and the internal force. It can be seen that during the free vibration the initial displacements do not affect the free vibration.

3.2 Vibration of simply supported column – fixed supports

The result represented by Eq.(46) in the case of the level of the load as the elastic critical load gives the zero frequency. This is out of reality. For example, the miner foreman knocks on the columns. The low tone (the low frequency) means the small force inside the column and the column must be wedged. The high tone (the high frequency) means the high level of the load and the additional columns must be used.

To improve the obtained result the following arrangement must be done (Fig.4.):

For the displacements and the initial displacements, we take

$$w = \alpha_1 \sin(\pi x/l), \quad w_0 = \alpha_0 \sin(\pi x/l),$$

$$u = [x, \sin(2\pi x/l)]^T [\alpha_2, \alpha_3]^T$$

But for the increment of the displacement, we assume

$$\Delta w = \Delta \alpha_1 \sin(\pi x/l), \quad \Delta u = \Delta \alpha_3 \sin(2\pi x/l)$$

Now, different basic variational functions are used for the displacements and for the initial displacements:

Finally, the incremental stiffness matrix is

$$\mathbf{K}_{INC} = \frac{\pi^4 EI}{l^4} \frac{l}{2} - \frac{\pi^2}{l^2} \frac{l}{2} F + EA \frac{\pi^4}{l^4} \frac{l}{2} \frac{\alpha_1^2}{2}$$

Then we get the expression for the square of the circular frequency

$$\omega^2 = \omega_0^2 \left(1 - \bar{F} + \frac{1}{2} \frac{\alpha_1^2}{r^2} \right) \text{ where } r = \sqrt{\frac{I}{A}}$$

is the radius of inertia.

(47)

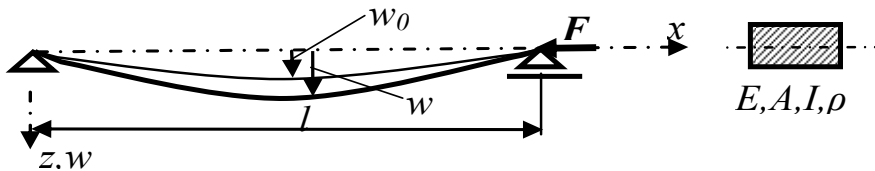


Figure 3. Simply supported column with initial displacement

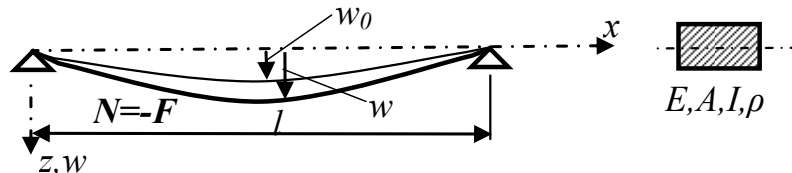


Figure 4. Simply supported column with initial displacement – fixed support

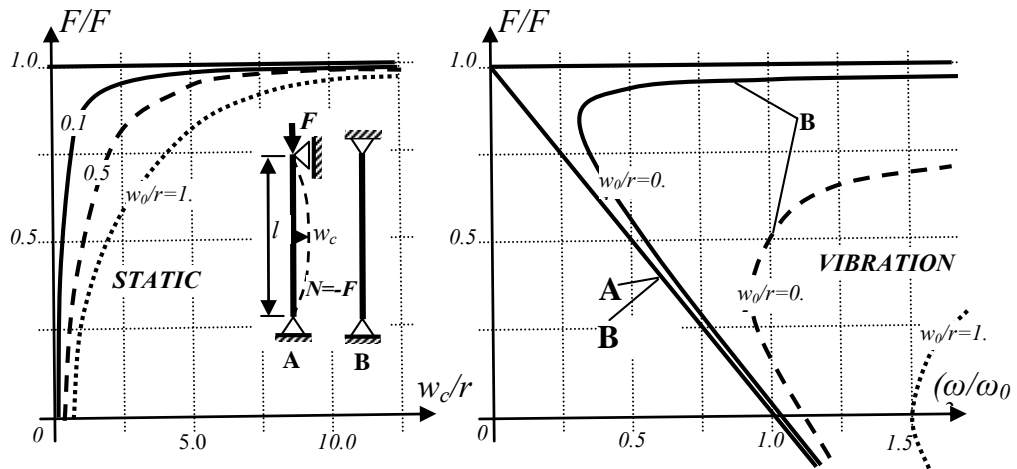


Figure 5. Stability and vibration of imperfect column

Thus, the result close to reality has been obtained. (Fig. 5) The displacement parameter „ α_1 “ is the function of the initial displacement and the level of the load. It means that the initial displacement enters the problem. If the load limits the level of the elastic critical load, the displacement and the frequency limits the infinity.

This example represents an advantage of the separation of the basic variational functions for the displacements and for the increments of the displacements.

3.3 Initial displacement as the second mode of buckling

A partial interesting problem is the influence of the mode of the initial displacement. In the previous part, we have supposed the initial displacement in the same mode as the first buckling mode (the mode of buckling related to the lowest elastic critical load). Due to that to obtain the solution by the analytical way was rather easy. The FEM has been used for the solution of more complicated examples.

Fig. 6. presents the solution of the buckling and the vibration of the column when the initial displacement has the mode related to the second mode of buckling.

Note. A lot of examples have been solved using the FEM. The obtained results can be presented in the dimensionless mode.

These results enable us to note some peculiarities. Even the initial displacement has the same mode as the second mode of the buckling ("the mode 2"), the collapse mode of the column is "the mode 1". The lowest elastic critical load is the maximum load. The mode of the vibration is "the mode 1" in all cases.

3.4 Experimental verification

The presented theoretical solutions are pointing to a substantial difference in the vibration of the beam at the moment when the critical load is reached. Considering sliding supports, the frequency should be zero. When supports are fixed, the frequency limits in infinity. This curiosity has been verified by an experiment.

The equipment for experimental verification of stability and vibration of beams loaded by pressure is shown in Fig. 7 and 8.

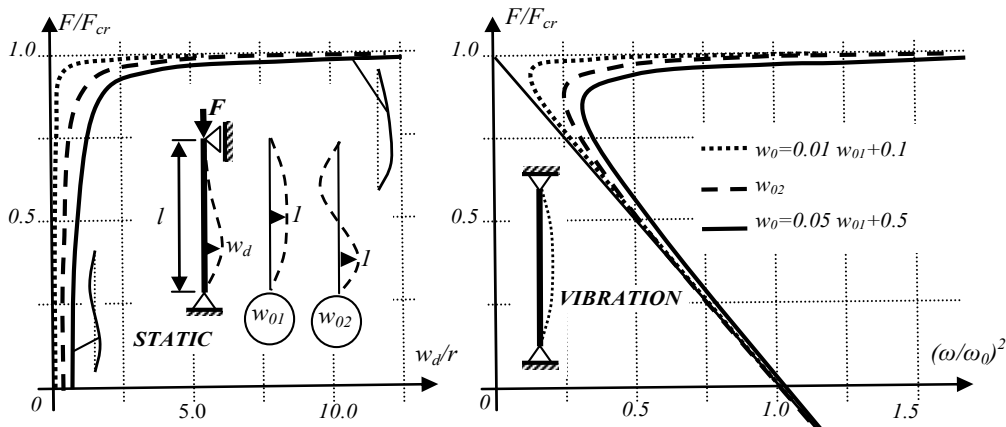


Figure 6. Stability and vibration of imperfect column with the initial displacement as the second mode of buckling

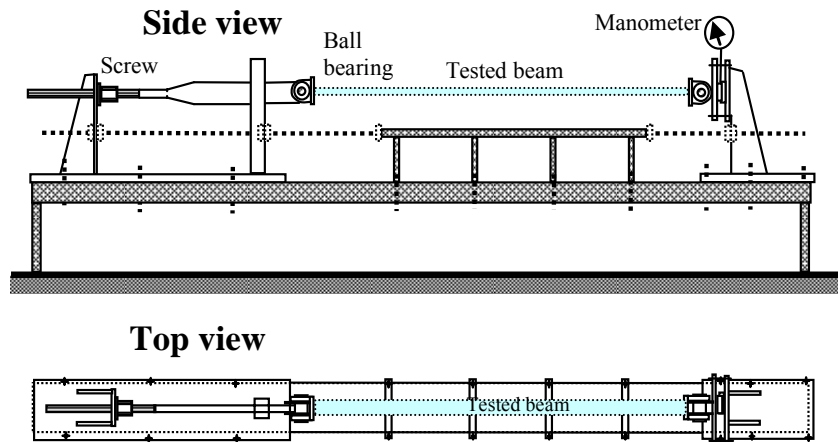


Figure 7. Scheme of the test set-up



Figure 8. General view of the test (the static behaviour)

The force (the load) is produced through the screw with a slight gradient (gradient 1.5 mm, average 30 mm), it means the load with the controlled deformation. The hinges are created by ball bearings in the jaw. The force is measured by manometer. The deflections are measured by mechanical displacement transducers fixed to the supporting steel structure. During measuring the frequency, the mechanical transducers are taken out and the accelerometer is attached.

Before the presentation of results, it is appropriate to make a note for specification of the mass matrixes due to end bearing (Fig. 9).

The mass matrix taking into account the effect of the end bearing will be

$$K_M = \rho A \frac{l}{2} + 2 * 0.06 * \sin \frac{\pi * 0.015}{l}$$

where the length of the beam is given in meters.

This effect of the end-bearing is dependent on the mass of the beam and is small (less than 1.5 %). To verify the dependence between the pressure force and frequency, the beams made of various types of materials have been analysed.

Steel hollow section profile Jäckl 30/15/1.5 mm

In the case of steel, the value of modulus of elasticity and the mass density are constant. When the exact dimensions of closed sections were measured, small problem occurred in measuring wall thickness.

The dimensions have been specified by measuring the weight of the profile. The rounded corners were considered in specification of cross-sectional characteristics. For further evaluation the following values were used

$$\text{Jäckl } 29.9 / 14.8 / 1.53, A = 121.4 \text{ mm}^2, I = 4286.0 \text{ mm}^4, r = 5.94 \text{ mm}, l = 1450 \text{ mm}$$

$$E = 210000 \text{ MPa}, \mu = 7850 \text{ kg/m}^3, F_{cr} = 4225.1 \text{ N}, \omega_0 = 144.2 \text{ s}^{-1}$$

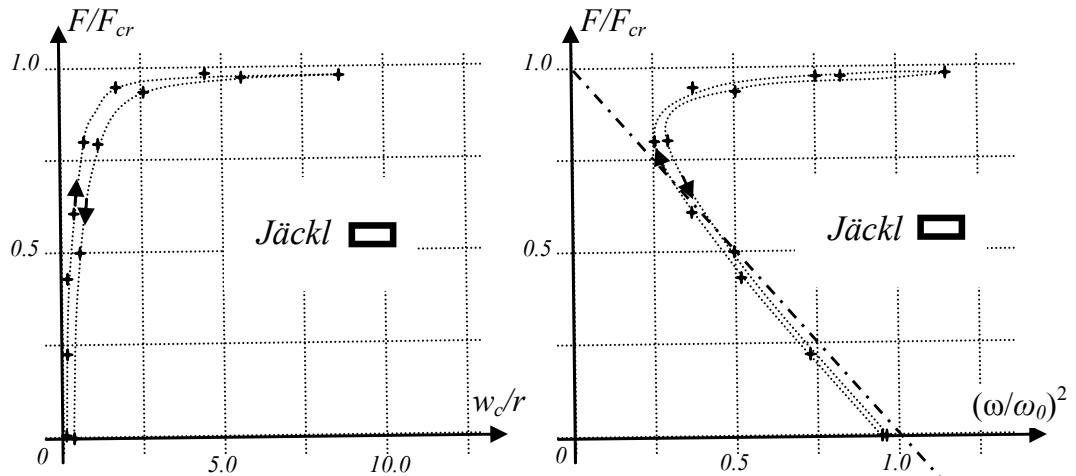


Figure 10. Results from measurements of the steel hollow thin-walled section – Jäckl

Timber beams

The modulus of elasticity of wood is an open question in the analyses of timber beams. In the presented measurements the critical load is identified at the moment of the increasing of the deformation without the increase of the force. Since the cross-sectional characteristics (the cross section, the moment of inertia) as well as the length of the beam have been known, using the Euler's elastic critical force, the modulus of elasticity can be evaluated. By measuring the weight of the profile, the mass density of wood has been easily and accurately evaluated. Subsequently, the natural circular frequency has been evaluated and two timber beams investigated.

The presented results confirmed undoubtedly a phenomenon that the frequency of the beam increases when the pressure force is near the critical level.

3.5 Vibration of frame

In the examples of the vibration of the columns, the problem could be arranged in the dimensionless equation. In the case of the frame, we have to use FEM. The obtained results are arranged into the dimensionless mode.

The geometry of the investigated frame is shown in Fig. 12. When we have an example where the mode of the vibration is similar to the mode of the buckling, the relation between the load and the square of circular frequency is linear and we are not able to take into consideration the effects of initial displacements. Generally, the behaviour of the column and the behaviour of the frame are similar. (Fig. 5 – alt A – movable support).

Timber beam 47 / 47 mm, $A = 2209 \text{ mm}^2$, $I = 406640 \text{ mm}^4$, $r = 13.57 \text{ mm}$, $l = 2040 \text{ mm}$
 $E = 10200 \text{ MPa}$, $\rho = 472 \text{ kg/m}^3$, $F_{cr} = 9836.7 \text{ N}$, $\omega_0 = 147.3 \text{ s}^{-1}$
 Timber beam 42 / 32 mm, $A = 1344 \text{ mm}^2$, $I = 114888 \text{ mm}^4$, $r = 9.24 \text{ mm}$, $l = 1650 \text{ mm}$
 $E = 9750 \text{ MPa}$, $\rho = 454 \text{ kg/m}^3$, $F_{cr} = 4060.8 \text{ N}$, $\omega_0 = 1154.9 \text{ s}^{-1}$

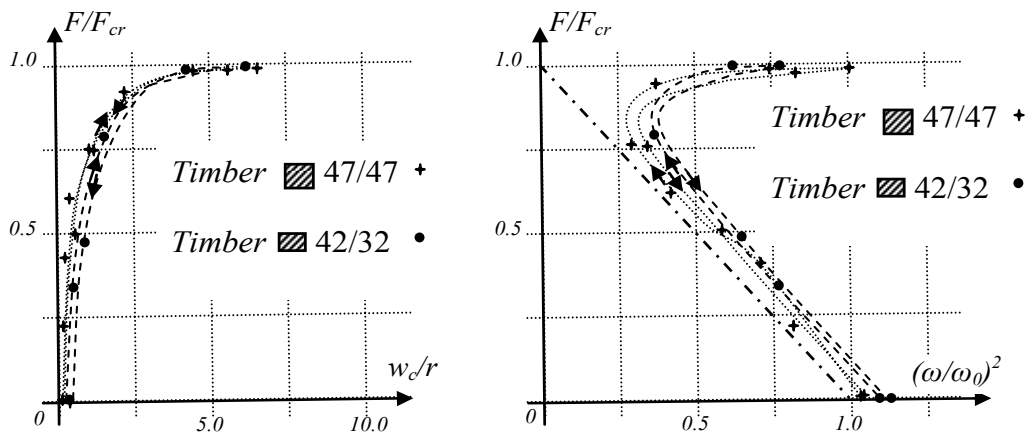


Figure 11. Results from the measurements of the timber beams

The load conditions have been arranged to get the mode of the buckling different to the mode of the vibration. In this case, the relationship between the load and the square of the circular frequency is non-linear (Fig. 13). Analogously as in the case of the column, we suppose a different boundary condition for the static load and for the vibration. If the point of the load application is fixed during the vibration process, we can take into consideration the effects of initial displacements. (We have supposed the same mode of initial displacements as the mode of buckling is.)

The modes of vibration for a different level of the load are presented as well (Fig. 13). In this case, we have supposed the frame without the initial imperfections. We can see that in the case of the higher level of the load ($F/F_{cr} > 0.6$), the mode of vibration is similar to the mode of the buckling.

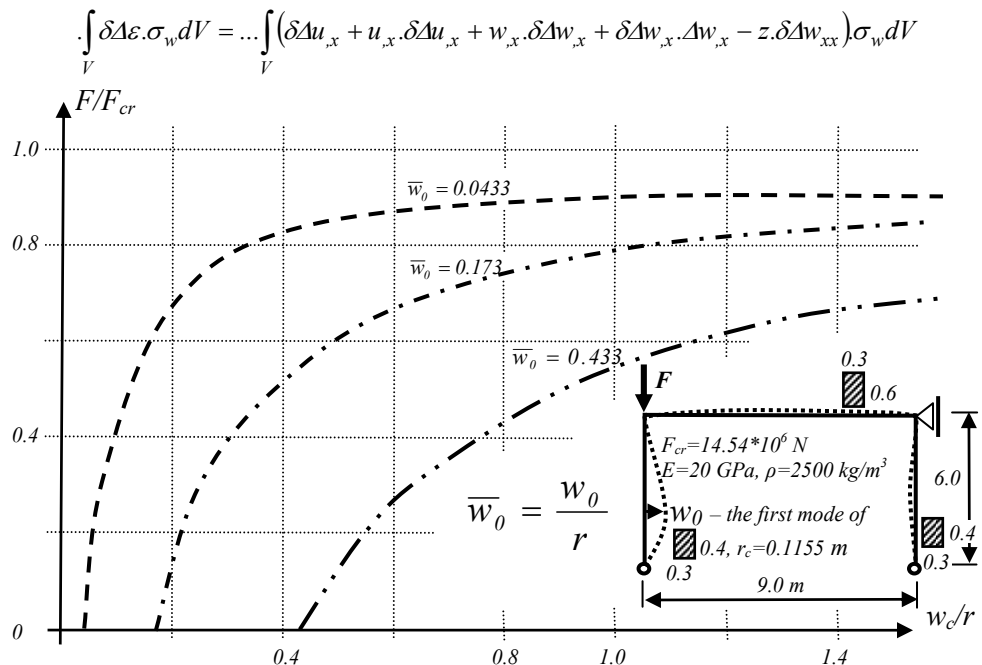


Figure 12. Load versus displacement for different values of initial displacements

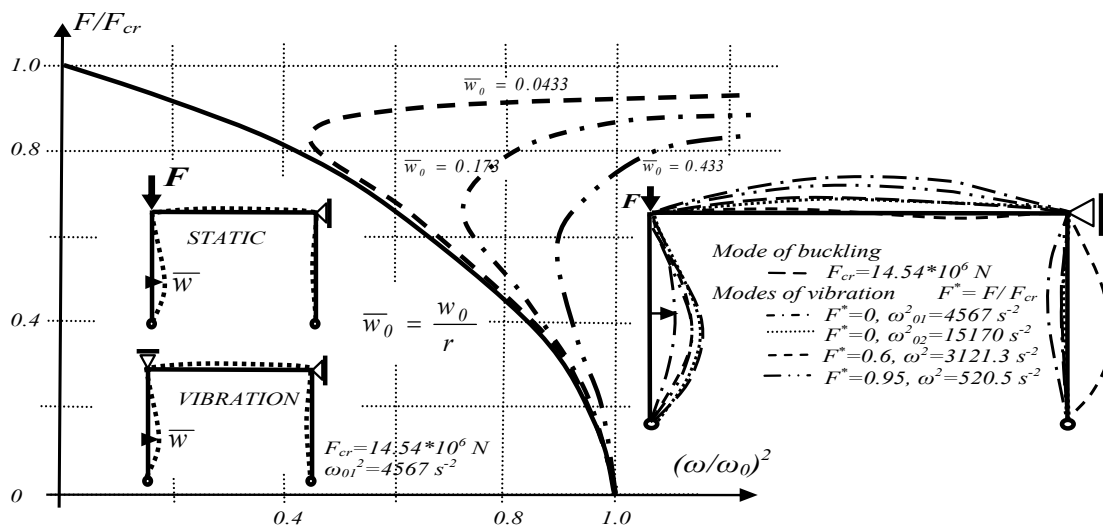


Figure 13. Influence of initial displacements on the frame vibration

3.6 Vibration and residual stresses

The residual stresses are typical in the welded steel structures, but we can ignore the residual stresses even in concrete structures, timber structures and many other structures as well. The question is if the residual stresses have any influence on the circular frequency. The situation is much different in the beam type structures in comparison to the plate structures.

The residual stresses have been mentioned in Eq.(5). In the case of the beam structures, this equation will be reduced

$$\sigma_x = E \cdot (\varepsilon_x - \varepsilon_{0,x}) + \sigma_w$$

The residual stresses produce the addition in the increment of the potential energy

In the case of the beam type of structures, the volume integration can be changed into the integration over the cross section and the integration over the length.

$$\int_V dV = \int_0^a \left(\int_A (\delta \Delta u_{,x} + u_{,x} \cdot \delta \Delta u_{,x} + w_{,x} \cdot \delta \Delta w_{,x} + \delta \Delta w_{,x} \cdot \Delta w_{,x} - z \cdot \delta \Delta w_{xx}) \sigma_w dA \right) dx =$$

All the derivations and the variations of the displacements functions are not any function of the cross section.

$$\int_0^a \left(\int_A (\delta \Delta u_{,x} + u_{,x} \cdot \delta \Delta u_{,x} + w_{,x} \cdot \delta \Delta w_{,x} + \delta \Delta w_{,x} \cdot \Delta w_{,x}) \int_A \sigma_w dA - \delta \Delta w_{xx} \int_A z \cdot \sigma_w dA \right) dx =$$

The residual stresses must be in equilibrium in the given cross section

$$\begin{aligned} \int_A \sigma_w dA &= 0, \quad \int_A z \cdot \sigma_w dA = 0 \quad \Rightarrow \\ \dots \int_V \delta \Delta \varepsilon \cdot \sigma_w dV &= 0 \end{aligned} \quad (48)$$

It is evident that **the residual stresses in the case of the beam structures have no influence on the circular frequency**.

Note. In the case of the statically indeterminate structure, Eq. (48) is not valid and the residual stresses could have the influence on the vibration.

There is much different situation in the case of the plate structures. In this case, the volume integration is divided into the integration over the thickness and the integration over the neutral surface. The integration of the residual stresses over the thickness is not zero and thus,

$$\int_V \delta \Delta \varepsilon \cdot \sigma_w dV = \int_{\Gamma} \left(\int_{-t/2}^{t/2} \delta \Delta \varepsilon \cdot \sigma_w dz \right) d\Gamma = \int_{\Gamma} \left(\delta \Delta \varepsilon \int_{-t/2}^{t/2} \sigma_w dz \right) d\Gamma \neq 0$$

Finally, **in the case of the plate structures, the residual stresses have an influence on the circular frequency**.

Expanding the example from Part 2.2 we can get the result for the square of the circular frequency of the square slender web loaded in compression

$$\omega^2 = \omega_0^2 \cdot (I - \bar{\sigma} + K(3\bar{\alpha}^2 - \bar{\alpha}_0^2)) \quad (49)$$

where $\omega_0^2 = \frac{\pi^4 Et^2}{3b^4(I-\nu^2)\rho}$ is the square of the circular frequency of a simply supported slender web and $K = 3(I-\nu^2)/8 = 0.34125$ (for $\nu=0.3$).

$$\int_A \left(\int_A (\delta \Delta u_{,x} + u_{,x} \cdot \delta \Delta u_{,x} + w_{,x} \cdot \delta \Delta w_{,x} + \delta \Delta w_{,x} \cdot \Delta w_{,x}) \int_A \sigma_w dA - \delta \Delta w_{xx} \int_A z \cdot \sigma_w dA \right) dx =$$

It is evident that, in comparison to the column, the circular frequency of the slender web is influenced by the initial displacement even in the case of the moving supports.

The influence of the fixed (unmovable) supports can be solved by the use of the following functions for the increments of the in-plane displacements

$$\Delta u = S_{x2} \cdot C_{y2} \cdot \Delta \beta_2 + S_{x2} \cdot \Delta \beta_3,$$

$$\Delta v = C_{x2} \cdot S_{y2} \cdot \Delta \gamma_2 + S_{y2} \cdot \Delta \gamma_3$$

The result can be arranged in the form

$$\omega^2 = \omega_0^2 \cdot \left(I - \bar{\sigma} + \frac{21 - 12\nu - 9\nu^2}{8} \bar{\alpha}^2 - \frac{3(I-\nu^2)}{8} \bar{\alpha}_0^2 \right) \quad (50)$$

Fig. 14 shows assumptions for distribution of residual stresses in the square slender web loaded in compression. We suppose the constant residual stresses through the thickness and then the approximate circular frequency can be expressed by the equation

$$\omega^2 = \omega_0^2 \cdot (I - \bar{\sigma} - \bar{\sigma}_{xw} - \bar{\sigma}_{yw} + K(3\bar{\alpha}^2 - \bar{\alpha}_0^2)) \quad (51)$$

$$\text{where } \bar{\sigma}_{xw} = \frac{\sigma_{xw}}{\sigma_{cr}}, \bar{\sigma}_{yw} = \frac{\sigma_{yw}}{\sigma_{cr}}.$$

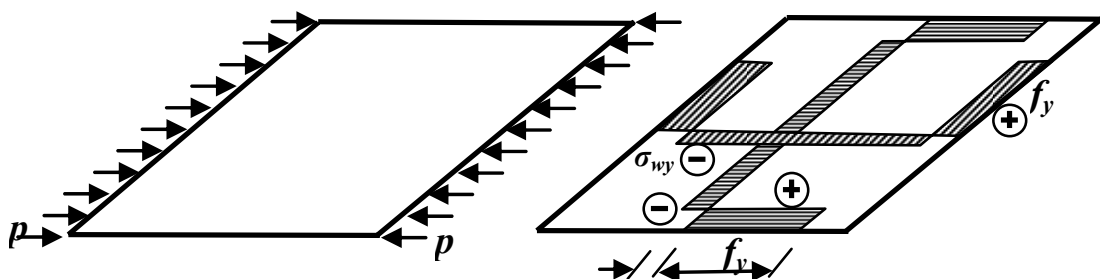


Figure 14. The distribution of the residual stresses in the slender web

One can see that residual stresses produce "shifting" of the level of the load.

Effect of residual stresses on circular frequency has been proved by experiment (Ravinger⁴). (Fig.15). Some results are presented in Figs. 16 and 17.



Figure 15. General view of experimental arrangement for the test of thin-walled panel

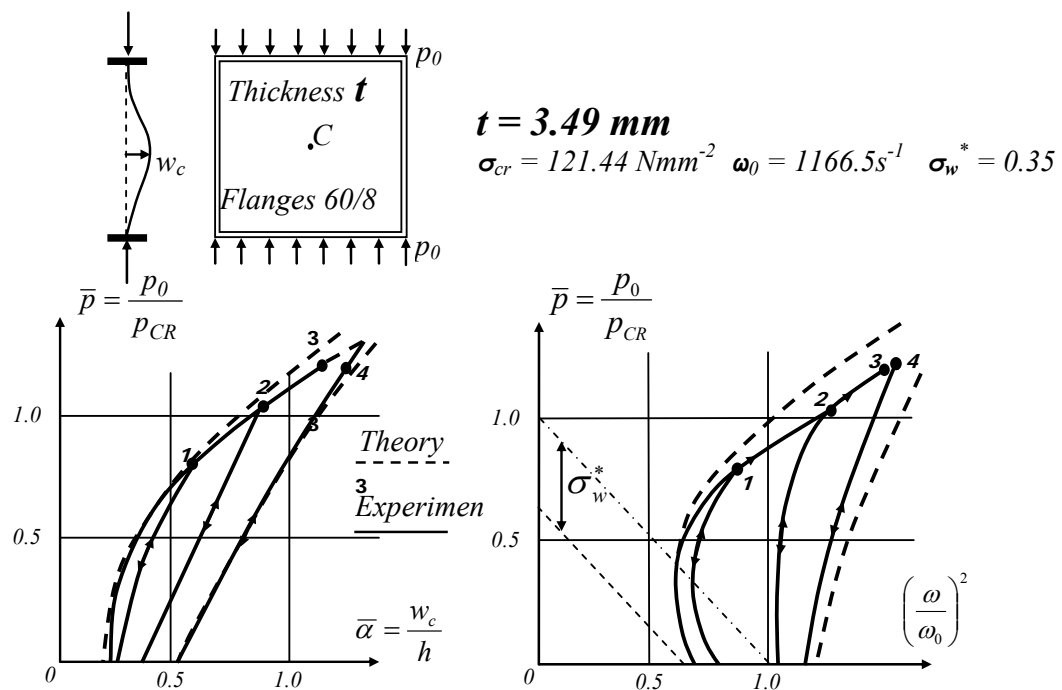


Figure 16. Comparison of theoretical and experimental results for the panel with $t=3.49$ mm thick web

$$t = 2.505 \text{ mm} \quad \sigma_{cr} = 65.95 \text{ Nmm}^{-2} \quad \omega_0 = 861.5 \text{ s}^{-1} \quad \sigma_w^* = 0.38$$

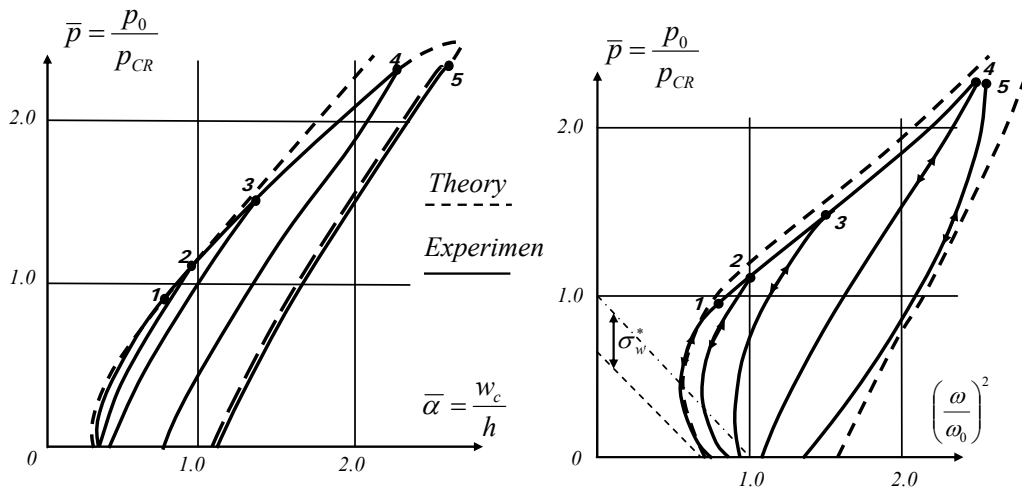


Figure 17. Comparison of theoretical and experimental results for the panel with $t=2.505 \text{ mm}$ thick web

4 CONCLUSION

The presented theory and results prove the influence of the natural frequency on the level of the load, on the geometrical imperfections and the residual stresses, too. This knowledge can be used as an inverse idea. Measuring of the natural frequencies provides a picture of the stresses and imperfections in a thin-walled structure. One idea how we can investigate the structure is presented in Fig. 18. Many times we are not able to measure the whole structure (global vibration) but even measuring local parts of structure (local vibration) can give us valuable results.

It is true that the relation of frequencies versus stresses and imperfections represents a sophisticated theory, but it is unlikely an obstacle for further investigation.

ACKNOWLEDGEMENT

This paper has been supported by Slovak Scientific Grant Agency.

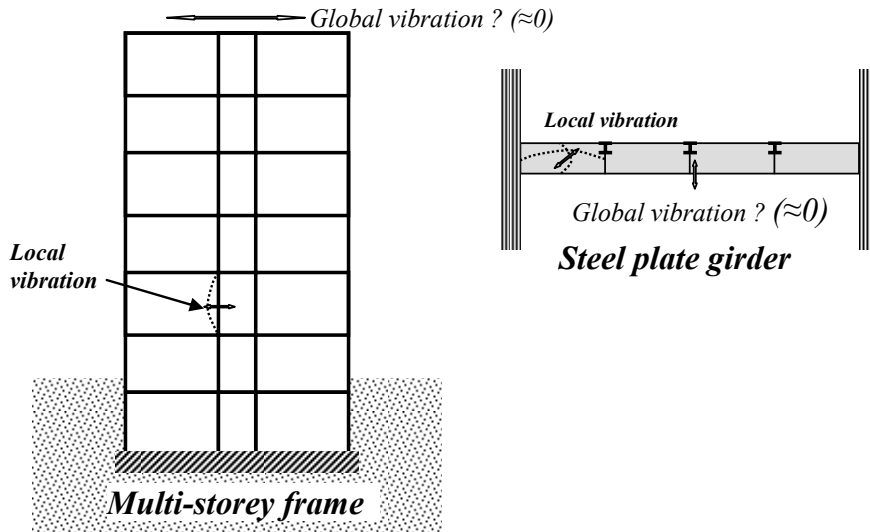


Figure 18. Scheme for non-destructive investigation of structure properties

5 REFERENCES

- [1] Bažant, Z. P. – Cedolin, L.: Stability of Structures: Elastic, Inelastic, Fracture and Damage Theories. Oxford University Press, New York, Oxford, 1991.
- [2] Bolotin, V. V.: The Dynamic Stability of Elastic System. CITL. Moscow, 1956 (In Russian. English translation by Holden Day. San Francisco, 1994.)
- [3] Burgreen, D.: Free Vibration of Pined Column with Constant Distance Between Pin-ends. *J. Appl. Mechan.*, 18, 1951. 135-139.
- [4] Ravinger, J.: Vibration of an Imperfect Thin-walled Panel. Part 1 : Theory and Illustrative Examples. Part 2: Numerical Results and Experiment. *Thin-Walled Structures*, 19, 1994, 1-36.
- [5] Ravinger, J. – Švolík, J.: Parametric Resonance of Geometrically Imperfect Slender Web. *Acta Technica CSAV*, 3, 1993, 343-356.
- [6] Ravinger, J.: Computer Programs – Static, Stability and Dynamics of Civil Engineering Structures. Alfa, Bratislava, 1990. (In Slovak)
- [7] Volmir, A.S.: Non-Linear Dynamic of Plates and Shells. Nauka. Moscow. 1972. (In Russian)

SUMMARY

STABILITY AND VIBRATION IN CIVIL ENGINEERING

Jan REVINGER

Von Kármán theory has been used for the description of the post-buckling behaviour of a thin-walled panel with imperfections and residual stresses. Using Hamilton's principle in incremental form the problem of free vibration has been established. Examples of buckling of a column, frame and a slender web loaded in compression emphasizing different types of support are presented. An influence of the mode of the geometrical imperfection is shown and an approximate solution taking into account the residual stresses is found.

Theoretical and numerical results are compared with the results from a laboratory experiment.

Key words: stability, post-buckling, vibration, finite element method, residual stresses

REZIME

STABILNOST I VIBRACIJE U GRAĐEVINARSTVU

Jan REVINGER

Teorija Von Kármán je korišćena u cilju opisivanja ponašanja tankih zidnih panela sa imperfekcijama i zaostalim naponima nakon izvijanja. Koristeći Hamiltonov princip u inkrementalnoj formi, uveden je problem slobodnih vibracija. U radu su dati primjeri izvijanja stubova, ramova i tankih ploča opterećenih na pritisak, naglašavajući različite vrste oslonaca. Dat je prikaz uticaja oblika geometrijske imperfekcije kao i približno rešenje, uzimajući u obzir zaostale napone.

Teorijski i proračunski podaci upoređeni su sa rezultatima dobijenim laboratorijskim ispitivanjem.

Ključne reči: stabilnost, stability, post-izvijanje, vibracije, metoda konačnih elemenata, zaostali naponi

MEHANIČKO NASTAVLJANJE ARMATURE

MECHANICAL REBAR SPLICING

Branko MILOSAVLJEVIĆ

STRUČNI RAD
PROFESSIONAL PAPER
UDK: 624.012.45.078.4

1 UVOD

Mehaničko nastavljanje armature, kao relativno nova tehnologija u građenju armiranobetonskih i spregnutih konstrukcija, intenzivno se razvija u poslednje dve decenije u svetu. Mnogo proizvođača, i sve širi assortiman proizvoda u vezi sa ovom tehnologijom, dovode do široke primene u građenju savremenih konstrukcija. Mehaničko nastavljanje armature preko spojnica (konektora ili kaplera), predstavlja svojevrsnu dopunu, a ne zamenu, klasičnog načina nastavljanja armature preklapanjem ili zavarivanjem. Odgovarajućom tehnološkom, ekonomskom i konstrukterskom analizom mogu se definisati mesta primene kod kojih je mehaničko nastavljanje armature bolji izbor od klasičnih načina nastavljanja.

2 VRSTE MEHANIČKIH ARMATURNIH SPOJNICA

U poslednjoj deceniji razvijeno je i patentirano mnogo različitih tipova mehaničkih spojnica. Po načinu prenošenja sile između dve nastavljene šipke armature, mehaničke spojnice mogu se podeliti u sledeće grupe [1]:

2.1 Mehaničke spojnice sa navojem

Kod ovog tipa spojnica, krajevi armaturnih šipki koje treba nastaviti se narezuju, i zatim nastavljaju uvrтанjem u spojnicu sa urezanim navojem (Slika 1). U zavisnosti od proizvođača, navozi mogu biti konični, ravni ili na proširenom delu šipke. Povoljnost koničnog navoja je mala razlika između prečnika armature i spojnice, jednostavno je pozicioniranje kraja šipke u spojnicu, uz mali ugao obrtanja za postizanje punog spoja. Za narezivanje koničnog navoja, neophodan je originalan, relativno složen

Mr Branko Milosavljević, dipl. građ. inž.
Građevinski fakultet Univerziteta u Beogradu, Bulevar kralja Aleksandra 73, Beograd, Srbija

1 INTRODUCTION

Mechanical rebar splicing, representing relatively new technology in reinforced concrete and composite structures construction is under fast development for several decades. Large number of manufacturers as well as wide assortment of products led to wider use of this technology in contemporary structures construction. Mechanical rebar splicing using couplers could be considered more as a supplement than substitution of classical rebar splicing by overlapping or welding. It is possible to determine locations and situations where mechanical rebar splicing is better solution than classical splicing, using appropriate technological, economic and structural analysis.

2 MECHANICAL COUPLER TYPES

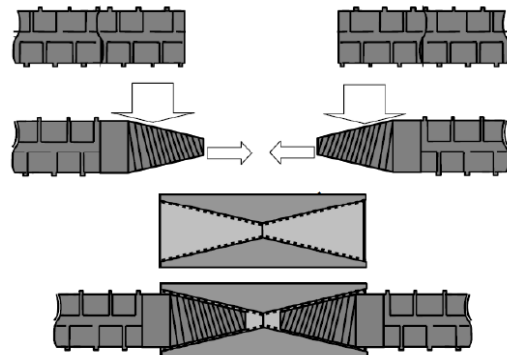
During the last decade, large number of different types of mechanical couplers were developed and patented. It is possible to classify mechanical couplers regarding the means of force transfer between two spliced bars, as follows [1]:

2.1 Threaded mechanical couplers

This type of couplers is qualified by threaded ends of reinforcing bars which are connected by crewing into the coupler with carved in threads (Figure 1). Depending on manufacturer, the threads could be conical, flat or on a thickened part of the bar. Advantage of conical threading is very small difference between coupler and bar outer diameter, as well as simple bar positioning into the coupler, with a minimum screw rotation angle to achieve full connection. Special tool is needed for conical threading

Mr Branko Milosavljevic, Civ.Eng.
University of Belgrade, Faculty of Civil Engineering, Bulevar kralja Aleksandra 73, Belgrade, Serbia

alat. Treba imati u vidu da svako narezivanje i urezivanje navoja na šipku i spojnicu utiče na konačne mehaničke karakteristike materijala, pogotovo na duktilnost i ponašanje pri cikličnom opterećenju.

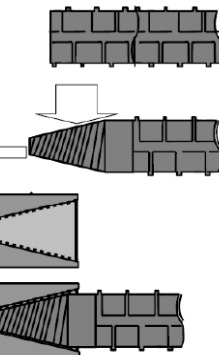


*Slika 1. Mehaničke spojnice s navojem
Figure 1. Threaded rebar couplers*

2.2 Spojnice sa ispunom cementnom ili epoxy emulzijom

Sistem spojница sa ispunom podrazumeva da se sila sa šipke prenese na ispunu, a zatim na spoljnju čauru. Spoljnja čaura ima dovoljnu dužinu da se omogući prenos sile sa šipke na ispunu prijanjanjem, a ujedno ima i funkciju utezanja ispune, čime se osigurava prenos sile sa rebara armature Šipke na ispunu. Ispuna može biti na bazi cementa, metala ili epoksi smole, i može se unositi u čauru pre ili posle postavljanja šipki. Spojnice sa ispunom mogu biti dvostrane (Slika 2), ili jednostrane, gde je čaura prethodno povezana s jednom od šipki zavarivanjem ili na drugi način.

ing of bar end. It should be noticed that every treading of a bar or coupler influences final material mechanical characteristics, specially the ductility and cyclic load behaviour.



*Slika 2. Mehaničke spojnice sa cementnom ispunom
Figure 2. Cementitious-grouted sleeve rebar-coupler*

2.3 Spojnice s deformisanom čaurom

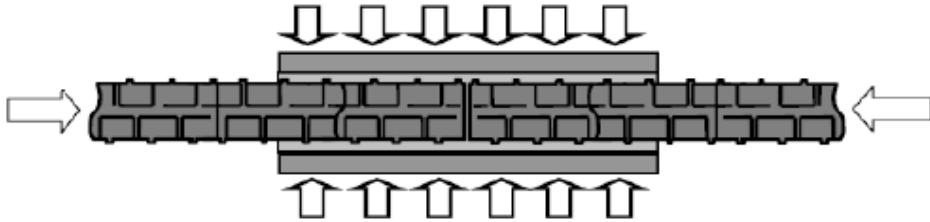
Metalna čaura se posebnim alatom plastično deformiše tako da nalegne na rebrastu armaturu i poprimi njen oblik, čime se omogućava transfer sile sa šipke na deformisanoj čauri i obrnuto (Slika 3.).

2.2 Grouted sleeve coupler

Grouted sleeve coupler system implies that the force transfers from the bar to the grout, than to the coupler sleeve. The sleeve should have sufficient length to ensure the force transfer from bar to grout by mechanical interlock, as well as to provide confinement to the grout. The grouts could be cement based, metallic, or adhesive, and it can be inserted into the sleeve before or after the positioning of the bar. Grouted sleeve couplers can be double-ended (Figure 2) or single-ended, where the sleeve is previously connected to the bar by some other mechanism.

2.3 Swaged sleeve coupler

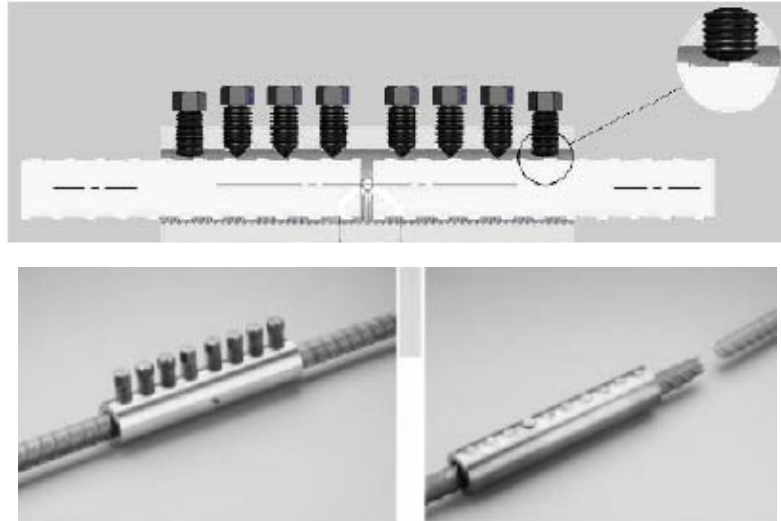
A metallic sleeve can be plastically deformed, swaged, onto the outside of a rebar, engaging the rebar's deformations and enabling load transfer from the bar to the sleeve and vice versa (Figure 3).



*Slika 3. Mehaničke spojnice s deformisanom čurom
Figure 3: Swaged-sleeve rebar-couplers*

2.4 Spojnice sa ugrađenim vijcima

Kod mehaničkih spojница sa ugrađenim vijcima, prenos sile se ostvaruje preko trenja i lokalnog moždaničkog dejstva vijka u kontaktu s površinom otrebene šipke. Po postavljanju šipke u spojnicu, posebnim alatom se priteže vijci, a zatim se odseca preostali deo vijka van gabarita čaure. Ovakva vrsta spojnice pogodna je za primenu kod sanacije i nastavljanja već građene armature, pogotovo na nedovoljno pristupačnim mestima, jer se ne zahteva obrada kraja šipke, a montaža se obavlja ručnim alatom.



*Slika 4. Mehaničke spojnice sa ugrađenim vijcima
Figure 4. Mechanical bolted rebar couplers*

3 PRIMENA MEHANIČKIH ARMATURNIH SPOJNICA

Mehaničke armaturne spojnice dizajnirane su prvenstveno za nastavljanje šipki armature u armirano-betonskim elementima. Namjenjene su za situacije kada klasični način nastavljanja armature - preklapanje i zavarivanje, nije moguće primeniti, na primer:

- kod nastavljanja armature s visokim procentima armature u preseku, i velikim profilima armature;
- kod nastavljanja maksimalno napregnute zategnute armature u elementima male širine (zidni nosači) ili malih dimenzija (zatege);
- kada, iz tehnoloških razloga, na prekidima betoniranja nije moguće prepustiti armaturu za preklop u potreboj dužini;

2.4 Bolted couplers

In case of bolted mechanical rebar couplers the forces transfer is conducted by friction and local dowel effect between the bolt and ribbed surface of the bar. After the bar placement into the coupler, special wrench is used to tighten the bolts and shear off their heads. This type of coupler is suitable for application in structural repairs and splicing of already built-in bars, especially at hard to reach places, because no previous bars end preparation is needed, and only hand tools are required.

3 THE APPLICATION OF MECHANICAL REBAR COUPLERS

The mechanical rebar coupler is designed for splicing reinforcement in concrete structural elements. They are designed for the situations where classical means of rebar splicing - by overlapping or welding are not applicable, such as:

- rebar splicing in elements with high reinforcement percentage and large rebar diameters,
- splicing of the fully loaded reinforcement in narrow structural elements (high beams) or elements with small dimensions (RC ties etc.)
- when, due to concreting technology, it is impossible to extend bars for overlapping at joints,

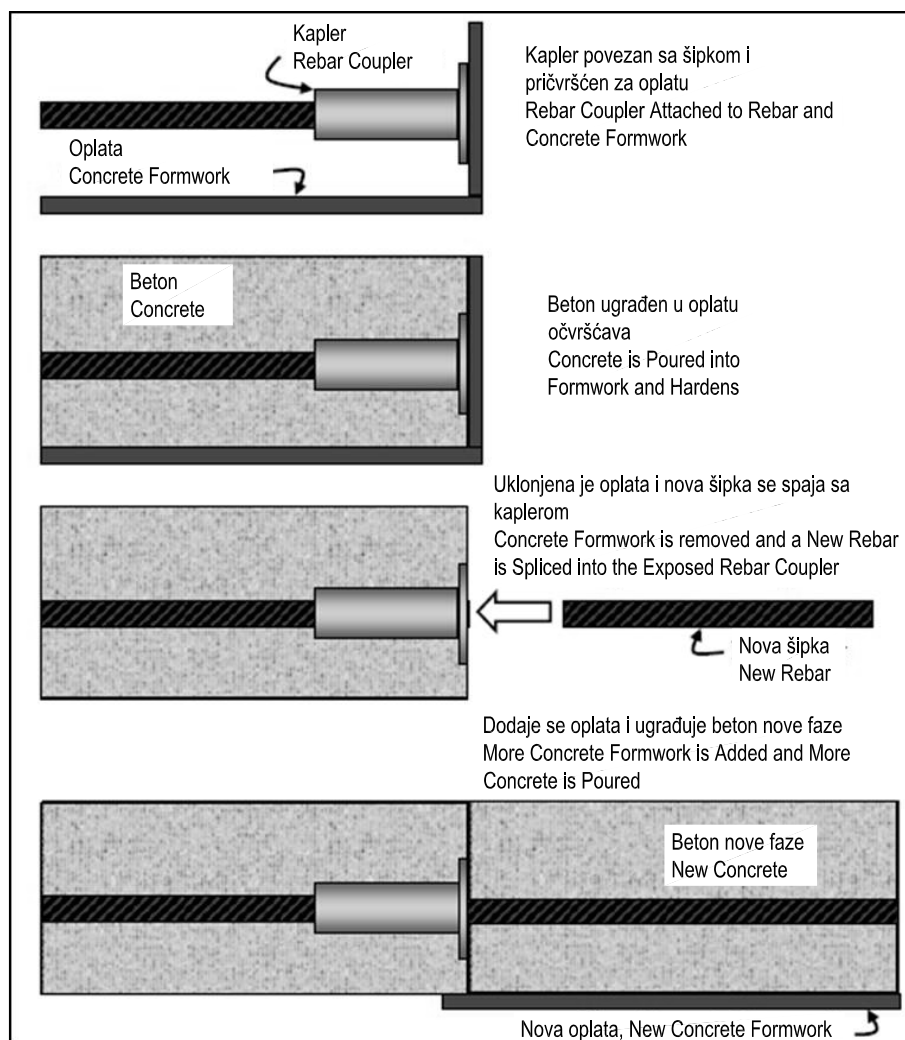
- kada je potrebno nastaviti više od 50% armature, a to propisima za nastavljanje preklapanjem nije dopušteno;
- kod specifičnih metoda građenja (na primer, metod gradnje *top-down*).

Posebna pogodnost primene mehaničkih spojница jeste mogućnost formiranja nastavaka armiranobeton-skih elemenata bez prekidanja oplate u prvoj fazi betoniranja, odnosno bez prepuštanja ankera kroz oplatu. Na taj način se omogućava upotreba velikih inventarskih komada oplate, klizne oplate i sličnog, bez njihovog oštećenja. Princip nastavljanja armature mehaničkim spojnicama kroz fazu betoniranja prikazan je na Slici 5.

- splicing of more than 50% of reinforcement in cases when such a amount of overlapping is unacceptable by relevant codes,

- in case of using specific building technologies (“*top-down*” building method, i.e.).

Particular advantage of mechanical rebar couplers use is the possibility to splice the reinforcement through construction joints without formwork interruption in the first phase of concreting, without extending the bars through the formwork. This enables the use of large formwork elements, sliding formwork, etc. without any damaging. The method of mechanical rebar splicing through construction joints is presented at Figure 5.



Slika 5. Nastavljanje armature mehaničkim spojnicam na prekidu betoniranja
Figure 5. Rebar-coupler creating continuity of reinforcing across construction joint.

Jedan od malobrojnih, ali veoma značajan primer primene mehaničkih spojница u srpskom građevinarstvu predstavlja Most preko Ade u Beogradu (Slika 6.). Pri izradi pilona korišćena je složena samopodizuća oplata. Da bi se izbeglo demontiranje oplate na mestu veze pilona sa sandučastom gredom mosta, pilon je betoniran u neprekidnom procesu, a veza sa gredom izvedena

A rare, but rather significant example of mechanical rebar couplers use in Serbian construction represents the Ada Bridge in Belgrade (Figure 6). A sophisticated self-lifting formwork was used for pylon construction. In order to avoid the formwork dismantling at the joint of the pylon and the bridge beam, pylon was continuously concreted, and afterwards connected to the beam.

naknadno. Veza armature grede i pilona izvedena je preko mehaničkih spojnica tipa LENTON, koje su prethodno ugrađene u pilon. Površina betona na pilonu, na mestu spoja s gredom mosta, posebno je projektovana sa odgovarajućim nišama, kako bi se, uz obradu površine betona na samom spoju, osigurao prenos izrazito visokih vrednosti statičkih uticaja na spoju pilona i grede, a naročito sila smicanja.

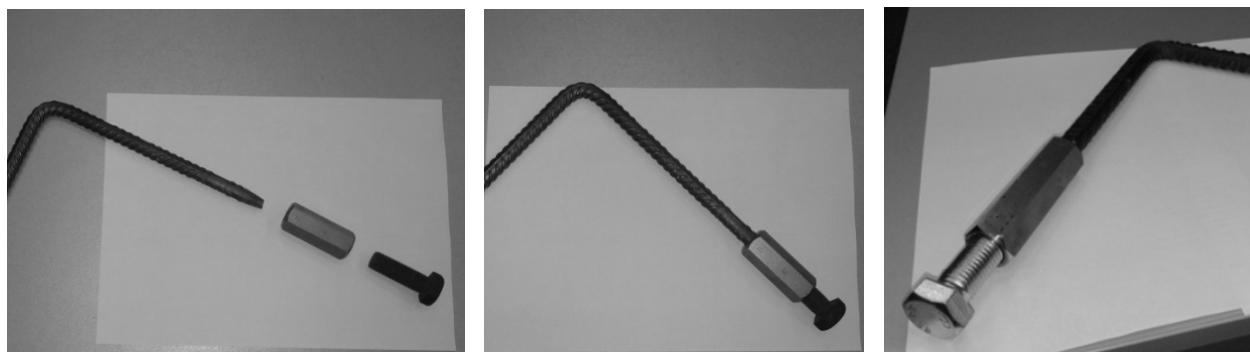
Rebar splicing was conducted using LENTON mechanical rebar couplers, previously embedded in pylon. The concrete surface at join area was specially designed, forming niches, including special surface preparation, in order to ensure the transfer of extremely large shear and other forces.



*Slika 6. Primena mehaničkih spojnica – Most preko Ade u Beogradu
Figure 6. Rebar Couplers Application – Ada Bridge in Belgrade*

Posebnu grupu mehaničkih spojnica čine spojnice za nastavljanje armaturne šipke i čeličnog završtanja (Slika 7) [6].

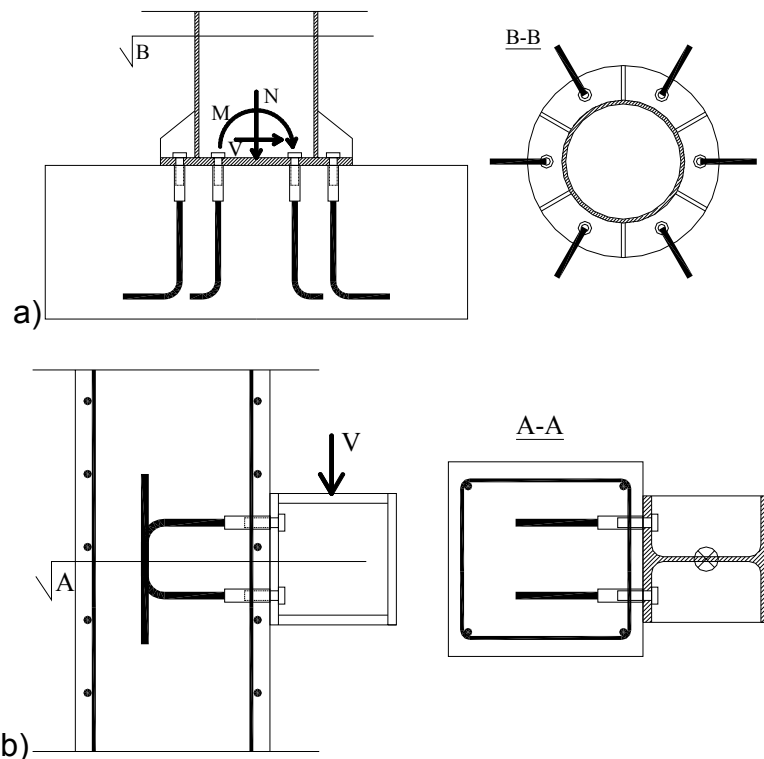
Particular mechanical rebar coupler type is the coupler designed for the connection of reinforcing bars and structural steel bolts (Figure 7) [6].



*Slika 7. Mehaničkih spojnica za zavrtnjeve
Figure 7. Rebar Bolt Couplers*

Osnovna namena ovakvih ankera jeste za vezu čeličnih stubova i armiranobetonskih temelja, kada se zavrtnji, dominantno aksijalno opterećeni usled uticaja iz stuba, sidre preko spojnice i armaturnog ankera u temelju (Slika 8 a). Ukoliko se ovakav koncept primeni na vezu čelične grede i stuba, zavrtnji i spojnice u vezi pretežno su opterećeni na smicanje (Slika 8 b).

The principal use of this coupler type is connection of steel columns and reinforced concrete foundations, where bolts, mainly axially loaded, due to the column forces, are anchored by the coupler and rebar anchor into the foundation (Figure 8a). If such a concept is applied on steel beam concrete column connection, bolts and couplers are mainly loaded in shear (Figure 8 b).



*Slika 8. Veza preko zavrtanja i mehaničke spojnice
Figure 8. Bolt-Rebar Coupler Connection*

Mogućnost primene mehaničkih spojница u okviru smičućih konektora sa čeličnim zavrtnjem relativno je slabo istražena, pogotovo za zavrtnjeve većih čvrstoća. Kod veze sa AB stubovima uobičajenih dimenzija, u zgradarstvu se javlja i problem pojave loma betona usled blizine ivice. Primena mehaničkih spojница kao elemenata smičućih konektora predstavlja predmet istraživanja u okviru šireg programa istraživanja smičućih veza u spregnutim konstrukcijama na Građevinskom fakultetu Univerziteta u Beogradu.

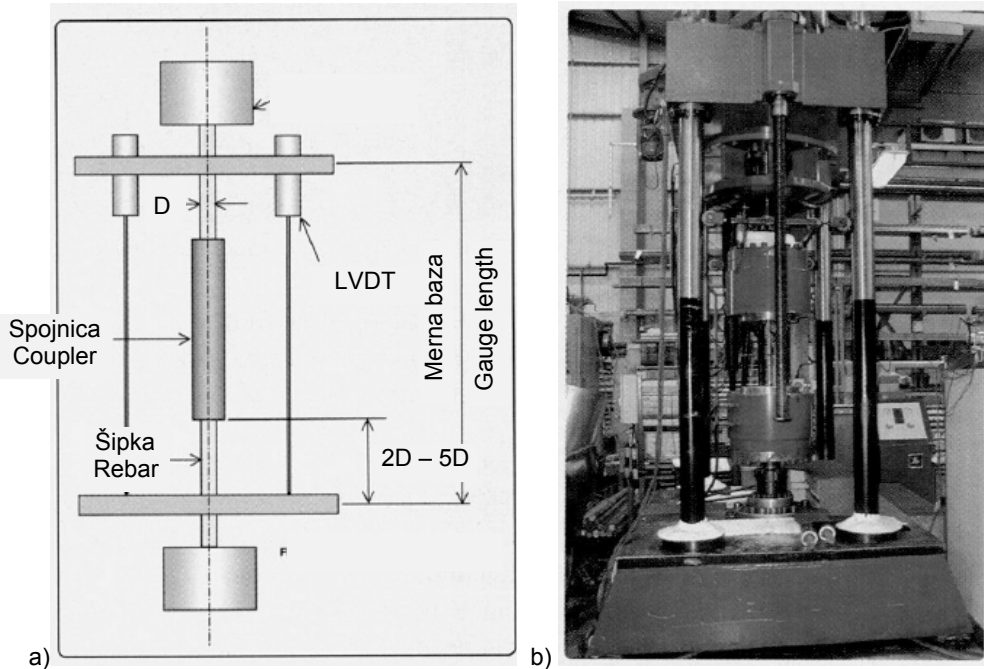
4 TEHNIČKI NORMATIVI ZA MEHANIČKO NASTAVLJANJE ARMATURE

Veoma brz i intenzivan razvoj sistema za mehaničko nastavljanje armature rezultovao je relativno velikim brojem proizvođača i komercijalnih patentiranih proizvoda. Budući da proizvođači potiču iz različitih zemalja, i postavljeni zahtevi u vezi s kvalitetom, mehaničkim karakteristikama i ponašanjem ovih spojница bili su različiti, kao i načini dokazivanja zahtevanih osobina. Ne tako davno, Fallon je ukazao na potrebu usvajanja jedinstvenog dokumenta koji bi definisao zahteve i način testiranja mehaničkih spojница. U svom radu [3] iznosi iskustva ispitivanja spojница koje proizvodi britanska firma ANCON, prikazujući tipičnu dispoziciju za ispitivanje mehaničkih spojница na staticko i dinamičko aksijalno opterećenje kao i ciklično opterećenje na zamor (Slika 9a), i aktuator koji se koristi za interna ispitivanja (Slika 9b).

The possibility of the use of mechanical couplers, as a part of bolted shear connectors, is rather poorly investigated, especially for high grade bolts. The concrete edge breakout is a problem with these connections at columns with usual cross-section dimension in common buildings. The mechanical couplers use in shear connections is one of the topics of the ongoing experimental, numerical and theoretical research of connections in composite structures at Civil Engineering Faculty of Belgrade University.

4 MECHANICAL REBAR SPLICING TECHNICAL REGULATIONS

Very fast and intensive mechanical rebar splicing system development resulted in large number of manufacturers and commercially patented products. Considering the fact that the manufacturers originate from different countries, the demands on quality, mechanical material characteristics and behaviour of these couplers were different, as well as the procedures for proving the required performance. Recently, Fallon pointed out the necessity of adopting the unified document prescribing requirements and testing procedures for mechanical rebar couplers. In his paper [3], he has presented the experience of mechanical couplers testing at British manufacturer ANCON facilities, presenting testing layout for mechanical couplers statically and dynamically axially loaded, as well as couplers cyclically tested on fatigue (Figure 9a). The actuator used for internal tests is also presented (Figure 9b).



Slika 9. Ispitivanje mehaničkih spojnica ANCON [3]
Figure 9. Mechanical couplers testing ANCON [3]

Evrokod za betonske konstrukcije propisuje, pored nastavljanja armature preklapanjem i zavarivanjem, mehaničko nastavljanje armature [2]. U međuvremenu, 2009. godine su usvojeni međunarodni standardi [4], [5], koji se odnose na nastavljanje armature mehaničkim spojnicama. U prvom delu standarda ISO 15835-1 definisani su zahtevi koje mehaničke spojnice moraju da ispunе, a u drugom delu ISO 15835-2 način ispitivanja. Propisani zahtevi za mehaničke spojnice odnose se na sledeće osobine:

Čvrstoća i duktilnost pri statičkom opterećenju: Čvrstoća mehaničkog nastavka mora biti najmanje jednaka proizvodu propisane gornje granice tečenja armature ($R_{eH,spec}$) i odnosa stvarne i propisane vrednosti napona tečenja za armaturu ($(R_m/R_{eH})_{spec}$). Ukupno izduženje pri najvećoj sili A_{gt} ne sme biti manje od 70% propisanog ukupnog izduženja pri maksimalnoj sili za armaturu, ali ne manje od 3% u absolutnom iznosu.

Proklizavanje (slip) pri statičkom opterećenju: Proklizavanje ne sme biti veće od 0,1mm.

Zamor pri cikličnom opterećenju u zoni elastičnosti: Mehanički nastavak mora da izdrži opterećenje na zamor od najmanje dva megacyklusa, sa obimom opterećenja $2\sigma_a$ od 60 MPa.

Ponašanje pri niskocikličnom opterećenju u elastoplastičnoj oblasti: Propisuje se maksimalno opterećenje i maksimalna zaostala deformacija za dva tipa niskocikličnog opterećenja kojima se modeliraju zemljotresi srednjeg i velikog intenziteta.

Sve navedene osobine mehaničkog spoja armature odnose se na aksijalno opterećenje. Treba napomenuti da ISO 15835-1 u tački 3.4 definiše mehaničke spojnice kao čaure ili narezane spojnice čija je namena da prenesu silu zatezanja ili pritiska s jedne na drugu šipku armature. Dakle, smicanje se u ovom standardu ne razmatra.

Eurocode for concrete structures allows use of mechanical splices, along with overlapping and welding [2]. In the meantime, during 2009, international standards [4] and [5], covering the area of mechanical splices was adopted. The first part of the standard ISO 15835-1 defines requirements for mechanical couplers and the second part, ISO 15835-2 defines the testing methods and procedures. Prescribed requirements for mechanical couplers relate to:

Strength and ductility under static forces: The strength of the mechanical coupler should not be less than product of specified characteristic (or nominal) yield strength value of the reinforcing ($R_{eH,spec}$) and the ratio of Specified tensile and characteristic yield strength value of the reinforcing bar ($(R_m/R_{eH})_{spec}$). Total elongation at maximum tensile force A_{gt} shall not be less than 70% of the specified characteristic value at maximum tensile force of the reinforcing bar, with a minimum value of 3%.

Slip under static forces: The total slip value measured shall not exceed 0,10 mm..

Fatigue properties under high cycle elastic loading: Mechanical splices shall sustain a fatigue loading of at least 2 megacycles with a stress range, $2\sigma_a$, of 60 MPa without failure.

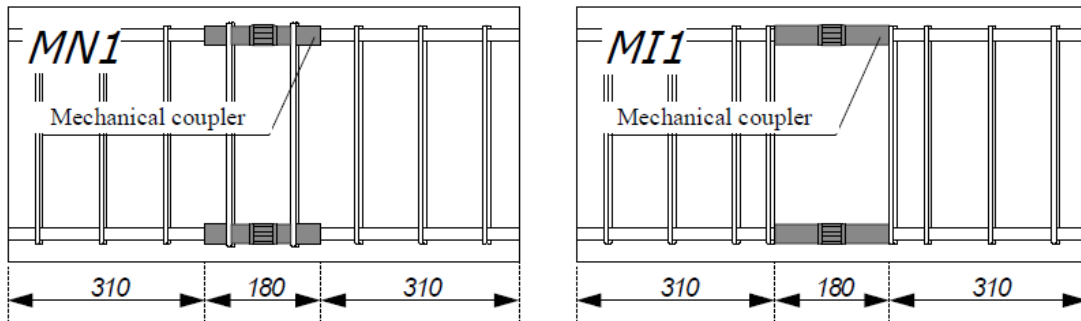
Properties under low cycle reverse elastic-plastic loading: There are two prescribed sets of low cycle fatigue requirements, one simulating moderate-scale earthquakes, and one simulating violent earthquakes.

All mechanical splice properties listed above are related to axial loading. It should be pointed out that ISO 15835-1, in paragraph 3.4, defines mechanical couplers as coupling sleeve or threaded coupler for mechanical splices of reinforcement bars for the purpose of providing transfer of axial tension and/or compression from one bar to the other. Shear is not considered.

Numerous papers are explaining mechanical rebar

U literaturi postoji relativno veliki broj radova koji objašnjavaju mehaničke nastavke armature, oblast i pogodnosti primene. Urađeno je i mnogo testova na zatezanje, uglavnom s namenom dobijanja tehničkih dopuštenja u pojedinim zemljama.

Pored radova koji se odnose na ispitivanje nosivosti i pomerljivosti armaturnih mehaničkih spojeva na zatezanje pri statičkom opterećenju, posebno treba istaći opsežno istraživanje praktično svih vrsta mehaničkih spojnica na zatezanje s kontrolisanom brzinom deformacije - sporom, srednje i velike brzine, u nameri da se utvrdi ponašanje ovih spojeva pri dinamičkom i incidentnom eksplozivnom opterećenju, gde su se najbolje pokazale spojnice s ravnim navojem (threaded rebar couplers) [7]. U radu Sanade i dr. [8] razmatran je uticaj načina poprečnog armiranja u zoni mehaničkog nastavka armature u armiranobetonskoj gredi pri visokim transverzalnim silama (Slika 10). Na slici desno je predloženi način armiranja, da bi se izbeglo pomeranje podužne armature od ivice preseka zbog nešto veće deblijine spojnice u odnosu na deblijinu šipke.



Slika 10. Poprečno armiranje u zoni mehaničkog nastavka
Figure 10. Transverse reinforcement at mechanical rebar splice

Ispitivanja su pokazala da ovakav način lokalnog pregrupisavanja poprečne armature u zoni visokih transverzalnih sila ne utiče na ponašanje armiranobetonske grede, i preporučuje ga za praktičnu primenu.

5 ZAKLJUČAK

U radu su prikazani različiti sistemi mehaničkog nastavljanja armature i definisane neke od situacija kada mehaničko nastavljanje ima prednost u odnosu na nastavljanje armature preklapanjem i zavarivanjem.

Razmatrani su novi internacionalni standardi za ispitivanje i dokaz kvaliteta sistema za mehaničko nastavljanje armature, nastali kao posledica potrebe za unificiranjem kvaliteta u ovoj oblasti koja se intenzivno razvija u svetu, s mnogim proizvođačima i varijacijama mehaničkih spojnica. Intenzivan razvoj proizvodnje, u određenoj meri, prate i istraživanja u ovoj oblasti. Predmet onih istraživanja čiji su rezultati dostupni javnosti, predstavlja ponašanje i nosivost mehaničkih spojeva pri statičkom, dinamičkom aksijalnom opterećenju, pri opterećenju koje se nanosi različitom brzinom. Istraživan je i lokalni uticaj mehaničkih spojnica na ponašanje armiranobetonskih elemenata opterećenih na smicanje. U radu je prikazan i sistem mehaničkih spojnika za povezivanje zavrtnja i armaturnog ankera, koji se

splicing in professional literature. Large number of splice tests in tensile were conducted, mostly in order to obtain the approval in different countries.

Along the papers related to testing of mechanical couplers capacity and slip under static axial loading, the extensive research of different mechanical splices types under load with controlled speed should be pointed out, conducted in order to determine the behaviour of mechanical splices under dynamic and explosion loads. Threaded rebar couplers showed best results in this research [7]. Sanada et al. [8] researched the influence of the transverse reinforcement arrangement in the zone of the mechanical rebar splice, under high shear loading (Figure 10). The right side of the picture presents the proposed way of stirrups arrangement, to avoid shifting longitudinal bars away from the section edge, due to somewhat larger diameter of the mechanical coupler.

Research results showed that the local stirrups rearrangement in the shear loaded area does not influence significantly the reinforced beam behaviour, so it is recommended for design use.

5 CONCLUSION

Different mechanical rebar splicing systems are presented, and design situations where mechanical splicing has advantage over reinforcement splicing by overlapping and welding are defined in this paper.

New international standards for testing and proof of systems for mechanical rebar splicing quality are considered. The development and publication of these standards have been initiated by the need for quality unification in this area that is developing rapidly worldwide, with large number of manufacturers and diversity of products. The intensive production development is, to some extent, followed by researching in this area. The scope of this research, available to the public, is behaviour and capacity of mechanical rebar splices under static and dynamic axial loading, and under the loading applied with different speed. The influence of the mechanical splices reinforced beam behaviour under shear load was also researched. Mechanical splicing system for rebar and bolt

može koristiti za vezu čeličnog i armiranobetonskog elementa.

Malobrojni su primeri primene mehaničkog nastavljanja armature u našoj zemlji. Jedan od značajnijih - veza pilona i grede Mosta na Adi u Beogradu - prikazan je u radu.

Može se zaključiti da intenzivan razvoj proizvodnje i primene mehaničkog nastavljanja armature u svetu, istraživanja u ovoj oblasti, kao i internacionalni standardi koji propisuju zahteve u pogledu kvaliteta i procedure dokaza kvaliteta, predstavljaju osnovu za razvoj odgovarajuće tehničke regulative u ovoj oblasti i u Srbiji. Usvajanje standarda i propisa u ovoj oblasti ubrzalo bi procedure dokaza kvaliteta i izdavanja atesta i odobrenja za pojedine sisteme mehaničkog nastavljanja armature, čime bi se proširila primena ovih sistema u svim situacijama kada oni predstavljaju bolje rešenje u odnosu na klasične načine nastavljanja armature.

connection, usable in steel and reinforced concrete structural elements connections, is presented in this paper. There are only few examples of mechanical rebar splicing in our country. The most significant one – the pylon and beam connection at Ada Bridge in Belgrade is presented in the paper.

It can be concluded that intensive development of production and use of mechanical rebar splicing systems, research in this area, as well as publication of international standards prescribing requirements for quality and procedures for proof of quality, is an excellent base for development of corresponding technical norms in Serbia. The legislation in this area would quicken proof of quality procedures, attest and approval issuing for individual products, leading to wider use of this system in all situations where it is in advantage over the classical reinforcement splicing.

6 LITERATURA REFERENCES

- [1] Brungraber G. R. Long-Term Performance of Epoxy-Bonded Rebar-Couplers. PhD thesis. University of California, San Diego 2009
- [2] EN1992-1-1: Eurocode 2 - Design of concrete structures. Part 1-1: General rules and rules for buildings. Brussels, Belgium: European Committee for Standardization (CEN); 2004.
- [3] Fallon J. Testing of reinforcing bar couplers. CONCRETE, April 2005; 24-25
- [4] ISO 15835-1:2009(E). Steels for the reinforcement of concrete - Reinforcement couplers for mechanical splices of bars. Part 1: Requirements
- [5] ISO 15835-2:2009(E). Steels for the reinforcement of concrete - Reinforcement couplers for mechanical splices of bars. Part 2: Test methods
- [6] Lenton katalog: Sustavi spajanja armature spojnicama s koničnim navojem. ERICO International Corporation 2008
- [7] Rowell S., Grey C., Woodson S., Hager K. High Strain-Rate Testing of Mechanical Couplers. Final report. Naval Facilities Engineering Service Center Port Hueneme, USA 2009
- [8] Sanada Y. Konishi D. Khanh N. Adachi T. Experimental study on intensive shear reinforcement for RC beams with mechanical couplers. fib Symposium Prague 2011. Proceedings ISBN 978-80-87158-29-6

MEHANIČKO NASTAVLJANJE ARMATURE

Branko MILOSAVLJEVIC

U radu su prikazani različiti sistemi mehaničkog nastavljanja armature i definisane neke od situacija kada mehaničko nastavljanje ima prednost u odnosu na nastavljanje armature preklapanjem i zavarivanjem. Razmatrani su novi internacionalni standardi za ispitivanje i dokaz kvaliteta sistema za mehaničko nastavljanje armature. U radu je prikazan i sistem mehaničkih spojnice za povezivanje zavrtnja i armaturnog ankera, koji se može koristiti za vezu čeličnog i armiranobetonskog elementa. Malobrojni su primeri primene mehaničkog nastavljanja armature u našoj zemlji. Jedan od značajnijih - veza pilona i grede Mosta na Adi u Beogradu - prikazan je u radu. Intenzivan razvoj proizvodnje i primene mehaničkog nastavljanja armature u svetu, istraživanja u ovoj oblasti, kao i internacionalni standardi koji propisuju zahteve u vezi s kvalitetom i procedurom dokaza kvaliteta, predstavljaju osnovu za razvoj odgovarajuće tehničke regulative u ovoj oblasti i u Srbiji, čime bi se proširila primena ovih sistema u svim situacijama kada oni predstavljaju bolje rešenje u odnosu na klasične načine nastavljanja armature.

Ključne reči: mehaničko nastavljanje armature, spojnice, testiranje, standard.

MECHANICAL REBAR SPLICING

Branko MILOSAVLJEVIC

Different mechanical rebar splicing systems are presented, and design situations where mechanical splicing has advantage over reinforcement splicing by overlapping and welding are defined in this paper. New international standards for testing and proof of systems for mechanical rebar splicing quality are considered. Mechanical splicing system for rebar and bolt connection, usable in steel and reinforced concrete structural elements connections, is presented in this paper. There are only few examples of mechanical rebar splicing in our country. The most significant one – the pylon and beam connection at Ada Bridge in Belgrade is presented in the paper. Intensive development of production and use of mechanical rebar splicing systems, research in this area, as well as the publication of international standards prescribing requirements for quality and procedures for proof of quality, represent very good base for development of the corresponding technical norms in Serbia. The legislation in this area would quicken proof of quality procedures, attest and approval issuing for individual products, leading to wider use of this system in all situations where it is in advantage over the classical reinforcement splicing.

Key words: Mechanical Rebar Splicing, Couplers, Testing, Standards

OTPORNOST MATERIJALA NA BAZI METALURŠKOG CEMENTA NA DEJSTVO KISELINA

RESISTANCE OF CEM III/B BASED MATERIALS TO ACID ATTACK

Ksenija JANKOVIĆ
Dragan BOJOVIĆ
Marko STOJANOVIĆ
Ljiljana LONČAR

ORIGINALNI NAUČNI RAD
ORIGINAL SCIENTIFIC PAPER
UDK: 666.946:620.193.4

1 UVOD

Trajnost konstrukcija veoma je važan parametar za njihovo projektovanje i izgradnju. Kada je beton izložen dejstvu kiselina prema EN 206-1 standardu, to znači da je u XA klasi izloženosti. Prema pH vrednosti, postoje tri klase: XA1, XA2 i XA3. Hemijska agresija takođe je definisana u Nacionalnom dodatku za agresivne sredine.

Otpornost betona na kiseline zavisi od: propljivosti, utvrđivanja u kojoj meri kiseline mogu da prodru u beton, alkalnosti i hemijskog sastava cementne paste [7].

Mineralni dodaci, kao što su leteći pepeo [2, 8], silikatna prašina i šljaka iz visokih peći [3, 9] poboljšavaju hemijsku otpornost zbog nižeg sadržaja CH, smanjenog odnosa Ca i Si u hidratima kalcijum silikata i fine strukture pora koju oni proizvode u betonu [2, 7, 10]. Mehanička aktivacija izazvala je dugoročno povećanje čvrstoće i unapredila sve performanse građevinskih kompozita smanjenjem hemijskih i mikrostrukturalnih nekompatibilnosti letećeg pepela [25].

Hemijska degradacija betona posledica je reakcija između sastojaka cementnog kamena, odnosno, kalcijum silikata, kalcijum aluminata, i posebno kalcijum hidroksida,

1 INTRODUCTION

Durability of structures is a very important parameter for its design and building. In the standard EN 206-1 acid attack means that concrete is in the XA exposure class. According to the pH value there are three classes: XA1, XA2 and XA3. Chemical attack is also defined in National code for aggressive environment.

Acid resistance of concrete depends on: the permeability, determination of the extent to which acids can penetrate into concrete, the alkalinity and the chemical composition of the cement paste [7].

Mineral additions, such as fly ash [2, 8], silica fume and blast-furnace slag [3, 9] improve chemical resistance because of the lower CH content, reduced Ca-to-Si ratio in calcium silicate hydrates and the refined pore structure they produce in concrete [2, 7, 10]. Mechanical activation promoted long-term strength enhancement and improved over-all performances of construction composites by minimizing the chemical and micro-structural incompatibility of fly ashes [25].

Chemical degradation of concrete is the consequence of reaction between the constituents of cement stone, i.e., calcium silicates, calcium aluminates, and

Dr Ksenija Janković, viši naučni saradnik
Institut IMS, Bulevar vojvode Mišića 43, 11 000 Beograd,
Srbija, e-mail: ksenija.jankovic@institutims.rs
Mr Dragan Bojović, dipl.inž.građ., istraživač-saradnik,
Institut IMS, Bulevar vojvode Mišića 43, 11000 Beograd,
dragan.bojovic @institutims.rs
Marko Stojanović, dipl.inž.građ., istraživač-pripravnik,
Institut IMS, Bulevar vojvode Mišića 43, 11000 Beograd,
marko.stojanovic@institutims.rs
Ljiljana Lončar, dipl.inž.građ., stručni savetnik, Institut IMS,
Bulevar vojvode Mišića 43, 11000 Beograd,
ljiljana.loncar@institutims.rs

Ksenija Janković, Ph.D., senior research associate
IMS Institute, Bul. vojvode Mišića 43, 11 000 Belgrade,
Serbia, e-mail: ksenija.jankovic@institutims.rs
Dragan Bojović, MSc, BScCE, research assistant, Institut
IMS, Bulevar vojvode Mišića 43, 11000 Beograd,
dragan.bojovic @institutims.rs
Marko Stojanović, MSc, research trainee, Institut IMS,
Bulevar vojvode Mišića 43, 11000 Beograd,
marko.stojanovic@institutims.rs
Ljiljana Lončar, BScCE, professional adviser, Institut IMS,
Bulevar vojvode Mišića 43, 11000 Beograd,
ljiljana.loncar@institutims.rs

kao i drugih sastojaka, sa određenim supstancama iz vode, rastvora zemljišta, gasova, para, i tako dalje.

Razvijen je kompjuterski model za predviđanje korozije u betonu usled agresije kiselinom [1].

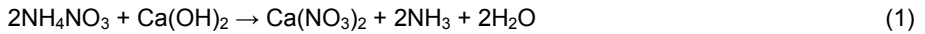
Otpornost na dejstvo mlečne i sirćetne kiseline od velikog je značaja, kako za podove u životinjskim objektima, tako i za silose [6]. Mlečna kiselina, koja se nalazi u otpadnim vodama silosa sa sirćetnom kiselinom ima veću agresivnost [2]. Degradacija cementnih materijala od strane organske kiseline ispitivana je i poređena sa sirćetnom kiselinom [13].

Sulfatna degradacija se primarno sastoji od uticaja sulfatnih jona na cementni kamen. Sulfatni ion je uzrok jedne od najopasnijih korozija, jer izaziva pojavu ekspanzivnih jedinjenja, od kojih je najvažnija etringita, $C_3A \cdot 3CaSO_4 \cdot 32H_2O$, u obliku prizmatičnih kristala [17]. Beton oštećen amonijum sulfatom, oštećen je ne samo ekspanzijom, već i omešavanjem cementnog matriksa.

Hemijske reakcije između sulfata i hidratisanih cementnih komponenti daju sledeće proizvode reakcije [14]: sekundarni gips ($CaSO_4 \cdot 2H_2O$), sekundarni etringit ($3CaO \cdot Al_2O_3 \cdot 3CaSO_4 \cdot 32H_2O$), tomasit ($CaSiO_3 \cdot CaSO_4 \cdot CaCO_3 \cdot 15H_2O$), brucit ($Mg(OH)_2$), M-S-H ($3MgO \cdot 2SiO_2 \cdot 2H_2O$) i silika gel ($SiO_2 \cdot xH_2O$).

Prema [27, 20], etringit i gips imaju ekspanzivni i destruktivni karakter, dok [22] tvrde da je doprinos gipsa ograničen, pri čemu ekspanzija etringita dominira. Formiranje tomasita dovodi do gubitka čvrstoće usled raspadanja proizvoda hidratacije koji nose čvrstoču (C-S-H) [28].

Rastvori amonijum-nitrata imaju snažan korozivni uticaj na cementne materijale [19, 23], što dovodi do raspada cementnih materijala prema sledećoj reakciji:



Amonijum-nitrat dekalcifikuje očvrsnu cementnu pastu zbog uklanjanja kalcijum-hidroksida (Eq. (1)). Ovo dovodi do dekalcifikacije i rastvaranja drugih proizvoda iz očvrsle cementne paste, kao i do smanjenja pH vrednosti. Shodno tome, čelična armatura može brzo korodirati.

Ponašanje i trajnost cementne matrice u kiseloj sredini i njen uticaj na imobilizaciju metala u procesu stabilizacije / očvršćavanja toksičnih otpada ispitano je pomoću testa Köch-Steinegger [12,16]. Ovaj test se zasniva na evaluaciji degradacije materijala u određenom medijumu prema gubitku mehaničkih osobina, posebno otpornosti na savijanje, na koju više utiče stepen degradacije nego na čvrstoću na pritisak. Uslov za otpornost na agresivne rastvore je da zatezna čvrstoća maltera nije manja od 70% u odnosu na referentne prizme negovane u vodi.

Ispitivani su malteri s različitim tipovima mešanih i sulfatno otpornih cementa u svinjcima [15]. Otpornost betona od cementa s krečnjakom [21] i cementa s letećim pepelom [26] na dejstvo sulfata pokazuje da sulfatno otporni cementi poboljšavaju hemijsku otpornost bez povećanja troškova. Mešavine se mogu klasifikovati prema svom uticaju na povećanje otpornosti na sulfate na sledeći način: mešavine s portland cementom i

above all calcium hydroxide, as well as other constituents, with certain substances from water, solutions of soil, gases, vapours, etc.

A computer model for prediction of concrete corrosion by acid attack is developed in [1].

The resistance against lactic and acetic acids has major importance, both for floors in animal buildings and silos [6]. Lactic acid, which is found in silage effluents with acetic acid presents a higher aggressiveness [2]. Degradation of cementitious materials by organic acid were investigated and compared to the acetic acid [13].

Sulphate degradation primarily consists of the impact of sulphate ions toward cement stone. The sulphate ion is the cause of one of the most dangerous corrosions, i.e. the corrosion of expansion and swelling, because it initiates the occurrence of expansive compounds, the most important one - ettringite, $C_3A \cdot 3CaSO_4 \cdot 32H_2O$, in the shape of prismatic crystals [17]. The concrete damaged by ammonium sulphate, is not only damaged by expansion, but also by softening of the cement matrix.

The chemical reactions between sulphates and hydrated cement components yield the following reaction products [14]: secondary gypsum ($CaSO_4 \cdot 2H_2O$), secondary ettringite ($3CaO \cdot Al_2O_3 \cdot 3CaSO_4 \cdot 32H_2O$), thaumasite ($CaSiO_3 \cdot CaSO_4 \cdot CaCO_3 \cdot 15H_2O$), brucite ($Mg(OH)_2$), M-S-H ($3MgO \cdot 2SiO_2 \cdot 2H_2O$) and silica gel ($SiO_2 \cdot xH_2O$).

According to [27, 20] ettringite as well as gypsum have an expansive and destructive character, while [22] claim that the contribution of gypsum is limited while the expansion of ettringite dominates. Thaumasite formation leads to strength loss due to the decomposition of the strength-forming hydration products (C-S-H) [28].

Ammonium nitrate solutions are very corrosive to cementations materials [19, 23], which leads to dissolution of cement-based materials according to the following reaction:



Ammonium nitrate decalcifies the hardened cement paste due to the removal of calcium hydroxide (Eq. (1)). This results in decalcification and dissolution of other products of hardened cement paste and leads to a reduction of the pH-value. Consequently, steel reinforcement corrosion may occur at an accelerated rate.

Behaviour and durability of cement matrices in acid media and its influence on metal immobilization in the stabilization/solidification process of toxic wastes was done using the Köch-Steinegger test [12,16]. This test is based on the evaluation of material degradation in a certain medium by its loss of mechanical properties, especially the flexural strength, which is more sensible to the degree of degradation in comparison with the compressive strength. Condition for resistance in aggressive solution means that flexural strength of mortar prisms is not less than 70 % of referent prisms cured in water.

Influence of pig slurry on mortar with different types of blended and sulphate-resistant cement was investigated [15]. Sulphate resistance of concrete with limestone cement [21] and fly ash cement [26] shows that sulphate-resistant cements improve the chemical resistance without cost increase. The mixtures could be

krečnjakom, mešavine s metalurškim cementom, mešavine s pucolanskim cementom, mešavine s metalurškim cementom i silikatnom prašinom, i mešavine s pucolanskim cementom i silikatnom prašinom [4].

Analizirajući rezultate ispitivanja maltera i betona izloženih 10% Na_2SO_4 , zaključeno je da je moguće da se dobije beton otporan na sulfatnu koroziju koristeći CEM II A-M (S-V) 42.5 N (minimalno 80% portland cementnog klinkera i do 20% dodatka zgure i silikatnog letećeg pepela). Beton s tom vrstom cementa nije otporan na rastvor amonijum-nitrita [11].

Upotreba visokog procenta zgure visokih peći (80%) smanjuje vreme nastajanja korozije uzoraka izloženih dejstvu sirčetne kiseline [18].

Značajno smanjenje degradacije betona usled kiselina zabeleženo je kod betona s metalurškim cementom [5].

Rad [24] predstavlja kritički pregled rezultata dobijenih mikroskopskim metodama.

U ovom radu je predstavljena otpornost maltera i betona s metalurškim cementom CEM III/B na koroziju uzrokovana sulfatnom, nitratnom, ureom, mlečnom i sirčetnom kiselinom. Skenirajuća elektronska mikroskopija (SEM) korišćena je da se ispita efekat agresivnih rastvora na mikrostrukturu i mehaničke osobine maltera. Za ocenu, korišćen je metod Köch-Steinegger.

2 EKSPERIMENTALNI RAD

Prikazano je ispitivanje na malteru i betonu usled uticaja pet agresivnih sredina - sulfatna, nitratna, urea, mlečna i sirčetna kiselina. Hemijska otpornost je ispitana u skladu s postupkom Koch-Steinegger.

Uzorci su napravljeni korišćenjem cementa CEM III/B 32.5 N - LH/SR (20-34% portland cementni klinker i 66-80% dodatka zgure).

Hemijski sastav cementa prikazan je u Tabeli 1.

*Tabela 1. Hemijski sastav cementa
Table 1. Chemical composition of cement*

SiO_2 (%)	31.82
Al_2O_3 (%)	7.36
Fe_2O_3 (%)	1.32
CaO (%)	44.21
MgO (%)	7.88
SO_3 (%)	2.92
S^{2-} (%)	0.42
Na_2O (%)	0.40
K_2O (%)	0.57
MnO	0.736
Gubitak žarenjem (%)	2.21
Loss on ignition (%)	
Cl^- (%)	0.014

Prizme od maltera 10x10x60 mm sastoje se od: 450 g cementa, 1350 g standardnog peska u skladu sa EN 196-1 i 200 g vode. Referentne prizme su čuvane u destilovanoj vodi. Njihova čvrstoća pri pritisku i pri savijanju data je u Tabeli 2. Pre nego što su prizme bile

classified in order of increasing sulfate resistance as follows: mixtures with Portland limestone cement, mixtures with blast furnace slag cement, mixtures with pozzolanic cement, mixtures with BFC plus SF, and mixtures with pozzolanic cement plus SF [4].

Analysing testing results of mortar and concrete exposed to 10% Na_2SO_4 it was concluded that it is possible to get concrete resistant to sulphate corrosion using CEM II A-M (S-V) 42.5 N (minimum 80% Portland cement clinker and up to 20% addition of slag and silicate fly ash). Concrete with that cement type is not resistant to ammonium nitrate solution [11].

The use of high percentage of blast-furnace slag (80%) decreases the time to initiate the corrosion for specimen subjected to acetic acid attack [18].

A significant reduction of acid deterioration was recorded for blast-furnace slag concrete [5].

Paper presents critical review of results obtained with microscopic methods [24].

The resistance to corrosion caused by sulphate, nitrate, carbamide, lactic and acetic acid on mortar and concrete with CEM III/B was presented. Optical and scanning electron microscopy (SEM) was used to examine the effect of aggressive solutions on the microstructure and mechanical properties of mortar. The results of the durability using the Köch-Steinegger method have been presented in this paper.

2 EXPERIMENTAL WORK

Testing the influence of five aggressive solutions - sulphate, nitrate, carbamide, lactic and acetic acid on mortar and concrete were presented. The chemical resistance was tested according to the Koch-Steinegger method.

The specimens were made by using cement CEM III/B 32.5 N - LH/SR (20 - 34 % Portland cement clinker and 66-80% additions of slag). The chemical composition of cement is shown in Table 1.

Mortar prisms 10x10x60 mm consist of: 450 g cement, 1350g standard sand according to EN 196-1 and 200g water. Referent prisms were stored in distilled water. Its compressive and flexural strength is given in the Table 2. Before the prisms were exposed to

izložene agresivnim rastvorima, negovane su jedan dan u kalupu i 27 dana u vodi. Testiran je uticaj 10% rastvora Na_2SO_4 , 2% rastvora NH_4NO_3 , 10% uree, 5% rastvora mlečne kiseline i 2% rastvora sirčetne kiseline na malter. Čvrstoća pri pritisku i čvrstoća pri savijanju određena je posle 28 i 56 dana čuvanja u agresivnim rastvorima.

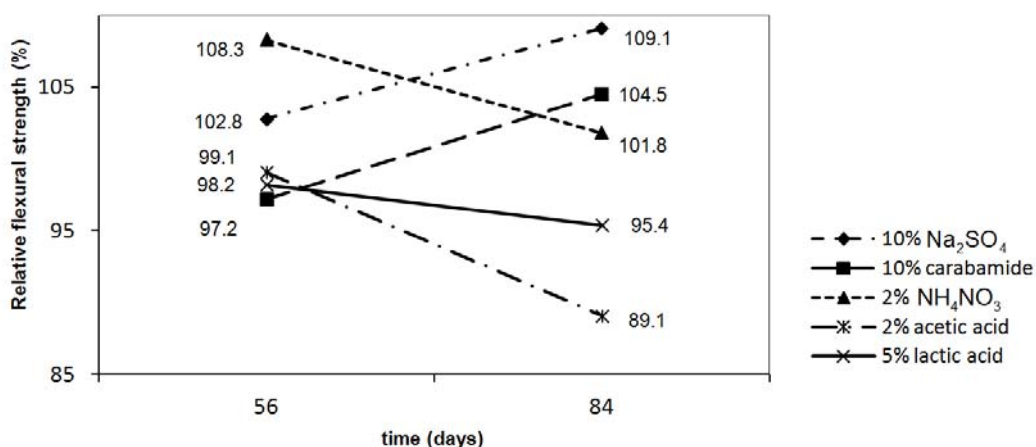
Na Slici 1-2, prikazani su rezultati ispitivanja kao prosečna vrednost od tri ispitana uzorka.

aggressive solutions, they were cured 1 day in the mould and 27 days in water. The influence of the 10 % Na_2SO_4 solution, 2 % NH_4NO_3 solution, 10% carbamide, 5% lactic acid solution and 2% acetic acid solution were tested. Compressive and flexural strength were determined after 28 and 56 days of storage in the aggressive solution.

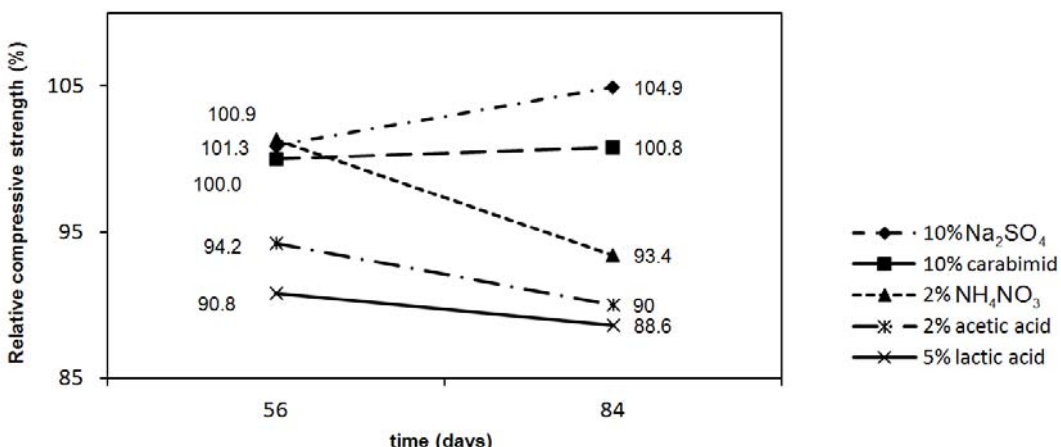
The results, as an average value of three specimens, are given in the Figures 1-2.

Tabela 2. Pritisna i savojna čvrstoća referentnog maltera
Table 2. Compressive and flexural strength of referent mortar

Vreme (dani) Time (days)	28	56	84
Čvrstoća pri pritisku (MPa) Compressive strength (MPa)	38.4	44.5	47.2
Čvrstoća pri savijanju (MPa) Flexural strength (MPa)	10.8	10.9	11



Slika 1. Relativna čvrstoća pri savijanju maltera u odnosu na vreme odležavanja u agresivnom rastvoru
Figure 1. Relative flexural strength of mortar vs. time in aggressive solution

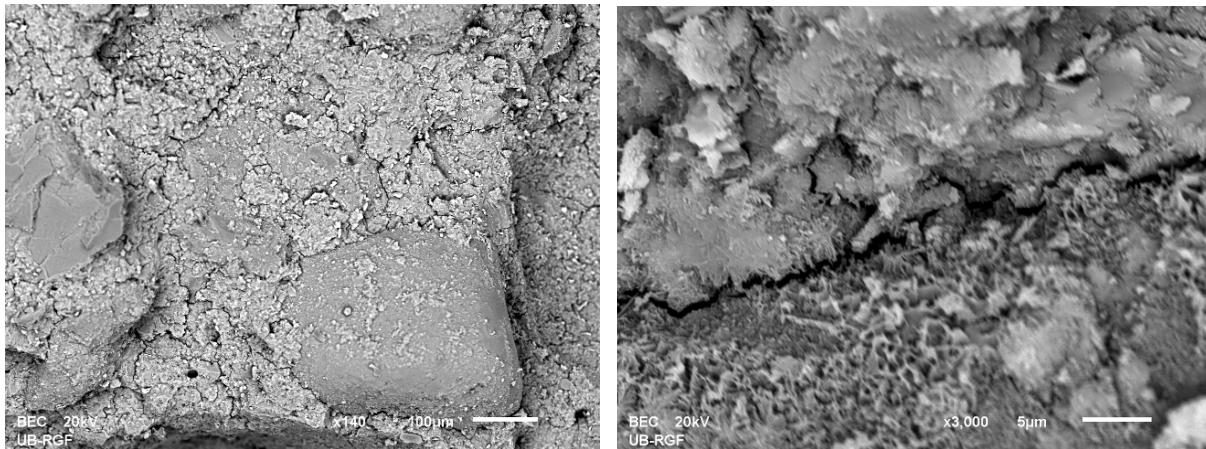


Slika 2. Relativna čvrstoća pri pritisku maltera u odnosu na vreme čuvanja u agresivnom rastvoru
Figure 2. Relative compressive strength of mortar vs. time in aggressive solution

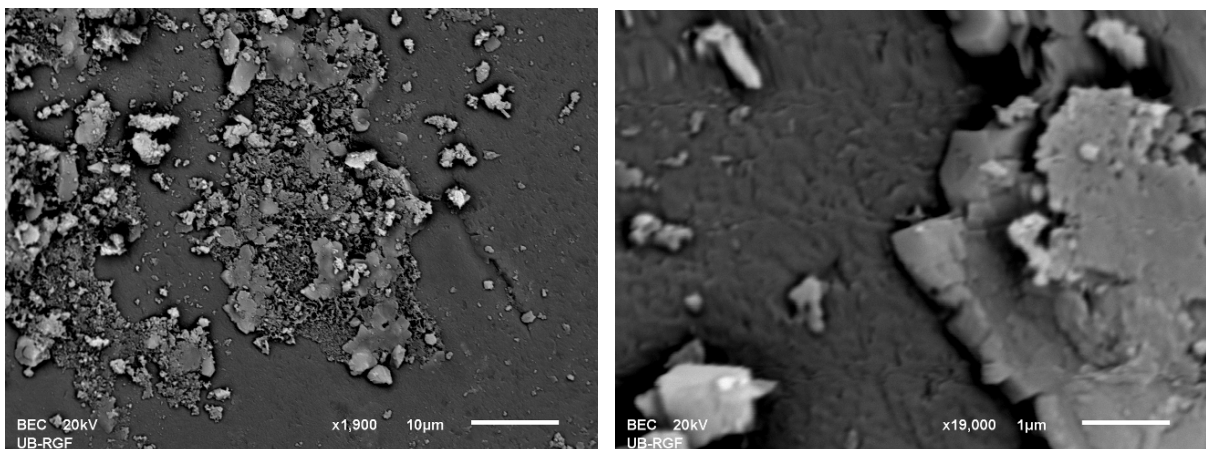
Smanjena čvrstoća pri savijanju uočena je kod uzoraka koji su čuvani u mlečnoj i sirčetnoj kiselini. Skenirajuća elektronska mikroskopija (SEM) korišćena je da se ispiša efekat agresivnih rastvora na mikrostrukturu i mehaničke osobine maltera. Tranzitna zona kvarcnog

Decrease of flexural strength was seen on specimens' immersion in lactic and acetic acid solutions. Optical and scanning electron microscopy (SEM) was used to show the effect of those aggressive solutions on the microstructure and mechanical properties of

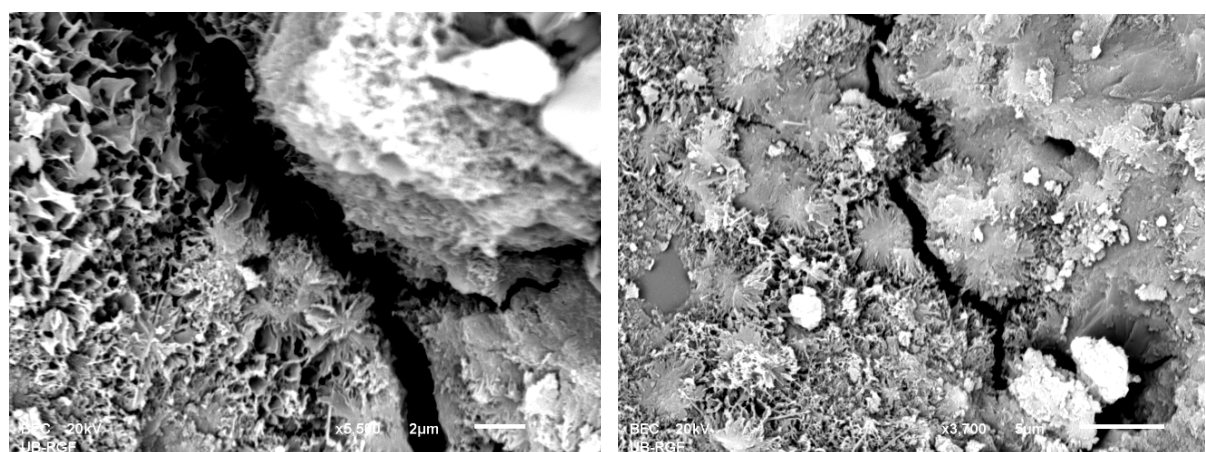
peska i C-S-H faze kod referentnog maltera prikazana je na Slici 3. Uzorci izloženi 2% rastvoru sirčetne kiseline prikazani su na Slici 4. Uzorci izloženi 5% rastvoru mlečne kiseline prikazani su na Slici 5.



Slika 3. SEM slika – Tranzitna zona kvarcnog peska i C-S-H faze
Figure 3. SEM image - Transition zone between quartz grain and C-S-H phase



Slika 4. SEM slika – Uzorci izloženi 2% rastvoru sirčetne kiseline
Figure 4. SEM image - Specimens exposed to 2% acetic acid solution



Slika 5. SEM slika - Uzorci izloženi 5% rastvoru mlečne kiseline
Figure 5. SEM image - Specimens exposed to 5 % lactic acid solution

mortar. Transition zone between quartz grain and C-S-H phase on referent mortar is shown on Figure 3. Specimens exposed to 2% acetic acid solution are shown on Figures 4. Specimens exposed to 5 % lactic acid solution are shown on Figures 5.

U drugoj fazi ispitivane su dve vrste betona. Uzorci su napravljeni sa istim cementom kao malter - CEM III / B 32,5 N - LH / SR, prirodnji agregat ($D_{max} = 16$ mm) iz reke Morave u Srbiji, superplastifikator (0,8%) i voda. Informacije o sastavu betona prikazane su u Tabeli 3. Količine komponentnih materijala usvojene su za dobijanje betona iste konzistencije.

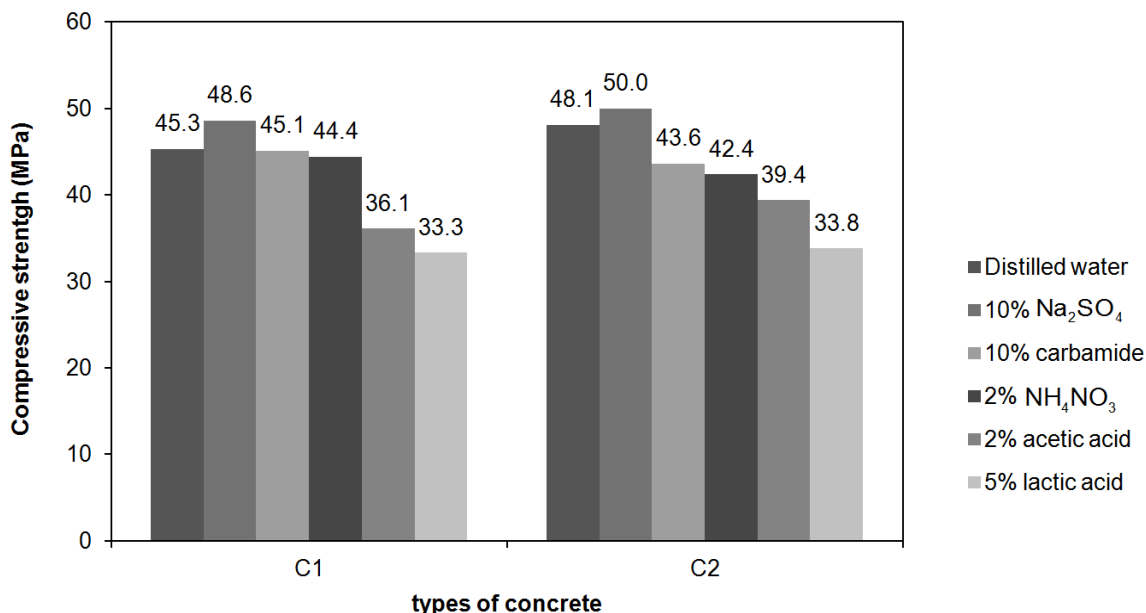
*Tabela 3. Količine komponentnih materijala betona
Table 3. Quantities of component materials of concrete*

Vrsta betona Type of concrete	C1	C2
Cement (kg/m ³) Cement (kg/m ³)	390	420
Agregat (kg/m ³) Aggregate (kg/m ³)	1830	1813
Voda (kg/m ³) Water (kg/m ³)	147	147
Dodatak (kg/m ³) Admixture (kg/m ³)	3,1	3,4

Pre nego što su kocke $7 \times 7 \times 7$ cm (minimalna dimenzija uzorka veća od $4 \times D_{max}$) bile izložene agresivnim rastvorima, negovane su jedan dan u kalupu i 27 dana u vodi. Čvrstoća uzorka pri pritisku ispitivana je nakon 28 i 84 dana (56 dana odležavanja u agresivnim rastvorima i referentnog betona u vodi). Na Slici 6 prikazani su rezultati ispitivanja kao prosečne vrednosti od tri uzorka.

In the second phase two types of concrete were tested. The specimens were made with the same cement as mortar – CEM III/B 32.5 N – LH/SR, natural aggregate ($D_{max}=16$ mm) from river Morava, Serbia, super plasticizer (0.8%) and water. Information about composition of concrete is shown in Table 3. Amounts of component materials were adopted to obtain concrete with the same consistency.

Before the cubes $7 \times 7 \times 7$ cm (minimum specimen dimension greater than $4 \cdot D_{max}$) were exposed to aggressive solutions, they were cured 1 day in the mould and 27 days in water. Compressive strength of specimens was tested after 28, and 84 days (56 days of storage in the aggressive solutions and referent concrete in water). The results, as an average value of three specimens, are given in the Figure 6.



*Slika 6. Čvrstoća betona pri pritisku nakon 84 dana
Figure 6. Compressive strength of concrete after 84 days*

Relativna čvrstoća pri pritisku prikazana je u Tabeli 4.

Relative compressive strength is shown in the Table 4.

Tabela 4. Relativna čvrstoća betona pri pritisku posle 56 dana u agresivnom rastvoru
Table 4. Relative compressive strength of concrete after 56 days in aggressive solution

Relativna čvrstoća pri pritisku (%) Relative compressive strength (%)	10% Na ₂ SO ₄	2% NH ₄ NO ₃	10% karbamid - urea 10% carbamide	5% rastvora mlečne kiseline 5% lactic acid solution	2% sirčetne kiseline 2% acetic acid
C1	107.3	98.0	99.6	73.5	79.7
C2	104.0	88.1	90.6	70.3	81.9

3 DISKUSIJA I ZAKLJUČAK

Posle 56 dana odležavanja prizmi od maltera u 10% rastvoru Na₂SO₄, čvrstoća pri savijanju prizmi je bila 9,1% veća nego kod kontrolnih uzoraka, dok je čvrstoća prizmi pri pritisku dostigla 104,9% vrednosti referentnih uzoraka negovanih u vodi. Posle 56 dana u 10% rastvoru uree, čvrstoća prizmi od maltera pri savijanju bila je 4,5% veća, ali je čvrstoća pri pritisku bila ista kao i kod kontrolnih uzoraka. Treći agresivan rastvor - 2% NH₄NO₃ veoma je korozivan za cementne materijale, ali je čvrstoća pri savijanju uzoraka koji su negovani 56 dana u njoj bila 1,8% veća nego kod referentnih uzoraka. Čvrstoća pri pritisku smanjena je za 6,6%. Sledеći agresivan rastvor - 2% sirčetne kiseline takođe je veoma korozivan za cementne materijale. Čvrstoća pri savijanju uzoraka koji su odležali 56 dana u tom rastvoru bila je manja za 10,9%. Čvrstoća pri pritisku dostigla je 90,0% vrednosti kontrolnih uzoraka. Rezultati ispitivanja uzoraka koji su odležali u 5% rastvoru mlečne kiseline su sledeći: nakon 56 dana u agresivnom rastvoru imali su smanjenu čvrstoću pri savijanju za 4,6%, a čvrstoća pri pritisku bila je 88,6% referentnog maltera.

Analizirajući rezultate čvrstoće pri savijanju prizmi napravljenih od maltera koje su izložene agresivnim rastvorima i kontrolnih uzoraka koji su negovani u vodi, može se zaključiti da je CEM III / B 32,5 N - LH / SR otporan na uticaj svih rastvora kojima su tretirani, jer je po Koch-Steinegger metodici uslov za otpornost na agresivne rastvore taj da čvrstoća pri savijanju prizmi od maltera treba da bude manja od 70% vrednosti za referentne prizme negovane u vodi.

Upoređujući rezultate čvrstoće pri pritisku betona napravljenih sa istim cementom, može se uočiti da uzorci, nakon 56 dana potapanja u rastvor sulfata, nitrata, uree, mlečne i sirčetne kiseline, imaju čvrstoću pri pritisku veću od 70% vrednosti referentnih uzoraka koji su negovani u vodi. Pokazano je da su mlečna i sirčetna kiselina veoma agresivni rastvori. Čvrstoća pri pritisku betona C1 izloženog 5% rastvoru mlečne kiseline dostigao je 73,5% vrednosti referentnog betona, dok je beton C2 negovan u istom rastvoru imao 70,3% čvrstoće uzoraka negovanih u vodi. Čvrstoća pri pritisku betona koji je odležao 56 dana u 2% rastvoru sirčetne kiseline smanjen je za oko 20% u odnosu na kontrolne uzorce betona negovanih u vodi.

Analizirajući rezultate ispitivanja maltera i betona izloženih sledećim rastvorima: 10% Na₂SO₄, 2% NH₄NO₃, 10% uree, 5% mlečne kiseline i 2% sirčetne

3 DISCUSSION AND CONCLUSION

After the 56 days in the 10 % Na₂SO₄ solution flexural strength of mortar prisms was 9.1 % greater than control specimens while compressive strength had 104.9 % value of referent specimens cured in water. After 56 days in 10% carbamide solution, flexural strength of mortar prisms was 4.5 % greater but compressive strength was at the same level as for control specimens. The third aggressive solution – 2 % NH₄NO₃ is very corrosive to cementations materials but flexural strength of the specimens cured 56 days in it was 1.8 % greater than referent. The compressive strength was reduced 6.6 %. The next aggressive solution – 2% acetic acid is also very corrosive to cementations materials. Flexural strength of the specimens cured 56 days in that solution was reduced 10.9%. Compressive strength reached 90.0 % of control specimens. Results of testing specimens' immersion in 5% lactic acid solution were: after 56 days in aggressive solution the flexural strength decreased 4.6 % and compressive strength was 88.6 % of referent mortar.

Analyzing flexural strength of mortar prisms exposed to aggressive solutions and control specimens stored in water, it can be concluded that CEM III/B 32.5 N – LH/SR is resistant to the influence of all treated solutions because the condition for resistance in aggressive solution is that the flexural strength of mortar prisms should be no less than 70 % of referent prisms cured in water according to Köch-Steinegger method.

When comparing the results of the compressive strength of concrete made with the same cement it can be seen that specimens, after 56 days immersion in sulphate, nitrate, carbamide, lactic and acetic acid, have more than 70% value of referent specimens cured in water. It was shown that lactic acid and acetic acid are very aggressive solutions. The compressive strength of concrete C1 exposed to 5% lactic acid solution reached 73.5 % of referent concrete, while concrete C2 cured in the same solution had 70.3 % of strength of the specimens cured in water. The compressive strength of concrete immersed 56 days in 2% acetic acid solution decreased about 20 % compared to control concrete cured in water.

Analysing the testing results of mortar and concrete exposed to 10% Na₂SO₄, 2% NH₄NO₃, 10% carbamide, 5% lactic acid and 2% acetic acid solution, it can be concluded that it is possible to get concrete resistant to that type of chemical corrosion using CEM III/B 32.5 N –

kiseline, može se zaključiti da je moguće dobiti beton otporan na taj tip hemijske korozije koristeći CEM III / B 32,5 N - LH / SR. Ovi rezultati se podudaraju sa istraživanjima uticaja zgure iz visoke peći na otpornost betona na organske kiseline ili dejstva sulfata [5].

ZAHVALNOST

U radu je prikazan deo istraživanja koje je pomoglo Ministarstvo za nauku i tehnološki razvoj Republike Srbije u okviru tehnološkog projekta TR 36017 pod nazivom: „Istraživanje mogućnosti primene otpadnih i recikliranih materijala u betonskim kompozitima, sa ocenom uticaja na životnu sredinu, u cilju promocije održivog građevinarstva u Srbiji”.

4 LITERATURA REFERENCE

- [1] Beddoe, R. E., Dorner, H. W., Modelling acid attack on concrete: Part I. The essential mechanisms, *Cement and Concrete Research*, 35, (2005), 2333–2339
- [2] Bertron, A., Duchesne, J., Escadeillas, G., Attack of cement pastes exposed to organic acids in manure, *Cement and Concrete Composites*, 27, (2005), 898–909
- [3] Bertron, A., Escadeillas, G., Duchesne, J., Cement pastes alteration by liquid manure organic acids: chemical and mineralogical characterization, *Cement and Concrete Research*, 34, (2004), 1823–1835
- [4] Girardi, F., Vaona, W., Di Maggio, R., Resistance of different types of concretes to cyclic sulfuric acid and sodium sulfate attack, *Cement & Concrete Composites*, 32, (2010), 595–602
- [5] Gruyaert, E., Van den Heede, P., Maes, M., De Belie, N., Investigation of the influence of blast-furnace slag on the resistance of concrete against organic acid or sulphate attack by means of accelerated degradation tests *Cement and Concrete Research*, 42, (2012), 173–185
- [6] De Belie N., Lenehan, J. J., Braam, C. R., Svennerstedt, B., Richardson, M., Sonck, B., Durability of Building Materials and Components in the Agricultural Environment, Part III: Concrete Structures, *Journal of Agricultural Engineering Research*, 76, (2000), 3–16
- [7] De Belie, N., De Coster, V., Van Nieuwenburg, D., Use of fly ash or silica fume to increase the resistance of concrete to feed acids, *Magazine of Concrete Research*, 49, (1997), 337–344
- [8] De Belie, N., De Bruyckere, M., Van Nieuwenburg, D., De Blaere, B., Attack of concrete floors in pig houses by feed acids: influence of fly ash addition and cement-bound surface layers, *Journal of Agricultural Engineering Research*, 68, (1997), 101–108
- [9] De Belie, N., Verschoore, R., Van Nieuwenburg, D., Resistance of concrete with limestone sand or polymer additions to feed acids, *Transactions of the ASAE*, 41, (1998), 227–233
- [10] Janković, K., Bojović, D., Nikolić, D., Lončar, Lj., Some Properties of Ultra High Strength Concrete”, *Građevinski materijali i konstrukcije*, Vol. 53, No. 1, Beograd, (2010), 43–51
- [11] Janković, K., Milić Lj., Stanković, S. and Šušić, N., Investigation of the mortar and concrete resistance in aggressive solutions, *Technical Gazette*, Vol. 21, No.1, (2014), 173–176
- [12] Koch, A., Steinegger, H., Ein Schnellprüfverfahren fur Zement auf ihr Verhalten bei Sulfatangriff –A rapid test method for cement behaviour under sulphate attack, *Zement-Kalk-Gips*, 7, (1960), 317–324.
- [13] Larreur-Cayol S., Bertron, A., Escadeillas, G., Degradation of cement-based materials by various organic acids in agro-industrial waste-waters, *Cement and Concrete Research*, 41 (2011), 882–892
- [14] Liu, Z. Study of the basic mechanisms of sulfate attack on cementitious materials, PhD, University of Ghent and Central South University, (2010)
- [15] Massana, J., Guerrero, A., Antoñ, R., Garcimartíñ a, M.A., Sañchez E., The aggressiveness of pig slurry to cement mortars, *Biosystems Engineering*, 114, (2013), 124–134
- [16] Macías, A., Goñi, S., Madrid, J., Limitations of Köch-Steinegger test to evaluate the durability of cement pastes in acid medium, *Cement and Concrete Research*, 29, (1999), 2005–2009
- [17] Miletic, S., Ilic, M., Ranogajec, J., Marinovic-Nedovic, R., Djuric, M., Portland ash cement degradation in ammonium-sulfate solution, *Cement and Concrete Research*, 28, (1998), 713–725
- [18] Queslati, O., Duchesne, J., The effect of SCMs on the corrosion of rebar embedded in mortars subjected to an acetic acid attack, *Cement and Concrete Research*, 42, (2012) 467–475
- [19] Pavlik, V., Corrosion of hardened cement paste by acetic and nitric acids, Part II: Formation and chemical composition of the corrosion products layer, *Cement and Concrete Research*, 24, (1994), 1495–1508

LH/SR. These results match with research of the influence of blast-furnace slag on the resistance of concrete against organic acid or sulphate attack [5].

ACKNOWLEDGMENTS

The work reported in this paper is a part of the investigation within the research project TR 36017 "Utilization of by-products and recycled waste materials in concrete composites in the scope of sustainable construction development in Serbia: investigation and environmental assessment of possible applications", supported by the Ministry for Science and Technology, Republic of Serbia. This support is gratefully acknowledged.

- [20] Santhanam, M., Cohen, M. D., Olek, J., Effects of gypsumformation on the performance of cement mortars during external sulfate attack, *Cement and Concrete Research*, 33, (2003), 325–332
- [21] Sotiriadis K., Nikolopoulou, E., Tsivilis, S., Sulfate resistance of limestone cement concrete exposed to combined chloride and sulfate environment at low temperature, *Cement & Concrete Composites*, 34 (2012), 903–910
- [22] Schmidt, T., Lotenbach, B., Romer, M., Neuenschwander, J., Scrivener, K.L., Physical and microstructural aspects of sulfate attack on ordinary and limestone blended Portland cements, *Cement and Concrete Research*, 39, (2009), 1111–1121
- [23] Schneider, U., Chen, S.W., Deterioration of high-performance concrete subjected to attack by the combination of ammonium nitrate solution and flexure stress, *Cement and Concrete Research*, 35, (2005), 1705–1713
- [24] Terzić, A., Pavlović, Lj., Radojević, Z., Primena mikroskopskih metoda u analizi mikrostrukture različitih tipova betona sa recikliranim agregatom, *Građevinski materijali i konstrukcije*, Vol. 52, No 1, (2009), 34–39
- [25] Terzić, A., Pavlović, Lj., Milićić Lj., Radojević Z., Aćimović-Pavlović Z., Svojstva vatrostalnog veziva na bazi otpadnog materijala, *Građevinski materijali i konstrukcije*, Vol. 55, No 2, (2012), 47–57
- [26] Torgal, F. P., Jalali, S., Sulphuric acid resistance of plain, polymer modified, and fly ash cement concretes, *Construction and Building Materials*, 23, (2009), 3485–3491
- [27] El-Hachem, R., Rozière, E., Grondin, F., Loukili, A., Influence of sulphate solution concentration on the performance of cementitious materials during external sulphate attack; *Concrete in Aggressive Aqueous Environments, Performance, Testing and modeling*, RILEM publications SARL, Toulouse, France, (2009)
- [28] Crammond, N., The occurence of thaumasite in modern construction – a review, *Cement and Concrete Composites*, 24, (2002), 393–402

REZIME

OTPORNOST MATERIJALA NA BAZI METALURŠKOG CEMENTA NA DEJSTVO KISELINA

Ksenija JANKOVIĆ
 Dragan BOJOVIĆ
 Marko STOJANOVIC
 Ljiljana LONČAR

Cementni materijali u poljoprivrednim i drugim industrijskim objektima izloženi su dejstvu kiselina. Zbog toga vek konstrukcija zavisi od trajnosti maltera ili betonskih elemenata u agresivnoj sredini. U radu je predstavljena otpornost na koroziju koja je uzrokovana sulfatnom, nitratnom, ureom, mlečnom i sirčetnom kiselinom. Skenirajuća elektronska mikroskopija (SEM) korišćena je da se ispita efekat agresivnih rastvora na mikrostrukturu i mehaničke osobine maltera. Hemijska otpornost prizmi od maltera i dve vrste betona testirana je prema metodi Koch-Steinegger. Kako je uslov za otpornost na agresivne rastvore taj da zatezna čvrstoća maltera nije manja od 70% u odnosu na referentne prizme negovane u vodi, može se zaključiti da su malter i beton, napravljeni sa CEM III/B, u ovom istraživanju otporni na sve kiseline kojima su tretirani.

Ključne reči: hemijska agresija, metalurški cement, Koch-Steinegger metod, trajnost

SUMMARY

RESISTANCE OF CEM III/B BASED MATERIALS TO ACID ATTACK

Ksenija JANKOVIĆ
 Dragan BOJOVIĆ
 Marko STOJANOVIC
 Ljiljana LONČAR

Cement based materials in the agricultural and other industrial structures are exposed to acid attack. That is the reason why the service life of structure depends on the durability of mortar or concrete elements in aggressive environment. Resistance to corrosion caused by sulphate, nitrate, carbamide, lactic acid and acetic acid was presented. Optical and scanning electron microscopy (SEM) was used to examine the effect of aggressive solutions on the microstructure and mechanical properties of mortar. The chemical resistance of mortar prisms and two types of concrete were tested according to the Koch-Steinegger method. As the condition for resistance in aggressive solution is that flexural strength of mortar prisms is no less than 70 % compared to referent prisms cured in water it can be concluded that mortar and concrete made with CEM III/B in this investigation are resistant to all treated acids.

Keywords: chemical aggression, CEM III/B, Koch-Steinegger method, durability

METODE ANALIZE FLATERA U FREKVENTNOM I VREMENSKOM DOMENU

FREQUENCY- AND TIME-DOMAIN METHODS RELATED TO FLUTTER INSTABILITY PROBLEM

Anina ŠARKIĆ
Miloš JOČKOVIĆ
Stanko BRČIĆ

ORIGINALNI NAUČNI RAD
ORIGINAL SCIENTIFIC PAPER
UDK: 624.21:533.6

1 UVOD

Kompleksno neustaljeno strujanje vetra oko tela obično je praćeno odvajanjem struje vetra i eventualnim ponovnim pripajanjem, što dovodi do fluktuirajućih površinskih pritisaka koji rezultuju dinamičkim silama veta. Ova vrsta opterećenja naziva se aerodinamičko opterećenje.

U principu, modeli sila (modeli opterećenja) koriste se za opisivanje efekata opterećenja vjetrom. Jedan jednostavan model opterećenja odnosi se na razmatranje nedeformabilne, fiksne konstrukcije i naziva se ustaljeni model opterećenja. Ukoliko se zanemare fluktacije izazvane turbulentijom, nastali pritisci rezultuju osrednjim silama: silom otpora duž pravca delovanja veta D , silom uzgona upravnom na pravac veta L i momenatom M . Na osnovu ovih sila, ustaljeni koeficijenti (ili koeficijenti sile) za otpor C_D , uzgon C_L i momenat C_M dobijeni su kao:

$$C_D = \frac{D}{\frac{1}{2} \rho U_\infty^2 B L_B}, \quad C_L = \frac{L}{\frac{1}{2} \rho U_\infty^2 B L_B}, \quad C_M = \frac{M}{\frac{1}{2} \rho U_\infty^2 B^2 L_B} \quad (1)$$

gde ρ predstavlja gustinu vazduha, U srednju brzinu vazduha, B i L_B su širina preseka mosta i dužina. Pošto ovi koeficijenti zavise od geometrijskog oblika preseka, najčešće se eksperimentalno određuju na osnovu standardnih testova u aerotunelu i tada su izraženi kao funkcija napadnog ugla α (slika 1). Ovi bezdimenzionalni

1 INTRODUCTION

Complex unsteady wind flow around the body which is usually followed by flow separation and eventual reattachments gives rise to fluctuating surface pressures resulting in dynamic wind forces. This kind of load is referred as aerodynamic load.

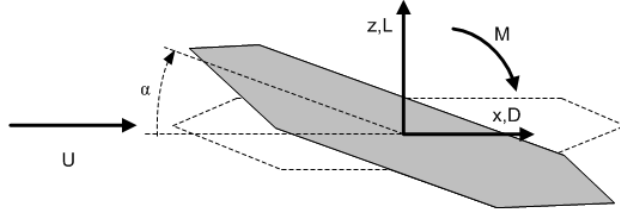
In general, force models (load models) are used to describe the loading effects from the wind. One simple load model is related to the consideration of non-deformable, fixed structure and it is called the steady load model. If the fluctuations due to the turbulence are neglected, the created pressures result in mean forces such as: along-wind drag force D , an across-wind lift force L and a pitch moment M . Based on these forces steady coefficients (or force coefficients) for drag C_D , lift C_L and moment C_M are obtained as:

where ρ represents the air density, U the mean wind velocity, B and L_B are the bridge deck width and length. Since these coefficients depend on geometrical shape of the cross-section, they are usually obtained experimentally from standard wind tunnel tests as a function of angle of attack α (Figure 1). These non-dimensional

dr Anina Šarkić, dipl.inž.građ., asistent, Građevinski fakultet, Univerzitet u Beogradu, Bulevar kralja Aleksandra 73, 11000 Beograd, anina@grf.bg.ac.rs
Miloš Jočković, msr.inž.građ., doktorand, Građevinski fakultet, Univerzitet u Beogradu, Bulevar kralja Aleksandra 73, 11000 Beograd, milosjockovic32@gmail.com
Prof. dr Stanko Brčić, dipl.inž.građ., Građevinski fakultet, Univerzitet u Beogradu, Bulevar kralja Aleksandra 73, 11000 Beograd, stanko@grf.bg.ac.rs

Anina Sarkic, Ph.D., University of Belgrade, Faculty of Civil Engineering, Boulevard of King Alexander 73, Belgrade, Serbia, anina@grf.bg.ac.rs
Milos Jockovic, M.Sc., University of Belgrade, Faculty of Civil Engineering, Boulevard of King Alexander 73, Belgrade, Serbia, milosjockovic32@gmail.com
Prof. Stanko Bracic, Ph.D., Faculty of Civil Engineering, University of Belgrade, Boulevard of King Alexander 73, 11000 Belgrade, Serbia, stanko@grf.bg.ac.rs

koeficijenti koriste se za prenos sila s modela u aerotunelu na model mosta s realnim dimenzijama koji se koristi pri projektovanju. Ovaj ustaljeni model opterećenja prikladan je za određivanje statičkih sila koje deluju na poprečni presek mosta i može se takođe nazivati i kvazištački model opterećenja.



Slika 1. Usvojena konvencija za sile od veta
Figure 1. Adopted convection for wind forces

Međutim, posmatranje potpuno nepokretne konstrukcije ne predstavlja ispravan pristup sagledavanju opterećenja od veta. Naime, fleksibilnost mostova se ne može zanemariti, pošto stvara potencijal za generisanje složene interakcije između fleksibilne konstrukcije i vetra koji je opstrujava. Mehanizam interakcije se može opisati na sledeći način. Sile nastale usled opstrujavanja vetra izazivaju pomeranja i/ili deformacije konstrukcije. Ukoliko su ta pomeranja i deformacije dovoljno veliki, oni utiču na način opstrujanja vetra oko konstrukcije i samim tim izazivaju promenu samih sila. Ova interakcija između fluida i konstrukcije se naziva aeroelastičnost i može dovesti do različitih aeroelastičnih fenomena.

Kao sledeći korak, može se uzeti u obzir aproksimacija vezana za kvaziustaljeni model kao dodatak na ustaljeni pristup. Ovaj model tretira pomeranje poprečnog preseka mosta. Ali, u ovom slučaju, ustaljeni model opterećenja proširen je na dinamiku, te se u svakom trenutku dejstvo vetra može modelovati pomoću ustaljenih izraza (jednačine (1)) za trenutnu konfiguraciju poprečnog preseka. Na ovaj način se zanemaruje memorija fluida. Ipak, ovo snažno pojednostavljenje pod određenim uslovima može dovesti do dobre aproksimacije sila.

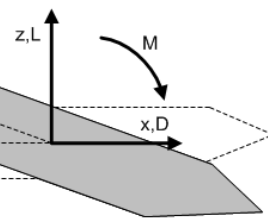
Međutim, nezgode kod višećih mostova koje su u prošlosti izazvane vетrom, kao što je katastrofa mosta Tacoma Narrows, pokazuju da su ove aproksimacije nedovoljne za opisivanje mehanizma interakcije i kao naredni korak je usledilo razvijanje neustaljenih modela sila.

2 FLATER

Flater predstavlja dinamičku nestabilnost gde energija uzeta iz strujanja veta povećava energiju oscilovanja mosta. Može dovesti do snažnih oscilacija s povećanjem amplituda, a time i do kolapsa konstrukcije.

Klasičan flater je aeroelastični fenomen kod kog se dva dominantna stepena slobode konstrukcije, naime rotacija i vertikalna translacija, sprežu u nestabilnu oscilaciju na koju utiče opstrujavanje vetra. Tipični poprečni preseci koji su podložni ovakvoj nestabilnosti su aeroprofilni i mostovi aerodinamičnog preseka. Kretanje je karakterisano silama veta koje tokom jednog ciklusa oscilovanja dodaju energiju u sistem. Ova

coefficients are used to transfer the forces from the wind tunnel model to design model of the bridge with real dimensions. This steady load model is appropriate for obtaining the static forces on the bridge deck, and it can be called also the quasi-static load model.



Slika 2. Usvojena konvencija za sile od veta
Figure 2. Adopted convection for wind forces

However, this consideration of perfectly motionless structure does not present a correct consideration of the wind loads. Namely, the flexibility of the bridge decks cannot be neglected, since it creates a potential in generating a complex interaction between flexible structure and circumfluent wind. The interaction mechanism can be described as follows. Forces produced from the surrounding flow are inducing displacements and/or deformations of a structure. If these displacements and deformations are large enough, they influence the flow field around the structure and consequently the forces change. This fluid-structure interaction is regarded as aero elasticity and can lead to different aero elastic phenomena.

As a next step of approximation a quasi-steady load model can be taken into account as an extension of steady approach. This model considers the motion of bridge cross-section. But in this particular case, steady load model is extended to dynamics, by imagining that at each instant the wind action can be modelled by using the steady expressions (Eq.(1)) related to the current configuration of the cross-section at that instant. In this way the fluid-memory is neglected. Still, this strong simplification under certain conditions can result in a good approximation of forces.

However, wind-induced accidents concerning the suspension bridges in the past, such as the famous collapse of the Tacoma Narrows bridge, proved that these approximations are insufficient to describe interaction mechanism and as a next step, development of unsteady force models followed.

2 FLUTTER

Flutter is a dynamic instability where the energy drawn from the wind flow increases the energy of the bridge deck oscillations. It can lead to violent oscillations with increase of amplitudes and therefore to the collapse of the structure.

Classical flutter is an aero elastic phenomenon, in which the two dominant degrees of freedom of the structure, namely rotation and vertical translation, couple in a flow-driven unstable oscillation. Typical cross-sections which are prone to this instability are airfoils and streamlined bridge decks. The motion is

razmena energije je vođena razlikom u fazi između vertikalnih i torzionih oscilacija ([1], [9]) i suprotstavlja se energiji koja se troši u prigušenju konstrukcije. Kritičan uslov ostvaruje se pri određenoj brzini veta, koja se naziva kritična brzina veta, i koja je vezana za izjednačavanje ukupnog prigušenja s nulom, odnosno konstrukcijskog i aerodinamičnog zajedno. Ovaj efekat je takođe povezan s promenom frekvencije oscilovanja. Naime, konstrukcija osciluje sa istom frekvencijom pri fleksionim i torzionim vibracijama – što se naziva kritičnom frekvencijom.

Odvajanje vrtloga nije neophodno za nastanak flatera, što uz činjenicu da se ovaj fenomen javlja pri brzini veta koja je iznad kritične brzine veta nastale usled odvajanja vrtloga, jasno izdvaja flater od rezonantnih problema ([3]). Na kritično stanje, nastalo usled flatera, može se uticati delovanjem na geometriju preseka, takođe na prigušenje i povećavanjem odnosa između svojstvenih frekvencija.

Mehanizam flatera proučavan je od strane [17] i [18], s ciljem određivanja svojstvenih oblika konstrukcije koji su odgovorni za flater, a nastalih usled modifikacije pomoću aeroelastičnih efekata. Ovi svojstveni oblici konstrukcije takođe se nazivaju i granama flatera.

Poprečni preseci koji nemaju aeroelastičan oblik podložni su jakom odvajaju struje veta koja vodi ka nestabilnosti koja je izražena pomoću jednog torzionog stepena slobode i koja se naziva torzioni flater. Praktično u blizini kritičnog stanja, strujanje veta predaje energiju uglavnom torzionom tonu.

U ovom radu akcenat je na klasičnom flateru i metodama za rešavanje flater-problema. Prikazani numerički primer takođe je vezan za tipičan poprečni presek mosta koji pripada grupi aerodinamičnih poprečnih preseka, gde je klasični flater značajan.

3 PRISTUP U FREKVENTNOM DOMENU

3.1 Model za flater kod mostova

S pretpostavkom da ravna ploča podleže malim harmonijskim oscilacijama pri vertikalnoj translaciji i rotaciji sa istom kružnom frekvencijom (kritičan uslov za nastanak flatera), neustaljene sile veta su izvedene u zatvorenoj formi u frekventnom domenu - Theodorsen [35]. Nažalost, slične analitičke funkcije koje daju zatvoreno rešenje za neustaljene sile veta, koje deluju na uobičajene poprečne preseke mostova, nije moguće odrediti. Razlog je u vezi sa opstrujavanjem vazduha oko oscilujućeg poprečnog preseka mosta, koje je znatno kompleksnije u poređenju sa opstrujavanjem oko ravne ploče, pre svega usled kompleksnih fizičkih fenomena kao što su masivno odvajanje strujanja, ponovno prijanjanje, odvajanje vrtloga i tako dalje. Ipak, analogna formulacija onoj koju je prezentovao Theodorsen, u smislu frekventno zavisnih parametara, zadržana je i u slučaju modela flatera kod mostova.

Scanlan [33] izveo je metodu u kome su aerodinamički parametri - flater derivati primenjeni za definisanje neustaljenih sile vezanih za uobičajene mostove. Flater derivati identifikovani su putem eksperimenata i koriste se za procenu sile veta nastalih usled kretanja konstrukcije (takođe se nazivaju i aeroelastične ili samopo- buđujuće sile). S tim u vezi, aerodinamični uzgon i momenat po jedinici dužine mosta mogu se izraziti u proši-

characterized by the fluid forces feeding energy into the system during one cycle of its oscillation. This exchange of energy is driven by the phase shift between the vertical and torsional oscillations ([1], [9]) and it counteracts the energy absorption by structural damping. The critical condition is reached by the certain wind speed, called critical wind velocity, related to the total zero damping, i.e. structural and aerodynamic damping together. This effect is also coupled with a variation of a frequency of oscillation. Namely, the structure oscillates with the same frequency in bending and torsion – called critical frequency.

Flow separation is unnecessary for the occurrence of flutter and also the fact that this phenomenon occurs at flow velocity above the critical vortex shedding one, clearly distinguishes the flutter from resonance problem ([3]). The critical state, related to flutter, can be influenced upon by acting on the geometry of the section, also on the damping and by increasing the ratio between natural frequencies.

Mechanism of flutter has been studied in [17] and [18], with the purpose of understanding which structural modes are responsible for the instability, as being modified by aero elastic effects. These structural modes are also called flutter branches.

Relatively bluffer cross-sections undergoing strongly separated flow are prone to the single degree of freedom torsional instability, which is called the torsional flutter. Basically in the neighbourhood of the critical condition the flow tends to insert the energy mainly in a torsional mode.

In this paper, classical flutter and its solutions are of main concern. Presented numerical example is also related to the typical bridge cross-section which belongs to the group of streamlined cross-sections, where classical flutter is of a main concern.

3 FREQUENCY-DOMAIN APPROACH

3.1 Bridge flutter model

Assuming that the flat plate undergoes small harmonic oscillations in heave and pitch with the same circular frequency (critical condition for the onset of flutter), the unsteady wind forces given in the frequency domain are derived in a closed form by Theodorsen [35]. Unfortunately, similar analytical functions giving a closed form expressions for the unsteady wind forces acting on a common bridge decks are impossible to obtain. The reason is related to the air flow around an oscillating bridge deck which is much more complicated than around a simple flat plate, primarily due to the complex physical phenomena such as massive separations, reattachment, shedding of eddies, etc. Nevertheless, an analogous formulation to the one presented by Theodorsen, in terms of frequency-dependent parameters, is kept also in the case of the bridge flutter models.

Scanlan [33] derived a method in which aerodynamic parameters - flutter derivatives are applied to define an unsteady forces related to the common bridge deck. The flutter derivatives are identified by experiments and used to estimate the occurring motion-induced forces (also called aero elastic or self-excited forces). Thus, the aero elastic lift and moment forces per unit length of span, can be expressed in the extended force model from [34]

renom modelu sila [34] pomoću diferencijalnih relacija:

$$L_{ae} = \frac{1}{2} \rho U^2 B \left[K H_1^* \frac{\dot{z}}{U} + K H_2^* \frac{B \dot{\alpha}}{U} + K^2 H_3^* \alpha + K^2 H_4^* \frac{z}{B} \right] \quad (2)$$

$$M_{ae} = \frac{1}{2} \rho U^2 B^2 \left[K A_1^* \frac{\dot{z}}{U} + K A_2^* \frac{B \dot{\alpha}}{U} + K^2 A_3^* \alpha + K^2 A_4^* \frac{z}{B} \right] \quad (3)$$

U ovim relacijama, $K=B\omega/U$ je redukovana frekvencija, a H_i^* , A_i^* ($i=1..4$) jesu flater derivati, dok ρ predstavlja gustinu vazduha, U srednju brzinu vетра, B širinu poprečnog preseka mosta. Obično se za određeni poprečni presek mosta određuje set flater derivata i svaki derivat se predstavlja kao bezdimenzionalna funkcija redukovane frekvencije.

Aeroelastični model sila predstavljen jednačinama (2) i (3) baziran je na dvema pretpostavkama. Prva je da samopobuđujuća sila uzgona i moment mogu biti opisani kao linearna funkcija pomeranja konstrukcije i njene rotacije (z ; α) i njihovih prvih i drugih izvoda (\dot{z} , $\dot{\alpha}$, \ddot{z} , $\ddot{\alpha}$), kao što se često koristi i kako je predstavljeno i u radu [11], kao:

$$F = F(z, \alpha, \dot{z}, \dot{\alpha}, \ddot{z}, \ddot{\alpha}) = P_z z + P_\alpha \alpha + P_{\dot{z}} \dot{z} + P_{\dot{\alpha}} \dot{\alpha} + P_{\ddot{z}} \ddot{z} + P_{\ddot{\alpha}} \ddot{\alpha} \quad (4)$$

gde F predstavlja ili aeroelastičnu силу uzgona L ili aeroelastični momenat M , a P_i ($i = z; \alpha$) jesu aeroelastični parametri sile. Validnost ove pretpostavke vezana je za ograničene amplitude oscilacija pri nastanku flatera ([34]). Uvodeći drugu pretpostavku o postojanju harmonijskog kretanja s jedinstvenom frekvencijom pri nastanku flatera, pomeranje i njegov prvi i drugi izvod mogu se izraziti kao:

$$x = \hat{x} e^{i\omega t}, \dot{x} = \hat{x} i\omega e^{i\omega t}, \ddot{x} = -\hat{x} \omega^2 e^{i\omega t} \quad (5)$$

gde je \hat{x} amplituda pomeranja ($x = z; \alpha$) i ω je kružna frekvencija kretanja. Iz jednačina (4) i (5) može se uočiti da se članovi koji se odnose na pomeranja i ubrzanja mogu kombinovati, što je u skladu s prikazom datim u jednačinama (2) i (3). Ovo omogućava interpretaciju flater derivata kao delova samopobuđujućih sile, koji se u dinamici konstrukcija vide kao aeroelastično prigušenje, pomoću derivata ($H_1^*, H_2^*, A_1^*, A_2^*$) i spregnute aeroelastične krutosti i mase, pomoću derivata ($H_3^*, H_4^*, A_3^*, A_4^*$).

Validnost ovog linearног modela samopobuđujućih sile vezanih za poprečni presek mosta predstavlja važnu temu. Jedan od važnih efekata jeste zavisnost flater derivata od amplitude kretanja ([23]).

Pored prikazane konvencije za flater deriveate postoje takođe i druge. Primeri se mogu pronaći kod [15] i [38].

3.2 Identifikacija flater derivata

Flater derivati se obično određuju eksperimentalno u aerotunelu za pojedinačne geometrije poprečnog preseka mosta. Za tu svrhu postoje dve glavne eksperimentalne strategije: metod slobodnih vibracija i metod prinudnih vibracija. Kod eksperimenata sa slobodnim vibracijama poprečni presek je elastično oslonjen pomoću opruga i eventualno prigušivača i

by the differential relations:

$$L_{ae} = \frac{1}{2} \rho U^2 B \left[K H_1^* \frac{\dot{z}}{U} + K H_2^* \frac{B \dot{\alpha}}{U} + K^2 H_3^* \alpha + K^2 H_4^* \frac{z}{B} \right] \quad (2)$$

$$M_{ae} = \frac{1}{2} \rho U^2 B^2 \left[K A_1^* \frac{\dot{z}}{U} + K A_2^* \frac{B \dot{\alpha}}{U} + K^2 A_3^* \alpha + K^2 A_4^* \frac{z}{B} \right] \quad (3)$$

In these equations, $K=B\omega/U$ is the reduced frequency and H_i^* , A_i^* ($i=1..4$) are the flutter derivatives, while ρ represents the air density, U the mean wind velocity, B is the bridge deck width. Usually, a set of flutter derivatives is evaluated for a specific cross-sectional shape of a bridge deck and each derivative is a dimensionless function of the reduced frequency.

The aero elastic force model presented in Eq.(2) and Eq.(3) is based on two assumptions. The first assumption is that the self-excited lift force and moment can be described as a linear function of the structural displacements and rotation (z ; α) and their first and second order derivatives (\dot{z} , $\dot{\alpha}$, \ddot{z} , $\ddot{\alpha}$), as commonly used and presented in [11], as:

$$F = F(z, \alpha, \dot{z}, \dot{\alpha}, \ddot{z}, \ddot{\alpha}) = P_z z + P_\alpha \alpha + P_{\dot{z}} \dot{z} + P_{\dot{\alpha}} \dot{\alpha} + P_{\ddot{z}} \ddot{z} + P_{\ddot{\alpha}} \ddot{\alpha} \quad (4)$$

where F represents either the aero elastic lift force L or the aero elastic moment M and P_i ($i = z; \alpha$) are aero elastic force parameters. The validity of this assumption is related to limited amplitudes of oscillations at the onset of flutter ([34]). Introducing a second assumption of the existence of harmonic motions with a single frequency at the onset of flutter, the displacement and its first- and second-order derivatives can be expressed as:

where \hat{x} is the amplitude of the displacement ($x = z; \alpha$) and ω is the circular frequency of motion. From Eq.(4) and Eq.(5) it can be observed that terms related to the displacements and accelerations can be combined, which is consistent with the representation in Eq.(2) and Eq.(3). This allows the interpretation of flutter derivatives as parts of self-excited forces, which feed back into the structural dynamics as aero elastic damping, through derivatives ($H_1^*, H_2^*, A_1^*, A_2^*$) and coupled aero elastic stiffness and masses, through derivatives ($H_3^*, H_4^*, A_3^*, A_4^*$).

The validity of this linear model for bridge deck self-excited forces is an important issue. One of the important effects is the dependence of flutter derivatives on the amplitude of motion ([23]).

Besides presented convention, there also exist other conventions for flutter derivatives. Examples could be found in [15] and [38].

3.2 Identification of flutter derivatives

Flutter derivatives are usually determined experimentally in wind tunnel tests for individual bridge deck geometries. For this purpose, two major experimental strategies exist: the free vibration method and forced vibration method. In the free vibration

postavljen je u aerotunel. Identifikacione tehnike za izdvajanje flater derivata mogu se naći u [7], [2], [29]. U slučaju testova prinudnih vibracija, potrebni su motor i kinematički mehanizam da pokreću model harmonički u svojim stepenima slobode. Samopobuđujuće sile mogu se dobiti direktno iz merenja sila ili iz pritisaka. Ovakvi primeri identifikacije flater derivata vezanih za pravougaone prizme mogu se naći u [17], [19] i [12]. Poređenje ove dve eksperimentalne tehnike – slobodnih i prinudnih vibracija – na primeru pravougaonog poprečnog preseka može se naći u [36] i [37]. Sveobuhvatnije poređenje metoda vezano za poprečne preseke koji se kreću od pravougaonih prizmi do aerodinamičnih preseka prikazano je u [28]. Izvori odstupanja eksperimentalnih rezultata i nepouzdanosti vezane za eksperimentalne metode istaknute su i analizirane. Implikacije uočenih razlika na nastanak flater nestabilnosti analizirane su u [5].

Za potrebe ove studije, primjenjen je metod prinudnih vibracija s predviđenim harmoničkim kretanjima i sile su direktno merene. Za takav identifikacioni metod je ključno odvajanje slabih signala vezanih za aeroelastične sile koje deluju na poprečnom preseku mosta od jakih signala vezanih za inercijalne sile samog modela. Rešenje je da se izvedu dva seta merenja. Referentno merenje s prinudnim vibracijama bez strujanja vazduha neophodno je za identifikaciju mehaničkog sistema modela. Nakon toga, merenja se ponavljaju sa identičnom frekvencijom oscilovanja i amplitudom pod dejstvom opterećenja vetra u aerotunelu. Budući da je primjenojeno prinudno harmoničko kretanje, ove merene sile takođe se pretpostavljaju kao harmoničke. Na ovaj način, merene sile bez strujanja vazduha F_0 i usled strujanja vetra F_w mogu se izraziti kao:

$$F_0 = \hat{F}_0 e^{i(\omega t + \varphi_0)}, F_w = \hat{F}_w e^{i(\omega t + \varphi_w)} \quad (6)$$

gde su \hat{F}_0 i \hat{F}_w amplitude sile, a φ_0 i φ_w fazna pomeranja ostvarena u odnosu na primjeno kretanje datu jednačinom (5), vezano za merenja bez strujanja vazduha i usled opterećenja vjetrom (slika 2), respektivno. Samopobuđujuće sile se dobijaju izračunavanjem razlike između ova dva seta merenja prema [14], sa slike 2:

$$\Delta F = F_w - F_0 \quad (7)$$

Može se pokazati da se flater derivati vezani za torzionalna kretanja dobijaju iz:

$$\frac{1}{2} \rho K^2 U^2 B \hat{\alpha} [H_3^*(K) + i H_2^*(K)] = \Delta L^\alpha(K) \quad (8)$$

$$\frac{1}{2} \rho K^2 U^2 B^2 \hat{\alpha} [A_3^*(K) + i A_2^*(K)] = \Delta M^\alpha(K) \quad (9)$$

a vezano za vertikalna kretanja iz:

$$\frac{1}{2} \rho K^2 U^2 \hat{z} [H_4^*(K) + i H_1^*(K)] = \Delta L^z(K) \quad (10)$$

$$\frac{1}{2} \rho K^2 U^2 B \hat{z} [A_4^*(K) + i A_1^*(K)] = \Delta M^z(K) \quad (11)$$

experiments a section model is elastically supported by springs and eventually a damper and mounted in a wind tunnel. Identification techniques for extracting the flutter derivatives can be found in [7], [2], [29]. In the case of forced vibration tests, a motor and a kinematic mechanism are necessary to drive the model harmonically in its degrees of freedom. Self-excited forces can be obtained directly through either force or pressure measurements. Such examples of identifying flutter derivatives related to the rectangular prisms using the pressure measurements can be found in [17], [19] and [12]. A comparison of both experimental techniques – free and forced vibration – on the rectangular cross-section can be found in [36] and [37]. More comprehensive comparisons of methods related to cross-sections ranging from rectangular prisms to streamlined sections are given in [28]. Sources of discrepancies of experimental results and uncertainties related to the experimental methods are pointed out and analyzed. Implications of these discrepancies to the onset of flutter instability have been analyzed in [5].

For the purpose of this study the forced vibration method with prescribed harmonic motions is applied and the forces are directly measured. For such an identification method the separation of the small signals of the aero elastic forces acting on the bridge deck model from the larger signals due to inertial forces of the model itself is crucial. A solution strategy is to perform two sets of measurements. A reference measurement with forced vibrations in still air is required in order to identify the mechanical system of the model. Then, the measurement is repeated with an identical oscillation frequency and amplitude under the action of the wind tunnel flow. Considering the applied forced harmonic motion these measured forces are also assumed harmonic. In this way, measured forces in still air F_0 and under the action of the wind F_w can be expressed as:

where \hat{F}_0 and \hat{F}_w are the force amplitudes and φ_0 and φ_w are the phase shifts related to the applied motion given in Eq.(5), regarding the measurements in still air and under the action of the wind (refer to Figure 2), respectively. The self-excited forces are obtained by calculating the difference between these two sets of measurements by [14], in Figure 2:

It can be shown that flutter derivatives related to the torsional motion can be obtained from:

and related to the vertical motion from:

ΔL^x i ΔM^x ($x=z,\alpha$) jesu pomenute razlike vezane za aeroelastični uzgon i aeroelastični momenat, respektivno, koje treba da se dobiju iz eksperimentata bez strujanja vazduha i pod dejstvom veta. U ovom radu, flater derivati su definisani prateći konvenciju po kojoj su sile uzgona i verikalno pomeranje definisani pozitivno na gore, dok su aeroelastični momenat kao i torzionalne deformacije pozitivne sa smerom kad je prednji kraj poprečnog preseka orijentisan na gore, kao što je prikazano na slici 1. Prema jednačini (6), samopobudjuće sile su takođe harmonijske u vremenu, ali s faznom razlikom u poređenju sa zadatim kretanjem preseka. Ovo svojstvo dozvoljava određivanje karakteristika sile kao što su amplituda i fazna razlika merenih signala. Mehaničke nepravilnosti u kinematičkom mehanizmu kao i odvajanje vrtloga od preseka mogu da poremete signal, zbog čega su naročito neophodni posebno stabilni algoritmi identifikacije - videti [22].

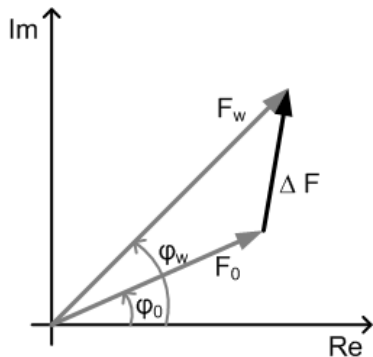
Prema tome, postupak se može sažeti kao:

- izvršiti testove s prinudnim oscilacijama bez strujanja vazduha i usled dejstva veta pri vertikalnom kretanju ili torzionom;
- izračunati najbolje uklapljen harmonik iste prinudne frekvencije da bi se dobili koeficijent amplitude sile i fazna razlika vezana za primenjeno kretanje, jednačina (6);
- izračunati razliku između dva merenja, jednačina (7);
- izračunati derivate na osnovu jednačina (8)-(11).

ΔL^x and ΔM^x ($x=z,\alpha$) are the mentioned differences of the aero elastic lift and the aero elastic moment, respectively, which should be obtained from the experiments in still air and under the action of wind. In this paper, flutter derivatives are defined following a convention after which the lift force and the heaving displacement are positive upwards, while the aerodynamic moment and the pitching rotation are positive nose-up, as it is shown in Figure 1. According to Equation (6) the self-excited forces are also harmonious in time, but with a phase shift compared to the prescribed motion of the deck. This characteristic allows determining force properties such as amplitude and phasing from the measured signals. As mechanical imperfections in the kinematic mechanism or vortex shedding from the section can disturb the signal, specifically stable identification algorithm are needed, see [22].

Thus, the procedure can be summarized as:

- perform forced oscillation tests in still air and under the action of the wind in either vertical (heave) or torsional (pitch) motion,
- calculate a best-fit harmonic of the same forcing frequency to obtain the force amplitude coefficients and phase shifts related to the applied motion, Eqs.(6)
- calculate the differences between two measurements, from Eq.(7)
- calculate the derivatives from Eqs.(8)-(11)



Slika 2. Identifikacija aeroelastičnih sile u kompleksnoj ravni ([20])
Figure 2. Identification of the aero elastic forces in the complex plane ([20])

3.3 Rešenje jednačina flatera

Kada su aeroelastične sile utvrđene (jednačine (2) i (3)), može se dobiti kritični uslov, odnosno kritična brzina veta za nastanak flatera. Najjednostavniji način za određivanje kritične brzine veta jeste da se posmatra krut model poprečnog preseka mosta sa dva stepena slobode (2DOF model); naime, posmatraju se vertikalno i torzionalno kretanje; 2DOF jednačine kretanja po jedinici dužine mogu se napisati kao:

$$m\ddot{z} + c_z \dot{z} + k_z z = L_{ae}$$

gde su L_{ae} i M_{ae} samopobudjuće sile predstavljene u jednačinama (2) i (3), m je masa, a I maseni moment inercije po jedinici dužine i k_z i k_α su krutosti, a c_z i c_α su

3.3 Solution of flutter equations

Once the aero elastic forces are established (Eq.(2) and Eq.(3)), the critical condition, i.e. critical wind velocity for the onset of flutter, can be calculated. The simplest way to establish critical wind velocity is to consider a rigid section model of the bridge deck with two degrees of freedom (2DOF model), namely vertical z (heave) and torsional α (pitch) motion are considered. The 2DOF equation of motion per unit span length can be written as follows:

$$I\ddot{\alpha} + c_\alpha \dot{\alpha} + k_\alpha \alpha = M_{ae} \quad (12)$$

where L_{ae} and M_{ae} are self-excited forces presented by Eq.(2) and Eq.(3), m is mass and I mass moment of inertia per unit length and k_z and k_α are stiffnesses and

koeficijenti prigušenja za respektivne stepene slobode.

Za slučaj kritičnog uslova kod flatera, vertikalno i torzionalno pomeranje može se posmatrati kao harmonijsko kretanje sa istom kružnom frekvencijom:

$$z(t) = \bar{z}e^{i\omega t}, \alpha(t) = \bar{\alpha}e^{i\omega t} \quad (13)$$

Posle zamene jednačina (2), (3) i (13) u jednačinu (12), formulisan je problem svojstvenih vrednosti stabilnosti kretanja, s frekvencijom flatera i kritičnom brzinom vetra kao nepoznatim:

$$\left[2\gamma_m \left(-1 + \frac{1}{X^2} + i2\zeta_z \frac{1}{X} \right) - (H_4^* + iH_1^*) \right] \frac{\bar{z}}{B} - (H_3^* + iH_2^*) \bar{\alpha} = 0 \quad (14)$$

$$- (A_4^* + iA_1^*) \frac{\bar{z}}{B} + \left[2\gamma_I \left(-1 + \frac{2\gamma_\omega^2}{X^2} + i2\zeta_z \frac{\gamma_\omega}{X} \right) - (A_3^* + iA_2^*) \right] \bar{\alpha} = 0 \quad (15)$$

gde su $\gamma_m = m/(\rho B^2)$ i $\gamma_I = I/(\rho B^4)$ bezdimenzionalne vrednosti mase i momenta inercije mase, respektivno, $\gamma_\omega = \omega_\alpha / \omega_z$ jeste odnos svojstvenih frekvencija, dok je $X = \omega / \omega_z$ nepoznata spregnutu frekvenciju, normalizovana u odnosu na svojstvenu frekvenciju vertikalnog oscilovanja.

Kako jednačine (14) i (15) predstavljaju homogen linearan sistem jednačina po \bar{z} i $\bar{\alpha}$, za dobijanje netrivijalnih rešenja determinanta mora da bude jednaka nuli. Kako jednačine (14) i (15) predstavljaju sistem jednačina s kompleksnim brojevima, oba dela determinante, i realan i imaginarni, moraju nestati, što dovodi do novog sistema jednačina:

$$R_4 X^4 + R_3 X^3 + R_2 X^2 + R_1 X + R_0 = 0 \quad (16)$$

$$I_3 X^3 + I_2 X^2 + I_1 X + I_0 = 0 \quad (17)$$

gde je:

$$\begin{aligned} R_4 &= 1 + \frac{1}{2\gamma_m} H_4^* + \frac{1}{2\gamma_I} A_3^* + \frac{1}{4\gamma_m \gamma_I} (H_4^* A_3^* - H_1^* A_2^* - H_3^* A_4^* + H_2^* A_1^*) \\ R_3 &= \zeta_\alpha \frac{\gamma_\omega}{\gamma_m} H_1^* + \zeta_z \frac{1}{\gamma_I} A_2^* \\ R_2 &= -1 - \gamma_\omega^2 - 4\zeta_z \zeta_\alpha \gamma_\omega - \frac{\gamma_\omega^2}{2\gamma_m} H_4^* - \frac{1}{2\gamma_I} A_3^* \\ R_1 &= 0 \\ R_0 &= \gamma_\omega^2 \\ I_3 &= \frac{1}{2\gamma_m} H_1^* + \frac{1}{2\gamma_I} A_2^* + \frac{1}{4\gamma_m \gamma_I} (H_4^* A_2^* - H_1^* A_3^* - H_3^* A_1^* + H_2^* A_4^*) \\ I_2 &= -2\zeta_z - 2\zeta_\alpha \gamma_\omega - \zeta_\alpha \frac{\gamma_\omega}{\gamma_m} H_4^* - \zeta_z \frac{1}{\gamma_I} A_3^* \\ I_1 &= -\frac{\gamma_\omega^2}{2\gamma_m} H_1^* - \frac{1}{2\gamma_I} A_2^* \\ I_0 &= 2\zeta_z \gamma_\omega^2 + 2\zeta_\alpha \gamma_\omega \end{aligned} \quad (18)$$

Na ovaj način je dobijen sistem jednačina s dve nepoznate. Nepoznate su X , koja sadrži spregnutu (flater) frekvenciju i kritična redukovana brzina U_{cr} , od

c_z and c_α damping coefficients, for respective degrees of freedom.

For the case of flutter critical condition, heave and pitch can be considered as harmonic motion with the same circular frequency:

$$z(t) = \bar{z}e^{i\omega t}, \alpha(t) = \bar{\alpha}e^{i\omega t} \quad (13)$$

After the substitution of Eqs.(2), (3) and (13) into Eqs.(12) eigenvalue problem of stability of motion is formulated with flutter frequency and the critical wind speed as unknowns:

$$(14)$$

$$(15)$$

where $\gamma_m = m/(\rho B^2)$ and $\gamma_I = I/(\rho B^4)$ are the nondimensional values of the mass and mass moment of inertia, respectively, $\gamma_\omega = \omega_\alpha / \omega_z$ is the frequency ratio of natural frequencies, while $X = \omega / \omega_z$ is the unknown coupling frequency, nondimensionalized regarding the heaving natural frequency.

Since Eq.(14) and Eq.(15) represent linear homogeneous system of equations of \bar{z} and $\bar{\alpha}$, to obtain nontrivial solutions, the determinant must be equal to zero. Since Eq.(14) and Eq.(15) presents system of complex number equations, both, real and imaginary part of the determinant must vanish, leading to the new system of equations:

$$(16)$$

$$(17)$$

where:

In this way a system of equations with two unknowns is obtained. The unknowns are X , containing the coupled (flutter) frequency, and the critical reduced velocity U_{cr} ,

koje zavise flater derivati. Rešenje se dobija grafičkim prikazom realnih rešenja X vezanih za obe jednačine u odnosu na U_{red} . Presek ovih krivih vodi ka rešenju flatera.

Generalno gledano, uočeno je da više stepeni tonova kod trodimenzionalnih konstrukcija može biti uključeno u flater nestabilnost. U tom slučaju, jednostavan 2DOF model nije dovoljan. Proračun se može obaviti na dva načina: primjenjujući aeroelastične sile direktno na trodimenzionalni model mosta pomoću metode konačnih elemenata, što se naziva direktni metod, ili posmatrajući odgovor konstrukcije, uzimajući u obzir samo odgovarajući broj svojstvenih tonova, što se naziva multimodalni metod. Diskusija u vezi s multimodalnim metodom prikazana je u [31]. Neki primeri implementacije sa odgovarajućim aplikacijama mogu se naći u [8] i [25]. U radu [10] direktni metod za flater analizu predstavljen je i upoređen s multimodalnim metodom. S jedne strane, direktni metod obezbeđuje učeće svih svojstvenih tonova, ali s druge strane, zahteva veću računarsku snagu.

4 PRISTUP U VREMENSKOM DOMENU

Flater derivati nisu pogodni za proračune u vremenskom domenu, jer su izraženi kao funkcija frekvencije. Kao pandan flater derivatima u vremenskom domenu mogu se izvesti funkcije koje nisu analitičke. Ovakve funkcije opisuju vremenski razvoj sila usled naglog infinitenzimalnog pomeranja konstrukcije i ove funkcije nazivaju se indicijalne funkcije. Prvi relevantni rad u kom je spomenuta mogućnost primene indicijalnih funkcija zabeležen je u [32].

Kako bi se definisale samopobuđujuće sile, istorija kretanja se posmatra kao niz ovih infinitenzimalnih inkremenata. Pod pretpostavkom linearnosti opterećenja, samopobuđujuće sile u vremenskom domenu (pandani jednačinama (2) i (3)) mogu se izraziti pomoću konvolucije ovih indicijalnih funkcija:

$$L_{ae}(s) = qBC_L' \left[\Phi_{L\alpha}(0)\alpha(s) + \Phi_{Lz}(0)\dot{z}(s) + \int_0^s \dot{\Phi}_{L\alpha}(s-\tau)\alpha(\tau)d\tau + \int_0^s \dot{\Phi}_{Lz}(s-\tau)\dot{z}(\tau)d\tau \right] \quad (19)$$

$$M_{ae}(s) = qB^2C_M' \left[\Phi_{M\alpha}(0)\alpha(s) + \Phi_{Mz}(0)\dot{z}(s) + \int_0^s \dot{\Phi}_{M\alpha}(s-\tau)\alpha(\tau)d\tau + \int_0^s \dot{\Phi}_{Mz}(s-\tau)\dot{z}(\tau)d\tau \right] \quad (20)$$

Aeroelastične sile u vremenskom domenu (jednačine (19) i (20)) izražene su u funkciji bezdimenzionalnog vremena $s=2Ut/B$. Kao što se može uočiti, četiri indicijalne funkcije – Φ_{il} koriste se za opisivanje aeroelastičnih sila, gde indeks i identificiše komponentu opterećenja L za uzgon ili M za aeroelastični momenat, a indeks l komponentu pomeranja koja se menja sukcesivno u koracima, z ili α .

Ove funkcije se obično određuju na osnovu odgovarajućih (merenih) flater derivata ([4], [26]). To se radi tako što se uzima tipična aproksimacija, predstavljajući indicijalne funkcije u vidu sume m eksponencijalnih grupa (filtera):

$$\Phi_{il}(s) = 1 - \sum_{k=1}^m a_{ilk} \exp(-b_{ilk}s) \quad (21)$$

that flutter derivatives depend on. The solution is obtained by plotting the real X solutions of both equations against U_{red} . The intersection of these curves leads to the flutter solution.

Generally speaking, it is observed that more modes of the three-dimensional structures can be involved in flutter instability. In this case, simple 2DOF model is insufficient. The calculation can be done in two ways: to apply aero elastic forces directly to the three-dimensional finite element model of the bridge, which is called a direct method, or to consider the structural response taking into account an adequate number of natural modes, called multimode method. The multimode method was discussed in [31]. Some examples of implementation with related applications can be found in [8] and [25]. In [10] a direct method for flutter analysis is presented and compared to the multimode method. Thus, direct method provides participation of all natural modes, but accordingly, it demands higher computational power as well.

4 TIME-DOMAIN APPROACH

The flutter derivatives are inadequately suited for the time domain calculations, due to being expressed as a function of frequency. As a counterpart to flutter derivatives in time domain, specific non-analytical functions can be derived. Such functions describe the time development of the forces due to the sudden infinitesimal structural motions and these functions are called the indicial functions. The first relevant work mentioning the possibility of using indicial functions is noted in [32].

In order to define the self-excited forces, the history of motion can be seen as a series of these infinitesimal step-wise increments. Under the assumption of linearity of load, the self-excited forces in time domain (counterparts of Eq. (2) and Eq.(3)) may be expressed as convolutions of these indicial functions:

$$Aero elastic forces in the time domain (Eq.(19) and Eq.(20)) are expressed as a function of a dimensionless time $s=2Ut/B$. As it may be observed, four indicial functions - Φ_{il} are used to describe the aero elastic forces, where subscript i indentifies the load component L for lift and M for aerodynamic moment and subscript l the motion component that experiences the step change z or α .$$

Usual practice to determine these functions is from the corresponding (measured) flutter derivatives ([4], [26]). This is done by taking the typical approximation, by representing the indicial function as a sum of m exponential groups (filters):

S ciljem uspostavljanja veza između indicijalnih funkcija i flater derivata, zadaje se harmonijsko kretanje u prethodno spomenutim konvolucionim integralima (jednačine (19) i (20)). Na ovaj način, aeroelastično opterećenje, dano konvolucionim integralima, izraženo je u frekventnom domenu, i u ovoj formi se može uporediti sa opterećenjem baziranim na flater derivatima (jednačine (2) i (3)), što dovodi do ovih relacija:

$$\begin{aligned} \frac{2\pi}{U_{red}} H_1^* &= -\left(\frac{dC_L}{d\alpha} + C_D\right) \left[1 - \pi^2 \sum_k a_{Lzk} \frac{1}{U_{red}^{*2} b_{Lzk}^2 + \pi^2} \right] \frac{2\pi}{U_{red}} A_1^* = -\frac{dC_M}{d\alpha} \left[1 - \pi^2 \sum_k a_{Mzk} \frac{1}{U_{red}^{*2} b_{Mzk}^2 + \pi^2} \right] \\ \frac{4\pi}{U_{red}^3} H_2^* &= -\frac{dC_L}{d\alpha} \left[\sum_k a_{Lak} \frac{b_{Lak}}{U_{red}^{*2} b_{Lak}^2 + \pi^2} \right] \frac{4\pi}{U_{red}^3} A_2^* = \frac{dC_M}{d\alpha} \left[\sum_k -a_{Mak} \frac{b_{Mak}}{U_{red}^{*2} b_{Mak}^2 + \pi^2} \right] \\ \frac{4\pi^2}{U_{red}^2} H_3^* &= -\frac{dC_L}{d\alpha} \left[1 - \pi^2 \sum_k a_{Lak} \frac{1}{U_{red}^{*2} b_{Lak}^2 + \pi^2} \right] \frac{4\pi^2}{U_{red}^2} A_3^* = \frac{dC_M}{d\alpha} \left[1 - \pi^2 \sum_k a_{Mak} \frac{1}{U_{red}^{*2} b_{Mak}^2 + \pi^2} \right] \\ \frac{2}{U_{red}^2} H_4^* &= \left(\frac{dC_L}{d\alpha} + C_D \right) \left[\sum_k a_{Lzk} \frac{b_{Lzk}}{U_{red}^{*2} b_{Lzk}^2 + \pi^2} \right] \frac{2}{U_{red}^2} A_4^* = -\frac{dC_M}{d\alpha} \left[\sum_k a_{Mzk} \frac{b_{Mzk}}{U_{red}^{*2} b_{Mzk}^2 + \pi^2} \right] \end{aligned} \quad (22)$$

S obzirom na prirodu ovih relacija, indicijalne funkcije (s bezdimenzionalnim koeficijentima a_{ilk} i b_{ilk} kao nepoznatim) mogu se identifikovati uz pomoć nelinearne optimizacije najmanjih kvadrata. Detalji u vezi s metodom koja je praćena u ovom radu, opisani su u [27].

Važno je napomenuti da je direktna eksperimentalna identifikacija indicijalnih funkcija takođe teorijski moguća i jedan primer je zabeležen u [5].

5 KVAZIUSTALJENA APROKSIMACIJA

Kao što je već napomenuto, uobičajeno je da se aeroelastične sile mere u aerotunelu na umanjenim modelima mostova. Posle toga se ove sile prenose na realni model mosta. Parametar sličnosti koji omogućava ovaj prenos naziva se redukovana brzina veta $U_{red} = U/Bf$.

U radu [20] ovaj se parametar sličnosti objašnjava posmatranjem vazduha iza pomerljivog poprečnog preseka mosta. Naime, usled prinudnih oscilacija poprečnog preseka mosta, vazduh iza tela takođe ispoljava kretanje sa istom frekvencijom, slika 3. Uzimajući u obzir dolazeću brzinu veta U , talasna dužina vazduha, koji je pod uticajem, može se proceniti kao $L_w = U T$, gde je T period prinudnih oscilacija. Tada se redukovana brzina može predstaviti kao:

$$U_{red} = \frac{U}{fB} = \frac{UT}{B} = \frac{L_w}{B} \quad (23)$$

Shodno tome, efekti memorije fluida postaju manji kada talasna dužina L_w raste, bilo povećavanjem brzine, ili smanjivanjem frekvencije oscilovanja. Za ove više redukovane brzine, strujanje veta se približava stanju koje je dobijeno u slučaju nepokretnog poprečnog preseka. U tom slučaju, aeroelastične sile mogu biti aproksimirane kvaziustaljenim pristupom (pomoću koeficijenata sila (jednačina (1))). Redukovana brzina od oko $U_{red} \approx 20$ ([13]) smatra se tačkom od koje kvaziustaljeni pristup može da se primeni umesto

In order to establish the relationships between indicial functions and flutter derivatives, harmonic motions are imposed into the previously mentioned convolution integrals (Eq.(19) and Eq.(20)). In this way the aero elastic load given by convolution integrals is expressed in the frequency domain, and in this form it can be compared to the load based on flutter derivatives (Eq.(2) and Eq.(3)), providing these relationships:

Due to the nature of these relationships, the indicial functions (with non-dimensional coefficients a_{ilk} and b_{ilk} as unknowns) can be then identified by means of nonlinear least-square optimisation. Further details of the method, which is followed within this work, are described in [27].

It is also worth of mentioning that direct experimental identification of indicial functions is theoretically also possible and one example has been noted in [5].

5 QUASI-STEADY APPROXIMATION

As already mentioned, the aero elastic forces are usually measured in the wind tunnel on the scaled bridge deck models. Later these forces are to be transferred to the design model of the real bridge. A similarity parameter which enables this transfer is called the reduced wind velocity $U_{red} = U/Bf$.

In [20] this similarity parameter is considered by observing the air behind moving bridge deck. Namely, due to the forced motion of the bridge deck, the air behind the body is also experiencing a motion with the same frequency, Figure 3. Taking into account the approaching wind velocity U , the wavelength of affected air can be estimated as $L_w = U T$, where T is the forced motion period. Then the reduced velocity can be presented as:

Consequently, the fluid-memory effects become smaller when the wavelength L_w is increasing, either by raising the velocity, or decreasing the oscillation frequency. For these higher reduced velocities the wind flow field approach conditions obtained in a case of a fixed cross-section. In this case the aero elastic forces can be approximated by quasi-steady approach (using the force coefficients (Eq. (1))). As a transition point for application of the quasi-steady approach instead of the unsteady one is found at the reduced velocity $U_{red} \approx 20$

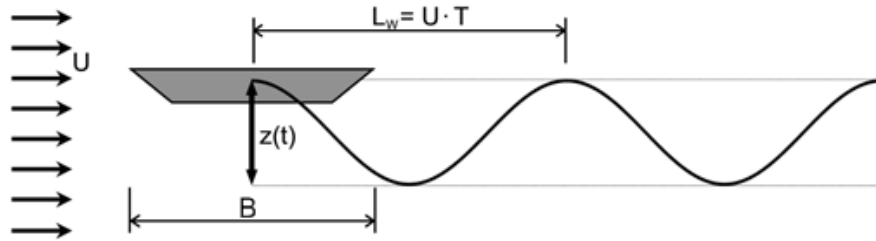
neustaljenog. Aeroelastične sile uz usvojenu pretpostavku kvaziustaljenosti mogu se izvesti kao:

$$L_{ae}^{qs} = qB \left[-\left(\frac{dC_L}{d\alpha} - C_D \right) \frac{\dot{z}}{U} + \frac{dC_L}{d\alpha} \alpha + \left(\frac{dC_L}{d\alpha} - C_D \right) \beta_z \frac{B}{U} \dot{\alpha} \right] \quad (24)$$

$$M_{ae}^{qs} = qB \left[-\frac{dC_M}{d\alpha} \frac{\dot{z}}{U} + \frac{dC_M}{d\alpha} \alpha + \frac{dC_M}{d\alpha} \beta_\alpha \frac{B}{U} \dot{\alpha} \right] \quad (25)$$

C_i su koeficijenti sila iz jednačina (1) a $dC_i/d\alpha$ su njihovi prvi izvodi. Bezdimentzionalni parametar β_i predstavlja parametar ekscentričnosti ([27]). Izvođenje jednačina (24) i (25) može se naći u [27].

([13]). Aero elastic forces based on quasi-steady assumption can be derived as:



Slika 3. Talasna dužina L_w , prema [20]
Figure 3. Wavelength L_w from [20]

6 NUMERIČKI PRIMER

6.1 Eksperimentalna postavka

Model simetričnog, aerodinamički optimizovanog jednočelijskog preseka nosača mosta (slika 4 levo) testiran je u aerotunelu s graničnim slojem na Univerzitetu u Bohumu (Ruhr – Universität Bochum). Aerotunel s nepovratnom vazdušnom strujom ima ukupnu dužinu od 9,4 m, širinu od 1,8 m i visinu od 1,6 m (slika 4 sredina). Turbulentna mreža se nalazi na ulazu u tunel, i proizvodi intenzitet turbulentcije od oko 3–4%, a integralna skala turbulentcije je oko 0,03 m.

Drveni model ima širinu od 0,36 m, visinu od 0,06 m i dužinu od 1,8 m. Ukupna masa modela je oko 4,9 kg. Model je horizontalno postavljen u aerotunelu (slika 4 desno). Na početku su sprovedeni testovi na fiksnom modelu. Model je postavljen na dva balansa sile, opremljena mernim trakama (koje mere sile) i koji se nalaze na bočnim stranama aerotunela. Merenja su realizovana pri različitim napadnim uglovima (-10° to 10°) s Reynolds-ovim brojem od oko 10^5 (ovo je određeno na osnovu širine preseka mosta).

Pored toga, flater derivati su dobijeni sprovodenjem testova s prinudnim vibracijama. Zbog toga, motor i kinematički mehanizam pokreću model mosta periodično u dva stepena slobode (vertikalno i torzionalno kretanje). U slučaju testova s prinudnim vibracijama, posebna pažnja se mora uzeti u obzir da bi se aeroelastične sile razdvajile od inercijalnih sila nastalih usled mase modela. Za tu svrhu se obavljaju dva seta merenja: jedno referentno merenje s prinudnim vibracijama bez strujanja vazduha i jedno merenje pod dejstvom veta, kao što se pominje u odeljku 3.2. Testovi s prinudnim vibracijama sprovedeni su koristeći Reynolds-ove brojeve u opsegu od $0,6 \cdot 10^5$ do $3,5 \cdot 10^5$. Amplitude prinudnih

6 NUMERICAL EXAMPLE

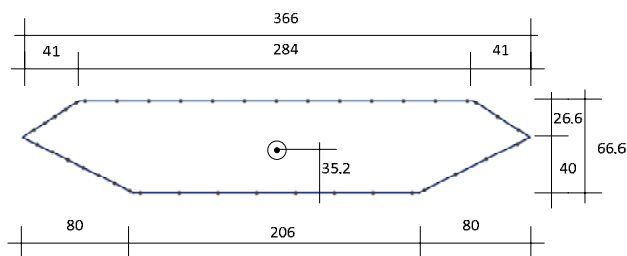
6.1 Experimental set-up

The model of a symmetric, aerodynamically optimized single-box section of a bridge girder (Figure 4 left) has been tested in the boundary layer wind tunnel at Ruhr-Universität Bochum. The open circuit wind tunnel has a total length of 9.4m, 1.8m width and 1.6m height (Figure 4 middle). A honeycomb grid is located at the inlet of the tunnel, generating turbulence intensity of around 3-4%, and having an integral turbulence length scale of around 0.03m.

The wooden model has a width B of 0.36m, a height H of 0.06m and a length L of 1.8m. The total mass of the model is about 4.9kg. The model is horizontally placed in the wind tunnel (refer to Figure 4 right). First, tests at the fixed model are carried out. The model is mounted on two force balances equipped with strain gauges (measuring the forces) which are located at each side of the wind tunnel. The measurements are realized at various angles of flow attack (-10° to 10°) with a Reynolds number of around 10^5 (based on the deck width of the bridge).

Furthermore, flutter derivatives are obtained performing forced vibration tests. Therefore a motor and a kinematic mechanism are driving the bridge deck model periodically in two degrees of freedom (vertical and torsional motion). In the case of forced vibration tests, special care has to be taken into account in order to separate the aero elastic forces from the inertial forces caused by the model's mass. For that purpose two sets of measurements are performed: one reference measurement with forced vibrations in still air and one measurement under the action of the wind, as it is also mentioned in section 3.2. The forced vibration tests are performed using Reynolds numbers in the range of

vibracija su oko 4 mm u slučaju vertikalnog kretanja i oko 1° za torzionalno kretanje. Opseg frekvencija vibracija za testove je od 1.0 do 6.6 Hz. Ostali detalji u vezi s merenjem u aerotunelu mogu se naći u [30], a u pogledu eksperimentalne platforme u [22].



0.6×10^5 to 3.5×10^5 . The forced vibration amplitudes are around 4mm in the case of heaving motion and around 1° for the torsional motion. The vibration frequency range for the test is 1.0 to 6.6Hz. Further details regarding the wind tunnel measurements can be found in [30] and concerning the used experimental rig in [22].



Slika 4. Model poprečnog preseka mosta postavljen na eksperimentalnu platformu
Figure 4. Model of the bridge deck section placed in the experimental rig

6.2 Rezultati i diskusija

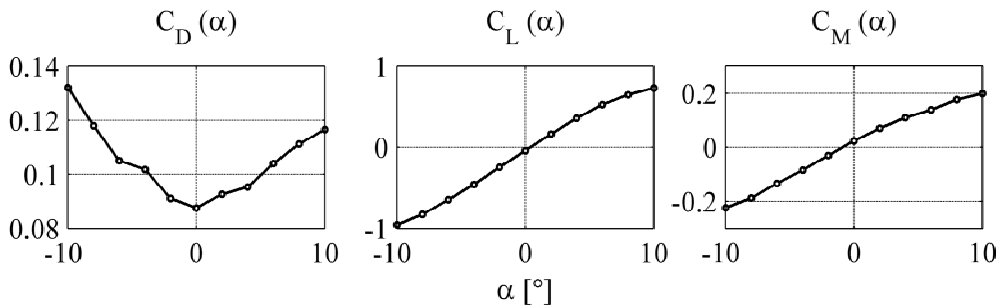
Dobijeni koeficijenti sile prikazani su na slici 5 u funkciji napadnog ugla. Brzina veta koji prilazi konstrukciji je 4 m/s. Koeficijenti C_i , $i=D, L$ i M iz jednačine (1) i gradjenti C'_i , neophodni za izražavanje aeroelastičnih sila pri kvaziustaljenoj aproksimaciji (jednačine (24) i (25)) pri osrednjem napadnom uglu od $\alpha = 0$, izvedeni su aproksimiranjem funkcije u obliku polinoma mernim tačkama sa slike 5. Odgovarajuće vrednosti su tada definisane kao vrednosti i gradjenti aproksimirane funkcije (funkcije u obliku polinoma) pri osrednjem napadnom uglu od $\alpha = 0$. Zbog prirode krivih otpora, uzgona i momenta sa slike 5, koeficijenti sile uzgona i momenta C_L i C_M aproksimirani su s linearnom funkcijom, a koeficijent sile otpora C_D aproksimiran je s polinomom drugog reda. Aproksimacije su izvedene za $-4^\circ \leq \alpha \leq 4^\circ$. Vrednosti određenih koeficijenata i njihovi prvi izvodi dati su u tabeli 1.

6.2 Results and discussion

Obtained force coefficients are plotted in Figure 5 as a function of the angle of the flow attack. The oncoming wind velocity is around 4 m/s. The coefficients C_i , $i=D, L$ and M from Eq.(1) and the gradients C'_i , necessary for expressing the aero elastic forces using the quasi-steady approximation (Eq.(24) and Eq.(25)), at the mean angle of attack $\alpha = 0$, are derived by fitting a polynomial function to the measured points presented in Figure 5. The respective values are then defined as the values and gradients of the approximation function at $\alpha = 0$ (polynomial function). Due to the nature of the drag, lift and moment force curves in Figure 5, the lift and the moment force coefficients C_L and C_M are approximated with a linear function and the drag force coefficients C_D is approximated by a polynomial of second order. The approximations are performed for $-4^\circ \leq \alpha \leq 4^\circ$. The values of respective coefficients and its first derivatives are given in Table 1.

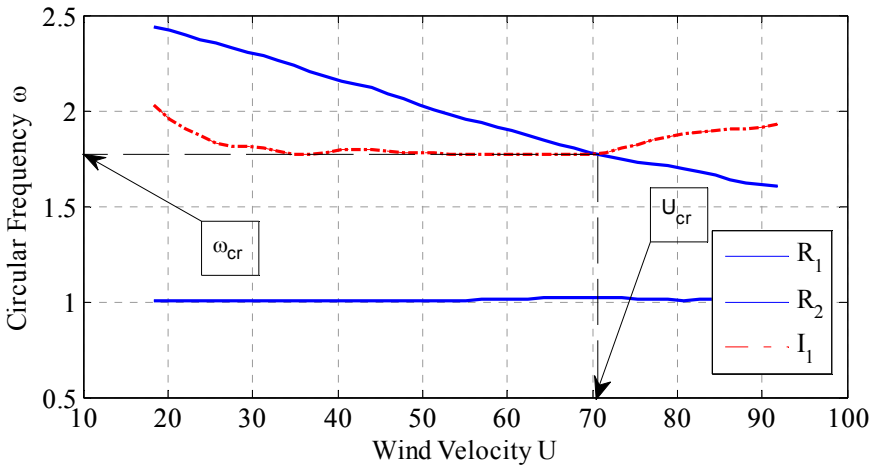
Tabela 1: Koeficijenti sile i njihovi prvi izvodi pri osrednjem napadnom uglu od $\alpha = 0$
Table 1: Force coefficients and its first derivatives at the mean angle of attack $\alpha = 0$

	C_D	C'_D	C_L	C'_L	C_M	C'_M
Statički eksperiment Static Experiment	0.0886	-0.0329	-0.0442	5.8513	0.0179	1.3984



Slika 5. Ustaljeni koeficijenti sile
Figure 5. Steady force coefficients

Svi osam flater derivata korišćenih u jednačinama (2) i (3) predstavljeni su na slici 7. Oni su mereni u opsegu redukovanih brzina do $U_{red}=30$ (gde je $U_{red}=U/Bf=2\pi/K$). Na osnovu ovih vrednosti, aeroelastično opterećenje može se odrediti pomoću jednačina (2) i (3). U ovom slučaju, konstruktivne karakteristike posmatranog mosta prikazane su u tabeli 2 i koristeći 2DOF model, opisan u odeljku 3.4, moguće je odrediti kritičnu brzinu. Stoga su na slici 6 prikazana realna rešenja X, realne i imaginarnе jednačine (jednačine (16) i (17)) u funkciji U_{red} . Prvi presek ovih krivih vodi ka flater rešenju. Kao što se može primetiti sa slike 6, dobijena je kritična brzina od oko $U_{cr}=70.46$ m/s.



Slika 6. Određivanje kritične brzine i kritične frekvencije
Figure 6. Determination of critical velocity and critical frequency

Kao dodatak flater derivatima koji su određeni iz testova u aerotunelu, na slici 7 su takođe prikazane i kvaziustaljene aproksimacije derivata. One su određene poređenjem koeficijenata koji se nalaze pored pomeranja i njihovih prvih izvoda koji su uzeti u obzir u dvema aeroelastičnim formulacijama: aeroelastične sile koje su bazirane na derivatima (jednačine (2) i (3)) i kvaziustaljenoj aproksimaciji (jednačine (24) i (25)). Kao što se može uočiti, nemaju svi flater derivati svoje pandane pri kvaziustaljenoj aproksimaciji. Oni koji nedostaju su derivati H_4^* i A_4^* , koji i nemaju odlučujuću ulogu kod praktičnih primera aerodinamike mostova. Može se primetiti da aproksimacije prate isti trend. Još jedna nepoznata u slučaju kvaziustaljene aproksimacije u vezi je sa izborom parametra ekscentričnosti β_i . Ovi parametri imaju veliki uticaj na najvažnije derivate vezane za prigušenje H_2^* i A_2^* . Naime, parametri β_i opisuju pozicije neutralnih tačaka odgovarajućih komponenata sile. U opštem slučaju poprečnog preseka mosta, zajednička neutralna tačka ne postoji ([26], [21]). Moguće rešenje bilo bi da se usvoje pozicije neutralnih tačaka u vezi s poprečnim presecima gde su one poznate, kao što je primer aeroprofil. Ipak, usled velikog uticaja na važne derivate H_2^* i A_2^* , β_i bi trebalo, ako je moguće, da budu određeni na osnovu dinamičkih testova (iz flater derivata). U ovom radu, prateći proceduru koja je opisana u [21], parametri su određeni na osnovu izmerenih H_2^* i A_2^* krivih, što vodi do $\beta z=1.761$ i $\beta \alpha=-1.378$. Na osnovu kvaziustaljenih flater

All eight flutter derivatives used in Eq.(2) and Eq.(3) are presented in Figure 7. They are measured for the range of reduced velocities till $U_{red}=30$ (where $U_{red}=U/Bf=2\pi/K$). Based on these values, aero elastic loads can be evaluated by the Eq.(2) and Eq.(3). In this case, the structural properties of the used bridge deck are given in Table 2 and using the 2DOF model described in section 3.4 critical velocity can be estimated. Therefore, in Figure 6 the real X solutions of real and imaginary equations (Eq.(16) and Eq.(17)) against U_{red} are plotted. The first intersection of these curves leads to the flutter solution. As it may be observed from Figure 6, the critical velocity around $U_{cr}=70.46$ m/s is obtained.

In addition to flutter derivatives evaluated from the wind tunnel tests, Figure 7 also shows quasi-steady approximations of derivatives. They are evaluated comparing the coefficients which stand beside considered displacements and their first derivatives in two aero elastic formulations: aero elastic forces based on the derivatives (Eq.(2) and Eq.(3)) and quasi-steady approximation (Eq.(24) and Eq.(25)). As may be observed, not all flutter derivatives have their counterparts in quasi-steady approximation. The missing ones are H_4^* and A_4^* which are not decisive related to practical examples of bridge aerodynamics. It can be remarked that the approximations are following the same trend. Another unknown in the case of quasi-steady approximation is related to the choice of eccentricity parameters β_i . They have strong influence on the most important damping derivatives H_2^* and A_2^* . Namely, parameters β_i describe the position of the neutral points for the respective force components. In general case of the bridge section a common neutral point does not exist ([26], [21]). One possible solution could be to adopt the positions of neutral points related to the certain cross-section where those positions are known, such as airfoil. Still due to the strong influence on important H_2^* and A_2^* derivatives, β_i parameters should be, if possible, evaluated from dynamic tests (from flutter derivatives). In this work, following the procedure described in [21] parameters are evaluated from measured H_2^* and A_2^* curves which leads to $\beta z=1.761$ and $\beta \alpha=-1.378$. Based

derivata sa slike 7, određena je kritična brzina kao konzervativnija vrednost od $U_{cr} = 66.97\text{m/s}$ u odnosu na kritičnu brzinu prethodno dobijenu s neustaljenim pristupom.

Kao što je već pomenuto u odeljku 4, koeficijenti indicijalnih funkcija se mogu identifikovati na osnovu nelinearne optimizacije pomoću metode najmanjih kvadrata. Kao primer će biti određeni nepoznati koeficijenti iz jednačine (21), koji su vezani za indicijalnu funkciju $\Phi_{L\alpha}$ koja opisuje silu uzgona usled rotacionog kretanja. Na osnovu uspostavljenih relacija između indicijalnih funkcija i flater derivata koje su prikazane u jednačinama (22), nepoznati koeficijenti se mogu odrediti na osnovu derivata H_2^* i H_3^* . Koristeći izmerene aeroelastične derivate H_2^* i H_3^* sa svojim diskretnim vrednostima pri redukovanim brzinama U_{red}^m , $m = 1, \dots, M$, funkcija greške $\varepsilon_{L\alpha}$ koja je potrebna da bude minimizovana može biti data kao:

$$\varepsilon_{L\alpha}(\mathbf{p}_{L\alpha}) = \sum_{m=1}^M \left[\frac{(D_{L\alpha}(\mathbf{p}_{L\alpha}, U_{red}^m) - \bar{D}_{L\alpha}^m)^2}{\sigma_{\bar{D}_{L\alpha}^m}^2} + \frac{(E_{L\alpha}(\mathbf{p}_{L\alpha}, U_{red}^m) - \bar{E}_{L\alpha}^m)^2}{\sigma_{\bar{E}_{L\alpha}^m}^2} \right] \quad (26)$$

gde je $D_{L\alpha} = -K^2 H_3^*$ a $E_{L\alpha} = -KH_2^*$ i K je redukovana frekvencija. Reprezentacija neustaljenih koeficijenata pomoću $D_{L\alpha}$ i $E_{L\alpha}$ pogodnija je zbog identifikacione procedure u odnosu na klasičnu reprezentaciju pomoću H_2^* i H_3^* , gde su vrednosti pri nižim redukovanim brzinama umanjene. Stoga bi vrednosti pri većim redukovanim brzinama imale veći uticaj na totalnu grešku, te bi se kao rezultat dobila slabija aproksimacija pri nižim redukovanim brzinama, gde je neustaljenost izraženija ([26]). Vektor $\mathbf{p}_{L\alpha}$, iz jednačine Eq.(26), sažima sve nepoznate parametre koji treba da budu određeni optimizacionom procedurom:

$$\mathbf{p}_{L\alpha} = [a_{L\alpha 1}, \dots, a_{L\alpha N_{L\alpha}}, b_{L\alpha 1}, \dots, b_{L\alpha N_{L\alpha}}]^T \quad (27)$$

gde su $a_{L\alpha i}$ i $b_{L\alpha i}$, $i=1-N_{L\alpha}$ bezdimenzionalni koeficijenti i $N_{L\alpha}$ je broj izabranih članova za aproksimaciju indicijalne funkcije $\Phi_{L\alpha}$. Ukoliko su ustaljeni koeficijenti kao i njihovi prvi izvodi nepoznati moguće je i njih tretirati kao nepoznate parametre.

Optimizacija se izvodi na osnovu algoritma 'pouzdane oblasti' ('trust-region' algoritma), koji je implementiran u Matlab-u i koristi analitičke izraze za gradijente greške $\partial \varepsilon_{il} / \partial p_{il}$ i $\partial^2 \varepsilon_{il} / \partial^2 p_{il}$ koji su izvedeni u radu [26]. Slične funkcije greške koriste se za identifikaciju ostalih indicijalnih funkcija. Sve četiri sračunate indicijalne funkcije za posmatrani poprečni presek prikazane su na slici 8.

Za aerodinamične poprečne preseke, s ravnomernim izgledom svih derivata, upotreba jedne ([3]) ili dve (kao kod Jones-ove aproksimacije Theodorsen-ove funkcije date u [16]) grupe eksponencijalnih članova dovoljna je da prikaže globalno ponašanje. U ovom slučaju, jedna eksponencijalna grupa je iskorisćena za opisivanje ponašanja svih indicijalnih funkcija. Za proveru kvaliteta identifikovanih indicijalnih funkcija, flater derivati mogu biti određeni na osnovu bezdimenzionalnih koeficijenata sadržanih u \mathbf{p}_{il} i jednačina (22). Stoga su na slici 9 takođe predstavljeni odgovarajući flater derivati koji su određeni na osnovu identifikovanih bezdimenzionalnih

on the quasi-steady flutter derivatives from Figure 7 critical velocity is evaluated as a more conservative value $U_{cr} = 66.97\text{m/s}$ when compared to the critical velocity obtained from previously shown unsteady approach.

As already mentioned in section 4, indicial functions coefficients may be identified by means of a nonlinear least-square optimization. As an example unknown coefficients from Eq.(21) related to the indicial function $\Phi_{L\alpha}$ which describe the lift force due to the pitch motion are going to be identified. Based on established relationships between indicial functions and flutter derivatives shown in Eqs.(22), unknown coefficients should be evaluated from the derivatives H_2^* and H_3^* . Using the measured aero elastic derivatives H_2^* and H_3^* at discrete values of the reduced wind velocity U_{red}^m , $m = 1, \dots, M$, the error function $\varepsilon_{L\alpha}$ can be established, which is to be minimized:

where $D_{L\alpha} = -K^2 H_3^*$ and $E_{L\alpha} = -KH_2^*$ and K is reduced frequency. The representation of unsteady coefficients in terms of $D_{L\alpha}$ and $E_{L\alpha}$ is more suitable for this identification procedure than the classical representation in terms of H_2^* and H_3^* where the values at low reduced velocities are scaled down. Therefore the values at high reduced velocities would be weighted too much in the total error, resulting in a poor approximation at low reduced velocities, where unsteadiness is more important ([26]). Vector $\mathbf{p}_{L\alpha}$, from Eq.(26), collects the unknown parameters which have to be determined through the optimisation procedure:

where $a_{L\alpha i}$ and $b_{L\alpha i}$, $i=1-N_{L\alpha}$ are nondimensional coefficients and $N_{L\alpha}$ is the number of terms chosen to approximate the indicial function $\Phi_{L\alpha}$. If the steady coefficients and their first derivatives are unknown it is possible to treat them as additional unknown parameters.

The optimization is performed by using a trust-region algorithm which is implemented in Matlab and using analytical expressions for the error gradients $\partial \varepsilon_{il} / \partial p_{il}$ and $\partial^2 \varepsilon_{il} / \partial^2 p_{il}$ developed by [26]. Similar error functions are used to identify other indicial functions. All four resulting indicial functions for the considered bridge deck are presented in Figure 8.

For streamlined cross-sections, with 'uniform' trends in all derivatives, the use of one ([3]) or two (Jones' approximation of Theodorsen's function given in [16]) groups of exponential terms is sufficient to capture the general behaviour. In this case one exponential group is used to describe the behaviour of all indicial functions. As a quality check for identified indicial functions, flutter derivatives can be evaluated based on the non-dimensional coefficients contained in \mathbf{p}_{il} and Eqs.(22). Therefore, Figure 9 also include the corresponding flutter derivatives evaluated based on identified non-dimensional coefficients a_{il} and b_{il} , related to the indicial

koeficijenta a_{il} i b_{il} , koji odgovaraju indicijalnoj funkciji $\Phi_{L\alpha}$ (na slici 9 obeleženo je sa „optimized“) i štaviše, pokazuju zadovoljavajuće poklapanje s merenim flater derivatima. Slična provera je izvršena i za ostale identifikovane indicijalne funkcije.

Ove funkcije, kroz formu konvolucionih integrala, mogu biti iskorišćene za određivanje kritične brzine veta. Naime, jednačine kretanja predstavljene u jednačini (12) mogu biti rešene u slučaju različitih brzina veta, samo u ovom slučaju, pomoću aeroelastičnih sila izraženih u vremenskom domenu (jednačine (19) i (20)). Povećavanjem brzine, kritična brzina se može odrediti kao brzina koja izaziva nestabilne-divergentne oscilacije. Uprkos tome, zbog ekvivalentnosti ova dva pristupa, frekventnog i vremenskog, oba rešenja moraju da konvergiraju. No ipak, neke prednosti u izboru jednog u odnosu na drugi pristup, trebalo bi uzeti u obzir. Naime, zabeleženo je u [27] da je, sa stanovišta računara, analiza stabilnosti obimnija u vremenskom domenu, pogotovo kada se uzmu u obzir komplikovaniji modeli od 2DOF, i stoga je analiza u frekventnom domenu poželjnija. Isti autori takođe navode da bi metod u vremenskom domenu trebalo da se koristi kod analize mostova kada je pristup u frekventnom domenu komplikovaniji (na primer, spregnuta analiza flatera i uticaja turbulencije, analiza koja uključuje lokalizovane prigušivače), ili kada nije moguć (na primer, analiza koja uključuje konstruktivne nelinearnosti, nelinearne prigušivače).

Tabela 2: Konstruktivne karakteristike posmatranog mosta¹
Table 2: Structural properties of considered bridge²

B[m]	m _z [kg/m]	m _a [kg/m]	f _z [Hz]	f _a [Hz]	ζ _z [-]	ζ _a [-]
18.3	12820	426000	0.142	0.355	0.006	0.005

7 ZAKLJUČCI

Dinamičke sile veta koje deluju na fleksibilne mostovske nosače nastaju usled turbulencije koja dolazi do konstrukcije, zatim koja je uzrokovana samom konstrukcijom, te vrtložnim tragom iza konstrukcije, kao i usled interakcije između konstrukcije i veta koji je opstrjava. Poslednji (aeroelastični) tip sila deluje kao dodatni dinamički uticaj na poprečni presek mosta. Te sile imaju potencijal da generišu aeroelastični mehanizam samopobuđujućih oscilacija nosača, i mogu da dovedu konstrukciju do dinamičke divergencije, stvarajući aeroelastični fenomen poznat kao flater.

Glavni cilj ovog rada je da predstave različite metode koje mogu da se koriste za rešenje problema flatera kod mostova. Kao prvi metod je predstavljen najčešće primenjivan pristup u frekventnom domenu u kom se koriste frekventno zavisni aerodinamični parametri poznati kao flater derivati. Razmatran je 2DOF model i definisan je problem svojstvenih vrednosti, koji kao rezultat daje kriti-

¹ Vrednosti su uzete iz [24], gde je sličan poprečni presek mosta posmatran pomoću multimodalne analize. Dva tona, vezana za savijanje i torziju, odgovaraju predstavljanim glavnim spregnutim tonovima u pomenutom članku.

function $\Phi_{L\alpha}$ (in Figure 9 marked as ‘optimized’) and moreover they show satisfying agreement with measured flutter derivatives. Similar check is also performed for other identified indicial functions.

These functions, in the form of convolution integrals can also be used to estimate critical wind velocity. Namely, the equations of motion presented in Eq.(12) can be solved for different wind velocities, only in this case, with the aero elastic forces expressed in the time domain (Eq.(19) and Eq.(20)). By increasing the velocity, the critical velocity can be estimated as one causing unstable, divergent oscillations. Nevertheless, due to the equivalency of these two approaches, namely frequency and time, both solutions should converge. Still, some preferences in choosing one or the other approach should be taken in consideration. Namely, it is noted in [27] that from the computational point of view, stability analysis in the time domain is more extensive, especially when considering more complicated models than 2DOF, and therefore frequency-domain analysis is preferable. The same authors also mention that the time-domain method should be used for bridge analyses where the frequency-domain approach is more complicated (e.g. coupled buffeting analysis, analyses including localized damping devices), or where it is inapplicable (e.g. analyses including structural nonlinearities, nonlinear damping devices).

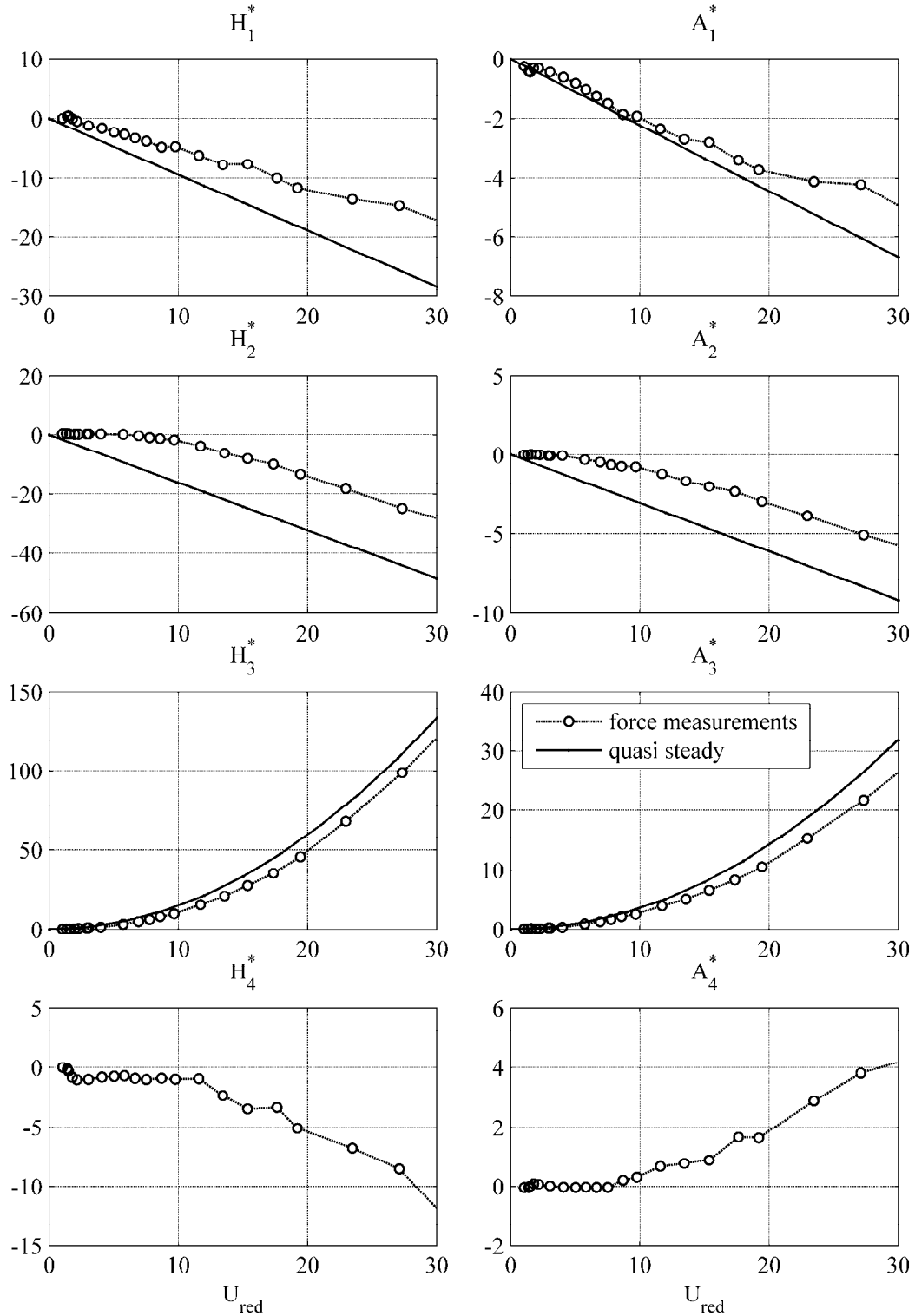
7 CONCLUSIONS

Dynamic wind forces upon flexible bridge girders evolve from the action of the incident, body- and wake-induced turbulence and from the interaction between the motion of the structure and the circumfluent wind. The latter (aero elastic) type of forces acts as the additional dynamic effect upon the girder cross-section. It has the potential to generate an aero elastic mechanism of self-excitation of girder oscillations, and it can bring the structure to dynamic divergence, creating aero elastic phenomenon called flutter.

The main objective of this paper is to present different bridge flutter methods which can be used to solve the flutter problem. At first, the most commonly used frequency-domain approach is presented in which frequency dependent aerodynamic parameters called flutter derivatives are applied. The 2DOF model is considered and eigenvalue problem is defined giving as the outcome critical wind speed - the main critical condition

² Values are taken from [24], where the similar bridge deck section is considered with the use of multimode analysys. Two modes, for heave and pitch, are corresponding to the presented main coupled modes from the related paper.

čnu brzinu veta - glavni kritični uslov za nastanak flatera. Kao sledeći korak, ekvivalentni pristup u vremenskom domenu, koji je baziran na indicijalnim funkcijama, sumiran je i zaključno je predstavljena aproksimacija vezana za kvaziustaljenu teoriju.

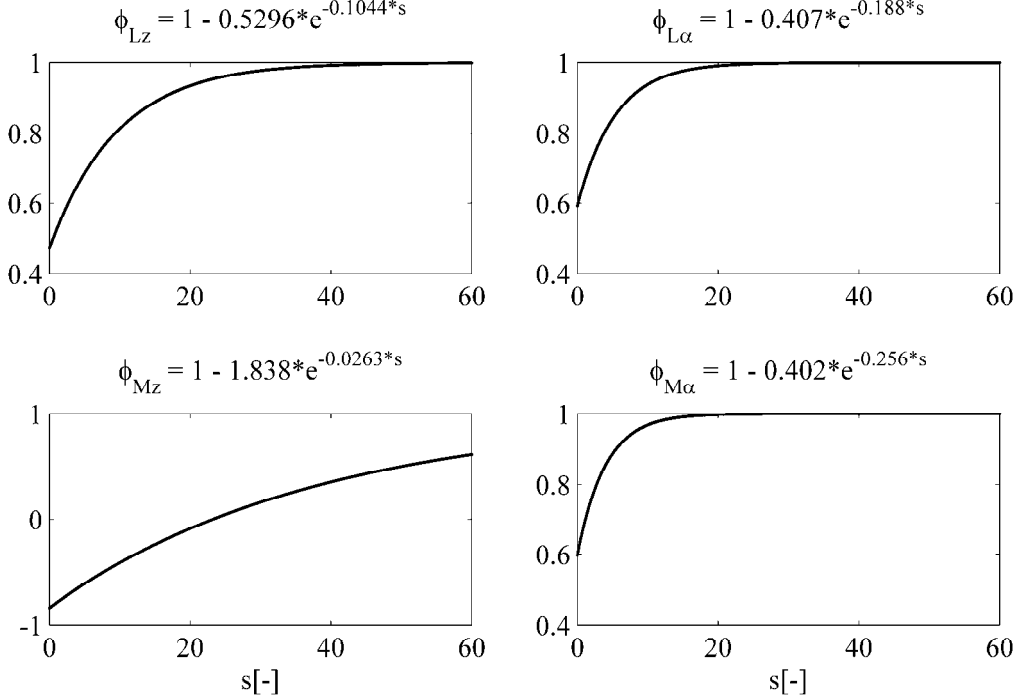


Slika 7. Flater derivati dobijeni direktno na osnovu merenja i korišćenjem kvaziustaljene aproksimacije
Figure 7. Flutter derivatives obtained directly from the measurements and using quasi-steady approximation

for the onset of flutter. As a next step, equivalent approach in time-domain, based on the indicial functions, is summarized and finally the approximation based on the quasi-steady theory is presented.

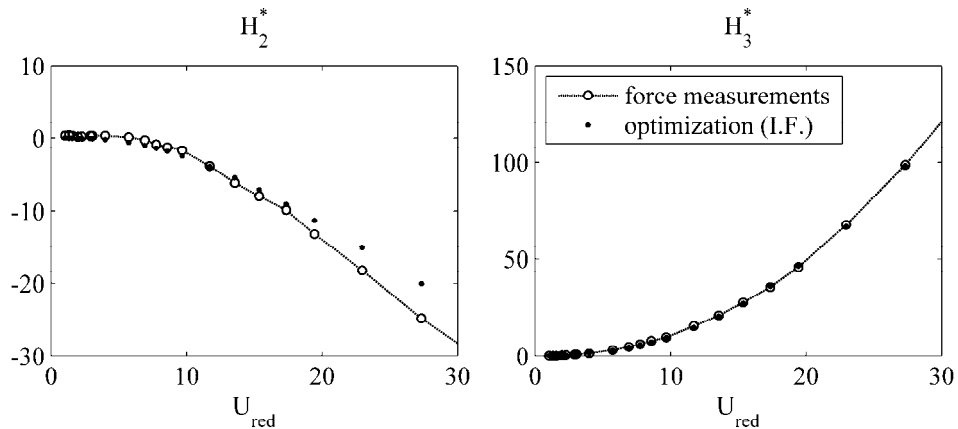
Prikazan je numerički primer jednog tipičnog poprečnog preseka mosta. S tom svrhom, serija eksperimenata je sprovedena u aerotunelu na fiksnom modelu postavljenom s različitim napadnim uglovima, kao i pomoću mehanizma za prinudne vibracije. Prikazane su identifikacione tehnike vezane za frekventno zavisne koeficijente – flater derivate i vremenski zavisne – indicijalne funkcije. Prednosti i mane prezentovanih pristupa su navedene.

A numerical example is offered related to one typical bridge deck cross-section. For that purpose, series of wind tunnel experiments conducted upon a rigid model placed under different angles of flow attack and by operating a forced vibration mechanism are performed. Identification techniques related to the frequency dependent coefficients – flutter derivatives and time dependent functions – indicial functions are provided. Advantages and disadvantages of the presented approaches are discussed.



Slika 8. Indicijalne funkcije

Figure 8. Indicial functions



Slika 9. Izabrani flater derivati dobijeni direktno na osnovu merenja u poređenju sa optimizovanim vrednostima dobijenim na osnovu procene indicijalne funkcije Φ_{La} sa slike 8

Figure 9. Selected flutter derivatives obtained directly from the measurements compared with optimized values obtained from indicial function estimation of the Φ_{La} from Figure 8

ZAHVALNOST

Autori zahvaljuju na uspešnoj saradnji prof. dr inž. R. Höffer-u (Ruhr University Bochum), na merenju u aerotunelu. Takođe, izražavaju zahvalnost za finansijsku podršku u okviru projekata TR 36046 Ministarstva prosvete, nauke i tehnološkog razvoja Republike Srbije, kao i za finansijsku podršku u okviru German Academic Exchange Service (DAAD) u vidu DYNET stipendije autoru MJ, za period jul-decembar 2013.

ACKNOWLEDGEMENT

The authors gratefully acknowledge the fruitful cooperation with Prof. Dr. Ing. R. Höffer, Ruhr University Bochum, related to the measurements in the wind tunnel. The financial support through the project TR 36046 of the Ministry of education, science and technological development of the Republic of Serbia, as well as the financial support provided by the German Academic Exchange Service (DAAD) in the framework of a DYNET scholarship for author MJ during period July–December 2013 is acknowledged.

8 LITERATURA REFERENCES

- [1] Bisplinghoff, R. L.; Ashley, H.; Halfman, R. L. (1996): *Aeroelasticity*. New York: Dover (Dover science books).
- [2] Bogunovic Jakobsen, J.; Hjorth-Hansen, E. (1995): Determination of the aerodynamic derivatives by a system identification method. In *Journal of Wind Engineering and Industrial Aerodynamics* 57, pp. 295–305.
- [3] Borri, C.; Costa, C. (2007): Cism courses and lectures. Edited by T. Stathopoulos: Springer Vienna.
- [4] Borri, C.; Höffer, R. (2000): Aeroelastic wind forces on flexible girders. In *Meccanica* 35 (10), pp. 1–15.
- [5] Caracoglia, L.; Jones, N. P. (2003): A methodology for the experimental extraction of indicial functions for streamlined and bluff deck sections. In *Journal of Wind Engineering and Industrial Aerodynamics* 91 (5), pp. 609–636.
- [6] Caracoglia, Luca; Sarkar, Partha P.; Haan, Frederick L., Jr.; Sato, Hiroshi; Murakoshi, Jun (2009): Comparative and sensitivity study of flutter derivatives of selected bridge deck sections, Part 2: Implications on the aerodynamic stability of long-span bridges. In *Engineering Structures* 31.
- [7] Chowdhury, Arindam Gan; Sarkar, Partha P. (2003): A new technique for identification of eighteen flutter derivatives using a three-degree-of-freedom section model. In *Engineering Structures* 25, pp. 1763–1772.
- [8] D'Asdia, Piero; Sepe, Vincenzo (1998): Aeroelastic instability of long-span suspended bridges: a multi-mode approach. In *Journal of Wind Engineering and Industrial Aerodynamics* 74–76 (0), pp. 849–857.
- [9] Fung, Y. (1993): An introduction to the theory of aeroelasticity: Dover Publications, Inc., New York.
- [10] Ge, Y. J.; Tanaka, H. (2000): Aerodynamic flutter analysis of cable-supported bridges by multi-mode and full-mode approaches. In *Journal of Wind Engineering and Industrial Aerodynamics* 86 (2–3), pp. 123–153.
- [11] Ge, Y.J.; Xiang, H.F (2008): Computational models and methods for aerodynamic flutter of long-span bridges. In *Journal of Wind Engineering and Industrial Aerodynamics* 96 (10-11), pp. 1912–1924.
- [12] Haan, F.L (2000): The effects of turbulence on the aerodynamics of long-span bridges. Department of Aerospace and Mechanical Engineering, Notre Dame, Indiana.
- [13] Höffer, R. (1997): Stationäre und instationäre Modelle zur Zeitbereichssimulation von Windkräften an linienförmigen Bauwerken. Doctoral Thesis. Ruhr-Universität Bochum, Germany, 1997.
- [14] Hortmanns, M. (1997): Zur Identifikation und Berücksichtigung nichtlinearer aeroelastischer Effekte. PhD Thesis. RWTH Aachen.
- [15] Jensen, A. G.; Höffer, R. (1998): Flat plate flutter derivatives – an alternative formulation. In *Journal of Wind Engineering and Industrial Aerodynamics* 74–76 (0), pp. 859–869.
- [16] Jones, R.T. (1940): The unsteady lift on a wing of finite aspect ratio. NACA Technical Report, 681.
- [17] Matsumoto, M. (1996): Aerodynamic damping of prisms. In *Journal of Wind Engineering and Industrial Aerodynamics* 59, pp. 159–175.
- [18] Matsumoto, M.; Daito, Y.; Yoshizumi, F.; Ichikawa, Y.; Yabutani, T. (1997): Torsional flutter of bluff bodies. In *Journal of Wind Engineering and Industrial Aerodynamics* 69–71, pp. 871–882.
- [19] Matsumoto, M.; Kobayashi, Y.; Shirato, H. (1996): The influence of aerodynamic derivatives on flutter. In *Journal of Wind Engineering and Industrial Aerodynamics* 60, pp. 227–239.
- [20] Neuhaus, C. (2010): Zur Identifikation selbsterregter aeroelastischer Kräfte im Zeitbereich. Doctoral Thesis. Bergischen Universität Wuppertal, Wuppertal. Bauingenieurwesen.
- [21] Neuhaus, C.; Höffer, R. (2011): Identification of quasi-stationary aeroelastic force coefficients for bridge deck section using forced vibration wind tunnel testing. In *EURODYN 2011* (Ed.): 8th International Conference on Structural Dynamics. Leuven, Belgium, pp. 1386–1392.
- [22] Neuhaus, C.; Roesler, S.; Höffer, R.; Hortmanns, M.; Zahlten, W. (2009): Identification of 18 Flutter Derivatives by Forced Vibration Tests – A New Experimental Rig. In : European & African Conference on Wind Engineering. 5th European & African Conference on Wind Engineering. Florence.
- [23] Noda, M.; Utsunomiya, H.; Nagao, F.; Kanda, M.; Shiraishi, N. (2003): Effects of oscillation amplitude on aerodynamic derivatives. In *Journal of Wind Engineering and Industrial Aerodynamics* 91.

- [24] Øiseth, O., Rönnquist, A., Sigbjörnsson, R. (2010): Simplified prediction of wind-induced response and stability limit of slender long-span suspension bridges, based on modified quasi-steady theory: A case study. In *Journal of Wind Engineering and Industrial Aerodynamics*, 98, 730-741.
- [25] Roesler, S. (2008): Entwicklung eines Berechnungswerkzeugs zum Nachweis der aeroelastischen Stabilität weitgespannter Brücken. Diplomarbeit. Bergische Universität Wuppertal, Germany.
- [26] Salvatori, L. (2007): Assessment and Mitigation of Wind Risk of Suspended-Span Bridges. Doctoral Thesis. TU Braunschweig, Germany, University of Florence, Italy.
- [27] Salvatori, L.; Borri, C. (2007): Frequency- and time-domain methods for the numerical modeling of full-bridge aeroelasticity. In *Computers and Structures* 85, pp. 675–687.
- [28] Sarkar, Partha P.; Caracoglia, Luca; Haan, Frederick L., Jr.; Sato, Hiroshi; Murakoshi, Jun (2009): Comparative and sensitivity study of flutter derivatives of selected bridge deck sections, Part 1: Analysis of inter-laboratory experimental data. In *Engineering Structures* 31.
- [29] Sarkar, Partha P.; Jones, Nicholas P.; Scanlan, R. H. (1992): System identification for estimation of flutter derivatives. In *Journal of Wind Engineering and Industrial Aerodynamics* 41-44, pp. 1243–1254.
- [30] Šarkić, Anina; Fisch, Rupert; Höffer, Rüdiger; Bletzinger, Kai-Uwe (2012): Bridge flutter derivatives based on computed, validated pressure fields. In *Journal of Wind Engineering and Industrial Aerodynamics*.
- [31] Scanlan, R. H. (1978): The Action of Flexible Bridges under Wind, I: Flutter Theory. In *Journal of Sound and Vibration* 60(2), pp. 187–199.
- [32] Scanlan, R. H.; Beliveau, J.-G; Budlong, K. (1974): Indicial aerodynamics functions for bridge deck. In *Journal of Engineering Mechanics* (100), pp. 657–672.
- [33] Scanlan, R.H; Tomko, J. (1971): Airfoil and bridge deck flutter derivatives. In *Journal of the Engineering Mechanics Division Proceedings of the ASCE* 97, pp. 1717–1737.
- [34] Simiu, E.; Scanlan, R. H. (1996): Wind Effects on Structures: Fundamentals and Applications to Design. third ed.: John Wiley, New York.
- [35] Theodorsen, T. (1934): General theory of aerodynamic instability and the mechanism of. NACA Technical Report 496.
- [36] Washizu, K.; Ohya, A. (1978): Aeroelastic instability of rectangular cylinders in a heaving mode. In *Journal of Sound and Vibration* 59, pp. 195–210.
- [37] Washizu, K.; Ohya, A. (1978): Aeroelastic instability of rectangular cylinders in a torsional mode due to transverse wind. In *Journal of Sound and Vibration* 72, pp. 507–521.
- [38] Zasso, A.(1996): Flutter derivatives: Advantages of new representation convection. *Journal of Wind Engineering and Industrial Aerodynamics*, 60, pp. 35-47.

REZIME

METODE ANALIZE FLATERA U FREKVENTNOM I VREMENSKOM DOMENU

Anina ŠARKIĆ
Milos JOČKOVIĆ
Stanko BRCIĆ

Fenomen flatera mostova predstavlja važan kriterijum stabilnosti, koji mora biti uzet u obzir tokom procesa projektovanja mosta. U ovom radu su prikazane različite metode koje se mogu koristiti pri rešavanju problema flatera. Najčešće korišćeni pristup je u frekventnom domenu i baziran je na formulaciji aeroelastičnih sile putem frekventno zavisnih koeficijenata koji se nazivaju flater derivati. Na osnovu ovako izraženih aeroelastičnih sila, određuje se kritična brzina veta, kao glavni uslov za nastanak flatera. Aeroelastične sile mogu se takođe izraziti i u vremenskom domenu, pomoću takozvanih indicijalnih funkcija. Ove funkcije su najčešće određene iz odgovarajućih flater derivata. U slučajevima kada su efekti memorije fluida zanemarljivi, kvaziustaljena teorija može se koristiti za aproksimaciju aeroelastičnih sila. Numerički primer tipičnog poprečnog preseka mosta prati prikazane pristupe.

Ključne reči: Flater, rešenje flatera, modeli opterećenja, flater derivati, indicijalne funkcije

SUMMARY

FREQUENCY- AND TIME-DOMAIN METHODS RELATED TO FLUTTER INSTABILITY PROBLEM

Anina SARKIĆ
Milos JOČKOVIĆ
Stanko BRCIĆ

Bridge flutter phenomenon presents an important criterion of instability, which should be considered in the bridge design phase. This paper presents different bridge flutter methods which can be used to solve the flutter problem. Most commonly used frequency-domain approach is based on the formulation of aero elastic forces with frequency dependent coefficients called flutter derivatives. The critical wind speed, as the main critical condition for the onset of flutter is obtained based on these aero elastic forces. Aero elastic forces can be also expressed in the time-domain, using so-called indicial functions. These functions are usually determined from the corresponding flutter derivatives. In situations when fluid-memory effects tend to become small the quasi-steady theory can be used as an approximation of aero elastic forces. A numerical example related to the typical bridge cross-section follows presented approaches.

Key words: Flutter, flutter solution, load models, fultter derivatives, indicial functions

UPUTSTVO AUTORIMA*

Prihvatanje radova i vrste priloga

U časopisu Materijli i konstrukcije štampaće se neobjavljeni radovi ili članci i konferencijska saopštenja sa određenim dopunama ili bez dopuna, prema odluci Redakcionog odbora, a samo izuzetno uz dozvolu prethodnog izdavača prihvatiće se i objavljeni rad. Vrste priloga autora i saradnika koji će se štampati su: originalni naučni radovi, prethodna saopštenja, pregledni radovi, stručni radovi, konferencijska saopštenja (radovi sa naučno-stručnih skupova), kao i ostali prilozi kao što su: prikazi objekata i istkustava - primeri, diskusije povodom objavljenih radova i pisma uredništvu, prikazi knjiga i zbornika radova, kao i obaveštenja o naučno-stručnim skupovima.

Originalni naučni rad je primarni izvor naučnih informacija i novih ideja i saznanja kao rezultat izvornih istraživanja uz primenu adekvatnih naučnih metoda. Dobijeni rezultati se izlažu kratko, jasno i objektivno, ali tako da poznavalač problema može proceniti rezultate eksperimentalnih ili teorijski numeričkih analiza i tok razmišljanja, tako da se istraživanje može ponoviti i pri tome dobiti iste ili rezultate u okvirima dopuštenih odstupanja, kako se to u radu navodi.

Prethodno saopštenje sadrži prva kratka obaveštenja o rezultatima istraživanja ali bez podrobnih objašnjenja, tj. kraće je od originalnog naučnog rada. U ovu kategoriju spadaju i diskusije o objavljenim radovima ako one sadrže naučne doprinose.

Pregledni rad je naučni rad koji prikazuje stanje nauke u određenoj oblasti, kao plod analize, kritike i komentara i zaključaka publikovanih radova o kojima se daju svi neophodni podaci pregledno i kritički uključujući i sopstvene radove. Navode se sve bibliografske jedinice korištene u obradi tematike, kao i radovi koji mogu doprineti rezultatima daljih istraživanja. Ukoliko su bibliografski podaci metodski sistematisovani, ali ne i analizirani i raspravljeni, takvi pregledni radovi se klasificuju kao stručni pregledni radovi.

Stručni rad predstavlja koristan prilog u kome se iznose poznate spoznaje koje doprinose širenju znanja i prilagođavanju rezultata izvornih istraživanja potrebama teorije i prakse. On sadrži i rezultate razvojnih istraživanja.

Konferencijsko saopštenje ili rad sopšten na naučno-stručnom skupu koji mogu biti objavljeni u izvornom obliku ili ih autor, u dogovoru sa redakcijom, bitno preradi i proširi. To mogu biti naučni radovi, naročito ako su sopštena po pozivu Organizatora skupa ili sadrže originalne rezultate prvi put objavljene, pa ih je korisno uz određene dopune učiniti dostupnim široj stručnoj javnosti. Štampaće se i stručni radovi za koje Redakcioni odbor oceni da su od šireg interesa.

Ostali prilozi su prikazi objekata, tj. njihove konstrukcije i istkustava-primeri u građenju i primeni različitih materijala, diskusije povodom objavljenih radova i pisma uredništvu, prikazi knjiga i zbornika radova, kao i obaveštenja o naučno-stručnim skupovima.

Autori uz rukopis predlažu kategorizaciju članka. Svi radovi pre objavljivanja se recenziraju, a o prihvatanju za publikovanje o njihovoj kategoriji konačnu odluku donosi Redakcioni odbor.

Da bi se ubrzao postupak prihvatanja radova za publikovanje, potrebno je da autori uvažavaju Uputstva za pripremu radova koja su navedena u daljem tekstu.

Upustva za pripremu rukopisa

Rukopis otkucati jednostrano na listovima A-4 sa marginama od 31 mm (gore i dole) a 20 mm (levo i desno). u Wordu fontom Arial sa 12 pt. Potrebno je uz jednu kopiju svih delova rada i priloga, dostaviti i elektronsku verziju na navedene E-mail adrese, ili na CD-u. Autor je obavezan da čuva jednu kopiju rukopisa kod sebe zbog eventualnog oštećenja ili gubitka rukopisa.

Od broja 1/2010. prema odluci Upravnog odbora Društva i Redakcionog odbora, radovi sa pozitivnim recenzijama prihvaćeni za štampu, publikovace se na srpskom i engleskom jeziku.

Svaka stranica treba da bude numerisana, a optimalni obim članka na jednom jeziku, je oko 16 stranica (30000 slovnih mesta) uključujući slike, fotografije, tabele i popis literature. Za radove većeg obima potrebna je saglasnost Redakcionog odbora.

Naslov rada treba sa što manje reči (poželjno osam, a najviše do jedanaest) da opiše sadržaj članka. U naslovu ne koristiti skraćenice ni formule. U radu se iza naslova daju ime i prezime autora, a titule i zvanja, kao i име institucije u podnožnoj napomeni. Autor za kontakt daje telefone, faks i adresu elektronske pošte, a za ostale autore poštansku adresu.

Uz sažetak (rezime) od oko 150 do 200 reči, na srpskom i engleskom jeziku daju se ključne reči (do deset). To je jezgrovit prikaz celog članka i čitaocima omogućuje uvid u njegove bitne elemente.

Rukopis se deli na poglavља i potpoglavlja uz numeraciju, po hijerarhiji, arapskim brojevima. Svaki rad ima uvod, sadržinu rada sa rezultatima, analizom i zaključcima. Na kraju rada se daje popis literature.

Kod svih dimenzionalnih veličina obavezna je primena međunarodnih SI mernih jedinica.

Formule i jednačine treba pisati pažljivo vodeći računa o indeksima i eksponentima. Autori uz izraze u tekstu definuju simbole redom kako se pojavljuju, ali se može dati i posebna lista simbola u prilogu.

Prilozi (tabele, grafikoni, sheme i fotografije) rade se u crno-beloj tehnički, u formatu koji obezbeđuje da pri smanjenju na razmere za štampu, po širini jedan do dva stupca (8cm ili 16.5cm), a po visini najviše 24.5cm, ostanu jasni i čitljivi, tj. da veličine slova i brojeva budu najmanje 1.5mm. Originalni crteži treba da budu kvalitetni i u potpunosti pripremljeni za presnimavanje. Mogu biti i dobre, oštре i kontrastne fotokopije. Koristiti fotografije, u crno-beloj tehnički, na kvalitetnoj hartiji sa oštrim konturama, koje omogućuju jasnju reprodukciju. Skraćenice u prilozima koristiti samo izuzetno uz obaveznu legendu. Prilozi se posebno označavaju arapskim brojevima, prema redosledu navođenja u tekstu. Objašnjenje tabela daje se u tekstu.

Potrebno je dati spisak svih skraćenica korišćenih u tekstu.

U popisu literature na kraju rada daju se samo oni radovi koji se pominju u tekstu. Citirane radove treba prikazati po abecednom redu prezimena prvog autora. Literatuру u tekstu označiti arapskim brojevima u uglastim zagradama, kako se navodi i u Popisu citirane literature, napr [1]. Svaki citat u tekstu mora se naći u Popisu citirane literature i obrnuto svaki podatak iz Popisa se mora navesti u tekstu.

U Popisu literature se navode prezime i inicijali imena autora, zatim potpuni naslov citiranog članka, iza toga sledi ime časopisa, godina izdavanja i pocetna i završna stranica (od - do). Za knjige iza naslova upisuje se ime urednika (ako ih ima), broj izdanja, prva i poslednja stranicapoglavlja ili dela knjige, ime izdavača i mesto objavljinja, ako je navedeno više gradova navodi se samo prvi po redu. Kada autor citirane podatke ne uzima iz izvornog rada, već ih je pronašao u drugom delu, uz citat se dodaje «citirano prema...». Neobjavljeni članci mogu se pominjati u tekstu kao «usmeno saopštenje».

Autori su odgovorni za izneseni sadržaj i moraju sami obezbediti eventualno potrebne saglasnosti za objavljinje nekih podataka i priloga koji se koriste u radu.

Ukoliko rad bude prihvaci za štampu, autori su dužni da, po uputstvu Redakcije, unesu sve ispravke i dopune u tekstu i prilozima.

Za detaljnija tehnička upustva za pripremu rukopisa autori se mogu obratiti Redakcionom odboru časopisa.

Rukopisi i prilozi objavljenih radova se ne vraćaju. Sva eventualna objašnjenja i uputstva mogu se dobiti od Redakcionog odbora.

Radovi se mogu slati i na e-mail: folic@uns.ac.rs ili miram@uns.ac.rs i dimk@ptt.rs

Veb sajt Društva i časopisa: www.dimk.rs

* Upustvo autorima je modifikovano i treba ga u pripremi radova slediti.

Izdavanje časopisa "Građevinski materijali i konstrukcije" finansijski su pomogli:



INŽENJERSKA KOMORA SRBIJE

**MINISTARSTVO ZA NAUKU I TEHNOLOŠKI
RAZVOJ SRBIJE**



**UNIVERZITET U BEOGRADU
GRAĐEVINSKI FAKULTET**



**DEPARTMAN ZA GRAĐEVINARSTVO
FAKULTET TEHNIČKIH NAUKA NOVI SAD**



INSTITUT IMS AD, BEOGRAD



**UNIVERZITET CRNE GORE
GRAĐEVINSKI FAKULTET - PODGORICA**